

The role of fungal lifestyle and secreted effectors in complex phyllosphere microbial communities



Inaugural-Dissertation

zur

Erlangung des Doktorgrades der Naturwissenschaften
(Dr. rer. nat.)

der Mathematisch-Naturwissenschaftlichen Fakultät
der Universität zu Köln

vorgelegt von

Katharina Eitzen

aus Hamm

Köln, 2021

Die Untersuchungen zur vorliegenden Arbeit wurden von November 2015 bis Juli 2019 am Lehrstuhl für Terrestrische Mikrobiologie an der Universität zu Köln unter der Betreuung von Herrn Prof. Dr. Gunther Döhlemann durchgeführt.

Erstgutachter: Prof. Dr. Gunther Döhlemann

Zweitgutachter: Prof. Dr. Bart Thomma

Drittgutachter: Prof. Dr. Eric Kemen

Tag der mündlichen Prüfung: 26.01.2022

I almost wish I hadn't gone down that rabbit-hole -
and yet - it's rather curious, you know, this sort of life!"
Lewis Carroll - *Alice's Adventures in Wonderland*

Zusammenfassung

Pflanzen stellen ein natürliches Habitat für diverse Mikroorganismen dar. Bei der Mehrzahl dieser handelt es sich um kommensale Mikroben, die sich als Nutznießer von toten Pflanzenresten ernähren. Dennoch ist eine Pflanze stetig einem Infektionsrisiko durch krankheitserregende Mikroorganismen ausgesetzt. Alle Organismen dieses Mikrobioms sind durch ein Interaktionsnetzwerk miteinander verbunden und können das pflanzliche Immunsystem sowohl direkt als auch indirekt beeinflussen. In natürlichen *Arabidopsis thaliana* Populationen wurde der Oomycete *Albugo laibachii* als sogenannter „Hub-Organismus“ identifiziert und spielt somit eine große Rolle für die Stabilität des mikrobiellen Netzwerks.

In dieser Arbeit wurde gezeigt, dass die epiphytische Hefe *Moesziomyces bullatus ex Albugo (Mba)* ein kommensaler Antagonist in der *A. thaliana* Phyllosphere ist und die Infektion des Pathogens *A. laibachii* drastisch reduziert. Trotz der nahen Verwandtschaft zu pathogenen Brandpilzen bleibt *Mba* unter natürlichen Bedingungen strikt apathogen. Mit Hilfe von Genomvergleichen und genetischer Manipulation konnten in dieser Arbeit neue Erkenntnisse zur Evolution eben dieser apathogenen Stämme erlangt werden. Des Weiteren zeigte die Generierung eines selbstkompatiblen Stammes, dass *Mba in-vitro* alle Voraussetzungen für eine erfolgreiche Pflanzeninfektionen aufweist.

Durch die Kombination von Transkriptomanalysen und reverser Genetik konnte zudem der Ursprung der antagonistischen Interaktionen von *Mba* erforscht werden. Hierbei wurde eine GH25 Hydrolase identifiziert, deren Lysozym-Aktivität maßgeblich an *Mba*'s Biokontrollaktivität beteiligt ist. Diese Ergebnisse können dabei helfen, mikrobielle Interaktionen in der *A. thaliana* Phyllosphere besser zu verstehen und diese Erkenntnisse auf Nutzpflanzen zu übertragen, um neue Strategien der biologischen Schädlingsbekämpfung zu entwickeln.

Abstract

In nature plants are challenged by several pathogenic organisms but are also colonized by numerous commensal microbes. Those microbes establish a network of interactions with their host and amongst each other. They can influence the plants health status by altering plant immune responses or directly antagonizing microbial pathogens. In wild *Arabidopsis thaliana* populations, the oomycete pathogen *Albugo laibachii* was identified as a hub organism and plays an essential role in structuring the leaf phyllosphere microbial network. In this thesis it was shown that the epiphytic yeast *Moesziomyces bullatus ex Albugo (Mba)* is an antagonistic member of the *A. thaliana* phyllosphere. While it is a close relative of pathogenic smut fungi, it stays mainly a pathogenic in nature. This work provides new insights into the evolution of epiphytic basidiomycete yeasts in comparison to their pathogenic relatives. Genetic manipulation of *Mba* showed that it still holds the potential to switch to pathogenic growth in vitro. Loss of pathogenicity in this strain is most likely the result of a mating type bias leading to death of one mating type in nature. Nevertheless, its genetic background makes it highly compatible in its epiphytic form. *Mba* reduces infections of *A. thaliana* by *A. laibachii* and antagonizes several bacterial members of the *A. thaliana* phyllosphere community. To functionally investigate the antimicrobial interactions of *Mba*, a high-quality annotated genome sequence and an efficient transformation system were established. The combination of transcriptomics, reverse genetics and recombinant protein production identified a GH25 hydrolase with lysozyme activity as a major effector of this microbial antagonism. Those findings are important to strengthen the understanding of microbial interactions within the *A. thaliana* phyllosphere and can be used in the future to develop novel strategies of microbiota-mediated disease protection.

Abbreviations

× g	Gravitational acceleration on earth (9.81m/s ²)	Kan	Kanamycin
°C	Degree Celsius	kb	Kilobases
µg	Microgram	KO	Knock-out
µl	Microliter	LRR	Leucine rich repeat
µm	Micrometer	M	Molar
µM	Micromolar	MAMP	Microbe-associated molecular pattern
A	Ampere	MAPK	Mitogen-activated protein kinase
aa	Amino acid	MgCl ₂	Magnesium chloride
bp	Base pairs	min	Minute(s)
Carb	Carbenicillin	ml	Milliliter
Cbx	Carboxin	mm	Millimeter
cDNA	Complementary DNA	mRNA	Messenger RNA
CDS	Coding sequence	ng	Nanogram
DAMP	Damage-associated molecular pattern	NLR	Nucleotide binding leucine rich repeat protein
DNA	Deoxyribonucleic acid	nm	Nanometer(s)
dpi	Days post infection	No.	Number
ETI	Effector-triggered immunity	Nt	Nucleotide
EtOH	Ethanol	O/N	Over night
ETS	Effector-triggered susceptibility	OD	Optical density
f.c.	Final concentration	p	Statistical probability value
FC	Fold change	PAMP	Pathogen-associated molecular pattern
FDR	False discovery rate	PCR	Polymerase chain reaction
Fly1	Fungalysin 1	Pep1	Protein essential during penetration 1
g	Gram	PI	Propidium iodide
GO	Gene Ontology	Pit2	Protein involved in tumours 2
h	Hour		
H ₂ O _{bid.}	Double distilled water		
JA	Jasmonic acid		

Abbreviations

PRR	Pattern recognition receptor
PTI	Pattern-triggered immunity
qPCR	Quantitative polymerase chain reaction
qRT-PCR	Quantitative real-time polymerase chain reaction
RNA	Ribonucleic acid
RNA-Seq	Ribonucleic acid sequencing
ROS	Reactive oxygen species
rpm	Rounds per minute
RT	Room temperature
s	Second(s)
SA	Salicylic acid
SAR	Systemic acquired resistance
See1	Seedling efficient effector 1
SP	Signal peptide
TE-buffer	Tris-EDTA buffer solution
Tin2	Tumour inducing 2
TM domain	Transmembrane domain
TOR	Target of Rapamycin
U	Unit (Enzyme activity)
V	Volt
v/v	Volume/volume
w/v	Weight/volume
WGA	Wheat germ agglutinin

Table of contents

Zusammenfassung	I
Abstract	III
Abbreviations	V
1 Introduction	1
1.1 Pest control in agricultural systems	1
1.2 Plant-microbe-microbe interactions	3
1.2.1 Plant microbiome composition and function	3
1.2.2 Biocontrol agents of the Rhizosphere	7
1.2.3 Biocontrol agents of the Phyllosphere	8
1.3 Basidiomycete yeasts as drivers of community structure	11
1.3.1 Biology of Ustilaginomycetes	11
1.3.2 Special features of anamorphic Ustilaginomycete strains	14
1.4 Aim of this study	17
2 Results	19
2.1 Morphology of <i>Mba</i>	19
2.2 The genome of <i>Mba</i>	22
2.3 Generation of a transformation system for <i>Mba</i>	30
2.3.1 The Self-compatible <i>Mba</i> strain CB1	32
2.3.2 The influence of Mannosylerythritol lipids on microbial community members.	36
2.4 Identification of microbe-microbe effector genes by RNA-Seq	38
2.5 Heterologous expression of a secreted <i>Mba</i> glycoside hydrolase	42
3 Discussion	45
3.1 Genetic repertoire of anamorphic Ustilaginomycetes	45
3.1.1 <i>Mba</i> still carries the genetic prerequisites for mating	45
3.1.2 Anamorphic strains tend to have a higher intron number	46
3.1.3 Chromosomal recombination in <i>Mba</i> affects genes important for virulence and mating	47
3.1.4 <i>Mba</i> possess effector genes important for pathogenicity	48

3.1.5	Integration of self-compatible mating genes enables pathogenic development of <i>Mba</i>	49
3.2	Mechanisms of biocontrol in <i>Mba</i>	51
3.2.1	Secondary metabolites and their function in biocontrol.....	51
3.2.2	Transcriptional reprogramming points to changes in nutrient acquisition....	51
3.2.3	GH43 enzymes could give an advantage in nutrient acquisition.....	52
3.2.4	GH25 hydrolases are important for biocontrol activity of <i>Mba</i> against <i>A. laibachii</i>	53
3.3	Conclusion and future perspectives.....	55
4	Material and Methods	57
4.1	Material.....	57
4.1.1	Chemicals.....	57
4.1.2	Buffers and solutions.....	57
4.1.3	Enzymes and antibodies.....	57
4.1.4	Commercial kits.....	58
4.2	Media and growth conditions for microorganisms.....	58
4.2.1	Media.....	58
4.2.2	Propagation of <i>A. laibachii</i>	59
4.2.3	Cultivation of <i>E. coli</i>	59
4.2.4	Cultivation of SynCom Bacteria.....	60
4.2.5	Cultivation of <i>M. bullatus</i> and <i>U. maydis</i>	60
4.2.6	Cultivation of <i>Pichia pastoris</i>	60
4.2.7	Determination of cell density.....	60
4.3	Microbial strains, oligonucleotides, and vectors.....	61
4.3.1	<i>A. laibachii</i> strain.....	61
4.3.2	<i>E. coli</i> strains.....	61
4.3.3	SynCom bacteria.....	61
4.3.4	<i>M. bullatus</i> and <i>U. maydis</i> strains.....	62
4.3.5	<i>P. pastoris</i> strains.....	63
4.3.6	Oligonucleotides.....	63
4.3.7	Plasmids.....	65
4.3.7.1	Plasmid for Cloning of PCR Products.....	65
4.3.7.2	Plasmids for <i>M. bullatus</i> and <i>U. maydis</i> transformation.....	66
4.3.7.3	Plasmids for the expression of recombinant proteins in <i>P. pastoris</i>	68
4.4	Microbiological methods.....	68

4.4.1	Transformation of <i>E. coli</i>	68
4.4.2	Blue-white screen of <i>E. coli</i> transformants	69
4.4.3	Transformation von <i>P. pastoris</i>	69
4.4.4	Transformation of <i>M. bullatus</i> and <i>U. maydis</i>	70
4.4.5	Mating assays of <i>M. bullatus</i> and <i>U. maydis</i>	71
4.4.6	Induction of filament and appressoria formation on artificial surfaces	71
4.4.7	Microbial confrontation assays.....	72
4.5	Molecular biological methods.....	72
4.5.1	Isolation of nucleic acids.....	72
4.5.1.1	Plasmid DNA isolation from <i>E. coli</i>	72
4.5.1.2	Isolation of genomic DNA from <i>M. bullatus</i> and <i>U. maydis</i>	73
4.5.1.3	RNA-Extraction of Latex-peeled samples	73
4.5.1.4	DNase-digest after RNA extraction	74
4.5.1.5	Purification of DNA	74
4.5.2	<i>In vitro</i> modification of nucleic acids.....	75
4.5.2.1	Restriction of DNA	75
4.5.2.2	Ligation of DNA fragments.....	75
4.5.2.3	A-tailing of PCR products	75
4.5.2.4	Fragment assembly using pGEM®-T Easy vector system	75
4.5.2.5	Fragment assembly using Gibson Assembly system	76
4.5.2.6	Polymerase chain reaction (PCR).....	76
4.5.2.7	cDNA synthesis	77
4.5.2.8	Sequencing of DNA	77
4.5.2.9	Sequencing of RNA	77
4.5.3	Separation and detection of nucleic acids.....	77
4.5.3.1	Agarose gel electrophoresis	77
4.5.3.2	Southern Blot analysis	78
4.6	Biochemical methods.....	80
4.6.1	Separation of proteins via SDS-PAGE.....	80
4.6.2	Staining of SDS-PAGE gels.....	81
4.6.3	Immunological detection of proteins via chemiluminescence (Western blot)	81
4.6.4	Expression of heterologous proteins in <i>P. pastoris</i>	82
4.7	Plant methods.....	83
4.7.1	Plant material and growth conditions	83
4.7.2	Seed sterilization	83

4.7.3	Infections of <i>A. thaliana</i> with <i>A. laibachii</i>	83
4.7.4	Virulence assay of <i>U. maydis</i> on maize.....	84
4.8	Microscopy.....	84
4.8.1	WGA-AF488/Propidium iodide co-staining of colonised maize tissue.....	84
4.8.2	Fluorescence microscopy.....	85
4.8.3	Image processing and measurement.....	85
4.9	Bioinformatics and computational data analysis.....	85
4.9.1	RNAseq analysis.....	85
4.9.2	Further bioinformatic analysis tools.....	85
5	Bibliography.....	87
6	Appendix.....	103
	Eidesstattliche Erklärung.....	115
	Delimitation of own contribution.....	117
	Acknowledgment.....	119

1 Introduction

1.1 Pest control in agricultural systems

To ensure food supply of a growing human population it is still necessary to higher the yield of common crops and to achieve a more sustainable and efficient agriculture (Edgerton, 2009; Ray et al., 2013). Increasing the productivity of plants does not only imply to higher the number of plants that can grow in a field, especially as space is a limiting factor. Most important is to elevate plants fitness, which includes food production and tolerance of plants against biotic & abiotic stresses (Boyer, 1982; Edgerton, 2009).

While pathogens and pests cause between 20 % and 30 % of global crop yield losses (Savary et al., 2019), there are different ways of agricultural pest control, which can be divided into the following subgroups: cultural control, trap cropping, use of pesticides, and biological control.

Cultural pest control is one of the oldest strategies of pest control and means the manipulation of the crop production system or the use of cultural practices to reduce or to eliminate pest populations. It comprises the adjustment of planting dates and the process of crop rotation, which helps to balance nutrient use and to diversify pest and weed communities (Hill, 1990; Dufour & Areas, 2001). Furthermore, it includes physical practices like tillage which can help to control soil inhabiting pests in crop fields by bringing the larvae to the surface or destroying crop residues which can harbor pests (Hill, 1990).

An alternative method of controlling pests is the use of trap crops. They attract the agricultural pest, usually insects, away from nearby crops to reduce losses in the field (Hokkanen, 1991; Shelton & Badenes-Perez, 2006). Unfortunately, only a small share of plants, showing significant effects in greenhouse experiments, can be used in larger commercial scales. A review of trap cropping experiments revealed that only 10 out of 100 plants have a successful effect in large fields. Nevertheless, in all 10 cases special effort was needed to prevent insect dispersal back into the main crop. This fact makes trap cropping inefficient for large agricultural fields, as pesticides or human actions still need to be applied in addition (Holden et al., 2012).

Another efficient way of pest control in agricultural fields is the application of chemical substances known as pesticides to prevent, destroy, repel, or mitigate a pest (Saravi & Shokrzadeh, 2011). As they can be sprayed to the fields in large scales by aircrafts or tractor-mounted crop sprayers they are easy to handle for farmers and have a high efficiency on large fields. Although the use of pesticides clearly improved crop quality and quantity in the past 50 years, the pathogens acquire resistances leading to a demand for

increasing pesticide dosages (Syed Ab Rahman et al., 2018; Ferraz et al., 2019). Even more pesticides are needed as farmers in industrialized countries often tend to use improved varieties which promise a better yield but tend to be more susceptible to pathogens (Kjær et al., 1990; Brown & Rant, 2013). The systemic use of those drugs can heavily impact the microflora of agrarian ecosystems by killing beneficial bacteria and fungi and will persist in the environment as a soil contaminant (Carvalho, 2006). To guarantee a stable food supply we still depend on agrochemicals for crop protection or growth-promoting products as fertilizers, as they are the most effective way of pest control (Saravi & Shokrzadeh, 2011). But as many agrochemicals are poisonous or hazardous to health and environment, the use of microbial based products that can protect crops against diseases is a promising alternative in pathogen control (Nishimoto, 2019).

This last way of pest control in agricultural fields includes the use of other organisms like insects, mites, weeds, or microorganisms to control specific diseases in the field. Compared to pesticides, biocontrol agents have diverse modes of action, e.g. antibiosis, parasitism, competition, or induced resistance in the host plant, which long time was thought to limit the ability of pathogens to develop resistance (Köhl et al., 2019). However, recent results concerning biocontrol management in agricultural systems have shown that this assumption is still debatable (Bardin et al., 2015). Even more it is needed to study the impact of microbes on natural enemies and on the natural community itself, as the introduction of organisms into a certain environment can have several side-effects on the biodiversity (Myers & Cory, 2017). The most challenging part in biocontrol research is the transition of biocontrol agents from the green house to the field, as several studies reported a loss of efficacy under commercial field conditions (Nicot et al., 2011). Main factors for failure of a biocontrol agent is the insufficient resistance to abiotic stresses in the field, the persistence on the target, the linkage of metabolite production to certain circumstances or the unstable quality of the formulated product (Ruocco et al., 2011).

1.2 Plant-microbe-microbe interactions

1.2.1 Plant microbiome composition and function

Plants are an important habitat for microorganisms like bacteria, filamentous fungi, yeasts, protists, and archaea, termed as the microbiota (Bordenstein & Theis, 2015). They form a functional entity with their multicellular host, which influences plant growth and productivity and is nowadays often referred to as the holobiont (Bordenstein & Theis, 2015). In this concept, evolutionary selection likely occurs between the plant and its microbiome but also among microbes (Rosenberg & Zilber-Rosenberg, 2016; Hassani et al., 2018). The plant itself harbors diverse habitats for microbiota that can roughly be divided into below- and aboveground environments, with the roots being in the soil and the leaves being located above the ground. In both habitats one can further distinguish between the episphere compartments named phyllosphere and rhizosphere, consisting of the plants outer surface and an endosphere compartment, including all inner parts of a plant tissue (Berg et al., 2014).

Those compartments form dynamic ecological niches, which are mostly determined by environmental factors and host genetics (Figure 1). They vary widely in their community composition with bacteria and fungi being the most prominent organism groups. Main bacterial phyla of the plant endosphere are for example Proteobacteria, Firmicutes and Bacteroidetes, while in the phyllosphere Actinobacteria and Acidobacteria are enriched (Trivedi et al., 2020). In contrast to bacteria, only two fungal genera dominate all plant compartments, namely Ascomycetes and Basidiomycetes. Arbuscular mycorrhizal fungi, which mainly belong to the phylum of Glomeromycota, on the other hand only play a minor role for community diversity although they have an important role in nutrient uptake (Trivedi et al., 2020).

In addition, also archaea, viruses and protists can be found as inhabitants of plants and can influence plant processes. Some protists are known to consume microorganisms and by this accelerate nutrient turnover in microbial communities (Gao et al., 2019). Those predator-prey interactions serve as strong drivers of microbial community assembly and can strongly affect the microbiome composition.

To use natural microbiota for increase in plant yield requires a rational design of stable microbial communities. For this it is important to understand, how plants are colonized by their microbiota, how microbes can influence the community and in which ways they affect their host plant. Information received from ecological, metagenomic or metabolomic studies can be visualized in microbial networks. Such networks are snapshots of an ecosystem and represent the complex interactions that can be found in nature. Every network consists of

1. Introduction

two different components – nodes and edges – while nodes represent each microbe in the ecosystem and edges are statistically significant interactions. The number of edges connected to a node is marked as its degree (Röttgers & Faust, 2018). Microbial networks can help to identify core microbiota, which consist of microorganisms that can be found persistent and ubiquitous on one host. In most cases they belong to key microbial taxa that carry the genetic repertoire to positively affect the plants fitness and are mainly the result of co-evolution (Trivedi et al., 2020). Those core microbes are maintained by the plant in high abundances over the entire lifetime and typical examples for core microbiome members belong to the bacterial families of Rhizobiales or Pseudomonadales (Garrido-Oter et al., 2018). In addition to the core microbes, a small number of microbes stand out in network analyses by having a high degree, what means they are highly interconnected microbes – so called “hub organisms”. Due to their strong biotic interactions, they directly shape the community structure and are of great importance for ecosystem structure and function (Agler et al., 2016; Röttgers & Faust, 2018; Trivedi et al., 2020).

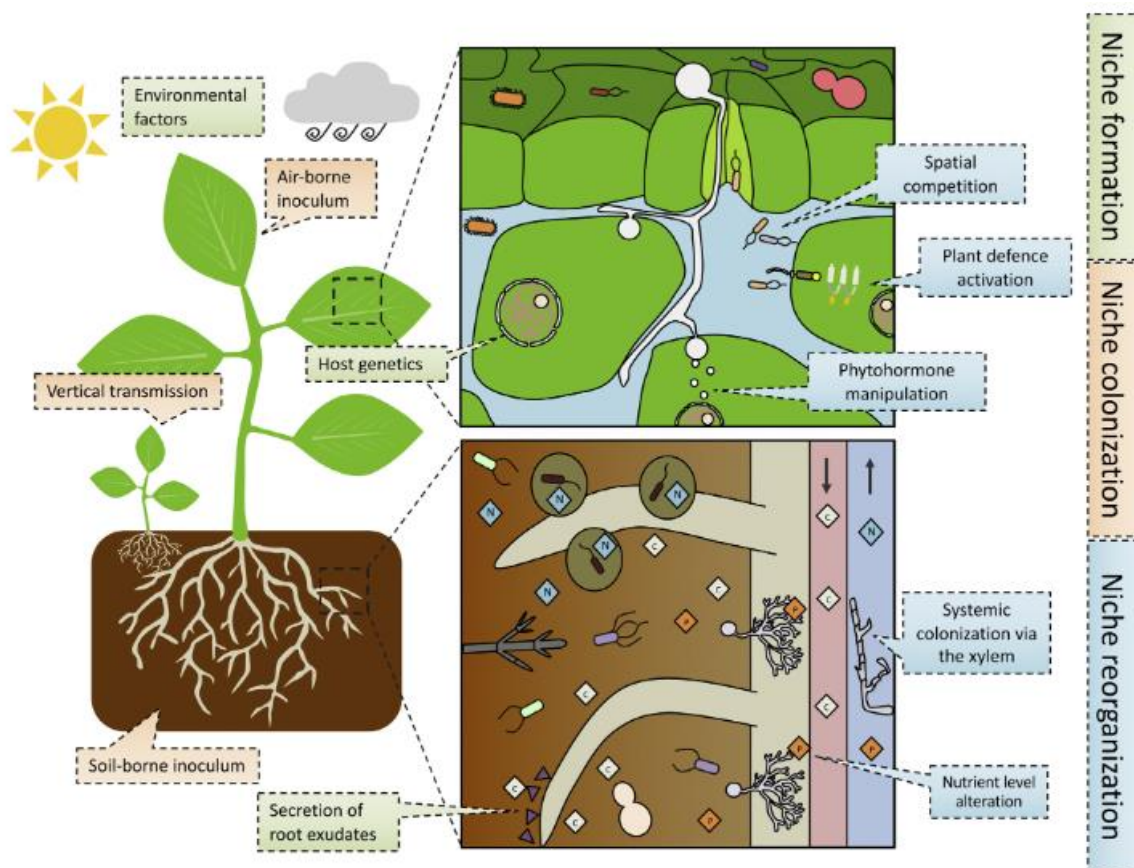


Figure 1: Formation of the plant holobiont. Environmental factors and host genetics shape a plants initial niche, that can be colonized by different microbes. The colonization itself can be achieved by soil- or air-borne microorganisms or via vertical transmission from plant to plant. Each colonizer requires a different set of adaptations which depends on the colonized tissue type. In the following, every microbe will begin to remodel its niche by leading to nutrient level alteration, spatial competition or by activating their hosts defense mechanisms. This can lead to dynamic adaptations of microbial niche inhabitants over time. Figure modified from (Kroll et al., 2017).

But how do microbes colonize a plant? Mainly, there are two different ways of colonization (Figure 1). In most cases colonization starts in the soil compartment, where an initial microbial community already exists and which is shaped by intermicrobial interactions like the secretion of antimicrobial metabolites (Trivedi et al., 2020). Exudates secreted by the plant roots, like organic acids or sugars, can be sensed and uptaken by some soil microbes. This confers a fitness advantage to a few microorganisms and further shapes community structure (Xing-Feng et al., 2014). As some microbes are capable of chemotaxis, they can actively initiate first colonization of the root environment by formation of a biofilm on the root surface (Trivedi et al., 2020). Genetically root colonizers show a higher amount of motility and nutrient transporter genes that help to colonize the plant and give a selective advantage (Levy et al., 2018). Furthermore, microbial symbionts can also be passed on to the next generation via vertical transfer. They can colonize the seeds via vascular connections or via pollen and are predominantly associated with a fitness advantage (Shade et al., 2017). The colonization of endophytic compartments needs specific adaptations like the production of lytic enzymes for the maceration of plant cell walls (Gao et al., 2010).

To protect themselves against pathogenic microbes, plants have evolved an innate immune system, which will recognize microbes with the help of membrane-localized (pattern recognition receptors; PRRs) and intracellular receptors (nucleotide-binding domain and leucine rich repeat containing receptors; NB-LRR; (Jones & Dangl, 2006)). PRRs can detect microbe- or damage-associated molecular patterns (MAMPs or DAMPs) like bacterial lipopolysaccharides, flagellin, fungal chitin or plant cytosolic proteins outside of the cell and induce PAMP-triggered immunity (PTI). It is characterized by a rapid Ca^{2+} burst and the generation of reactive oxygen species (ROS), leading to the activation of defense related mitogen-activated protein kinases (MAPKs), and production of phytohormones like salicylic acid (SA), jasmonic acid (JA) and ethylene (ET; (Macho & Zipfel, 2014)). To cope with those defense mechanisms endophytic bacteria for example evolved a specific detoxification system to catalyze the dismutation of superoxide into oxygen and hydrogen peroxide (Alquéres et al., 2013). Consequently, endophytes try to overcome the plants defense mechanisms and secrete small proteins called effectors into the apoplast or the plant cell (Asai & Shirasu, 2015). They are supposed to act as decoys to interfere with PTI, leading to effector-triggered susceptibility (ETS; (Hardoim et al., 2015; Levy et al., 2018)). It is speculated that many of those proteins emerged from convergent evolution and horizontal transfer of genes from plants to microbes. NB-LRRs represent the second line of immune response and can recognize microbial effectors, resulting in effector-triggered immunity (ETI; (Jones & Dangl, 2006)). It is generally an amplified version of PTI and leads to a

hypersensitive response (HR) at the infection site and systemic acquired resistance (SAR; (Tsuda & Katagiri, 2010; Cui et al., 2015)).

After colonizing the plant microbes have the ability to alter a colonized niche due to spatial competition, plant defense activation, phytohormone manipulation, systemic colonization via xylem or nutrient level alteration, which transforms every niche to a highly dynamic environment (Figure 1;(Kroll et al., 2017)). Successful colonization of roots for example can change the root architecture, which leads to different niche colonization patterns of other microbial groups (Trivedi et al., 2020).

As plants are sessile organisms, they depend on the nutrients available in their surrounding environment. The plant microbiota can play an essential role in nutrient acquisition for example by facilitating the uptake of inorganic phosphor or iron from the soil (Jin et al., 2010; Brito et al., 2020). Symbiotic interactions of plants with arbuscular mycorrhizal fungi or rhizobium bacteria help the plant to take up organic nitrogen that is otherwise not bioavailable in the soil (Backer et al., 2018). In addition to improved nutrient supply, associated microbes can contribute to disease resistance or improve stress tolerance. But is the plant's immune system also able to distinguish between good and bad microbes? To tackle this question, Vannier et al. (2019) hypothesized that the immune system of plants and the microbiota can instruct each other beyond the known co-evolutionary arms race. They proposed to add two components to the known plant immune responses, termed microbiota modulated immunity (MMI), and direct microbial competition (DMC; Figure 2). Root microbiota for example can stimulate the plants immune system by manipulating JA and ET signaling and due to this activate induced systemic resistance (ISR) mechanisms. The plant will be transferred into a state of emergency and its resistance to pathogens will be enhanced (Pieterse et al., 2014). Even more, some epi- and endophytic microbes manipulate the phenylpropanoid metabolism in tomato plants. As this pathway is also involved in SA synthesis it leads to a fortification of cell walls and higher stress resistance (Chialva et al., 2018). Under stress conditions plants are also able to recruit specific microbes due to the secretion of specific root exudates. One typical example for this is the production of scopoletin, which has antimicrobial activity and selects for beneficial microbes under iron or phosphorus stress conditions (Stringlis et al., 2018). DMC on the other hand supplements the plants innate immune systems as rhizosphere and endophytic microbes help battling pathogens by producing antimicrobial compounds like hydrolytic enzymes or antibiotics (Carrión et al., 2019). In a consequence it is needed to understand how complex microbe-microbe and microbe-plant interactions contribute to the plant's immune responses to implement this knowledge into rational design of synthetic microbial communities with a function in plant protection.

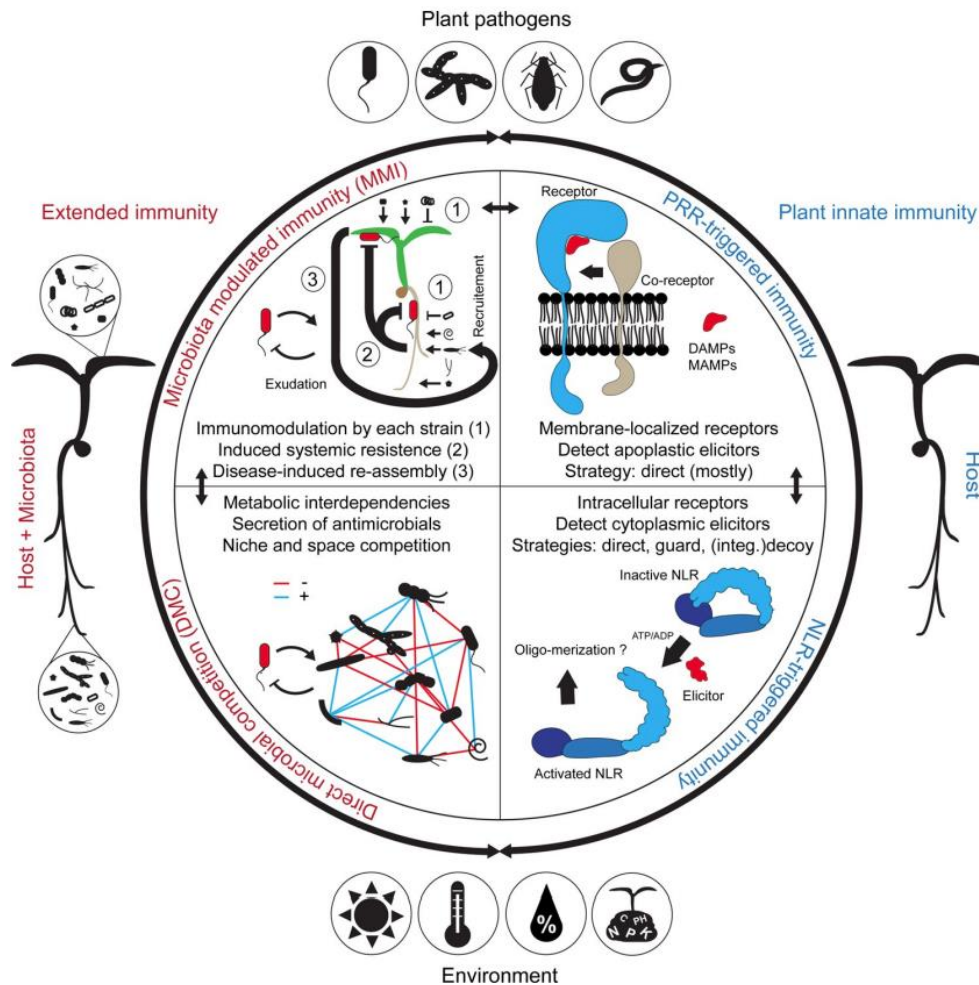


Figure 2: Proposed model for microbiota-mediated extension of the plant immune system. Host immune responses can be distinguished as PRR-triggered immunity and NLR-triggered immunity. While membrane localized PRRs recognize MAMPs and DAMPs extracellularly, NLRs recognize effectors secreted by pathogens intracellularly. Microbiota on the other hand can modulate the innate immune system by activating ISR or protect actively against pathogens by secreting antimicrobial substances. Figure modified from (Vannier et al., 2019).

1.2.2 Biocontrol agents of the Rhizosphere

In nature, plants abundantly form beneficial associations with soilborne microbes that are improving plant growth, but also affecting the soil ecosystem and its biodiversity. While the bulk soil contains billions of microbes, the rhizosphere community structure differs a lot, as plants secrete exudates which are shaping their microbiome (Mendes et al., 2011). Well studied examples of symbiotic microbes in roots are mycorrhizal fungi that improve the uptake of water and minerals like phosphate (Parniske, 2008), or *Rhizobium* bacteria that form a symbiosis with leguminous plants by fixing atmospheric nitrogen for the plant (Spaink, 2000). But also nonsymbiotic associations with plant-growth-promoting rhizobacteria (PGPR) and fungi (PGPF) can have a beneficial effect on plant fitness by eliciting an ISR response (Lugtenberg & Kamilova, 2009; Shores et al., 2010), which can effectively suppress a broad spectrum of pathogens and even insect herbivores (Van Wees

et al., 2008; Pineda et al., 2010). In addition, some PGPR like *Pseudomonas* spp., *Arthrobacter* spp. and *Bacillus* spp. are known to produce phytohormones like auxin, cytokinin and gibberellin and by this alter the plants hormone levels. This can lead to improved nutrient uptakes or higher stress tolerance resulting in elevated plant growth and fitness (Compant et al., 2019). Increasing importance of transferring those natural phenomena to pest and disease control is reflected by the raising number of studies carried out during the last 20 years (Ciancio et al., 2019).

Examples for commercially available biocontrol agents of the rhizosphere are the products Serenade® and Root Shield®. Serenade® comprises of dried *Bacillus amyloliquefaciens* (former *subtilis*) strain QST 713 spores, which are known to secrete cyclic lipopeptides (LPs) of the surfactin, iturin and fengycin families, which antagonizes several phytopathogens like *Fusarium* spp. or *Pythium* spp. (Cawoy et al., 2014; Zalila-Kolsi et al., 2016) and additionally triggers induced systemic resistance mechanisms to prime plants against other pathogen attacks (Compant et al., 2005; Cawoy et al., 2014; Zalila-Kolsi et al., 2016). The active agent of Root Shield® is *Trichoderma harzianum* strain T-22, which is a good colonizer of the root surface and by this outcompetes several plant pathogens. In addition, it can actively attack other fungi by secreting cell wall degrading enzymes (Yang et al., 2009) and acts, similar to Serenade®, mainly against *Fusarium* root rot, soil-borne *Rhizoctonia* or *Pythium* root rot.

1.2.3 Biocontrol agents of the Phyllosphere

In addition to rhizosphere biocontrol agents, a newly growing field of research focuses on microbial biocontrol in the phyllosphere, which comprises of all aerial parts of a plant and is dominated by the leaves. A leaf itself is divided in three main parts, the epidermis, the mesophyll, and the vascular tissue (Oguchi et al., 2018), which can be seen in the cross-section in Figure 3. The outer layer of a leaf is called epidermis and forms a boundary that separates the leaf's inside from its surrounding environment. As the cuticle prevents transpiration, active gas exchange takes place at the stomata. The mesophyll is located between the two epidermal layers and is the main photosynthetic active tissue. It consists of palisade and spongy mesophyll cells, in which the vascular tissue is embedded. One vein can be separated into the xylem, which transports water and minerals from the root to the leaf and the phloem, in which photosynthesis products, mainly sugars, are transported from source to sink (Oguchi et al., 2018). Parts of a leaf, that are frequently colonized by several microorganisms, are the leaf surface and the apoplast (Vorholt, 2012).

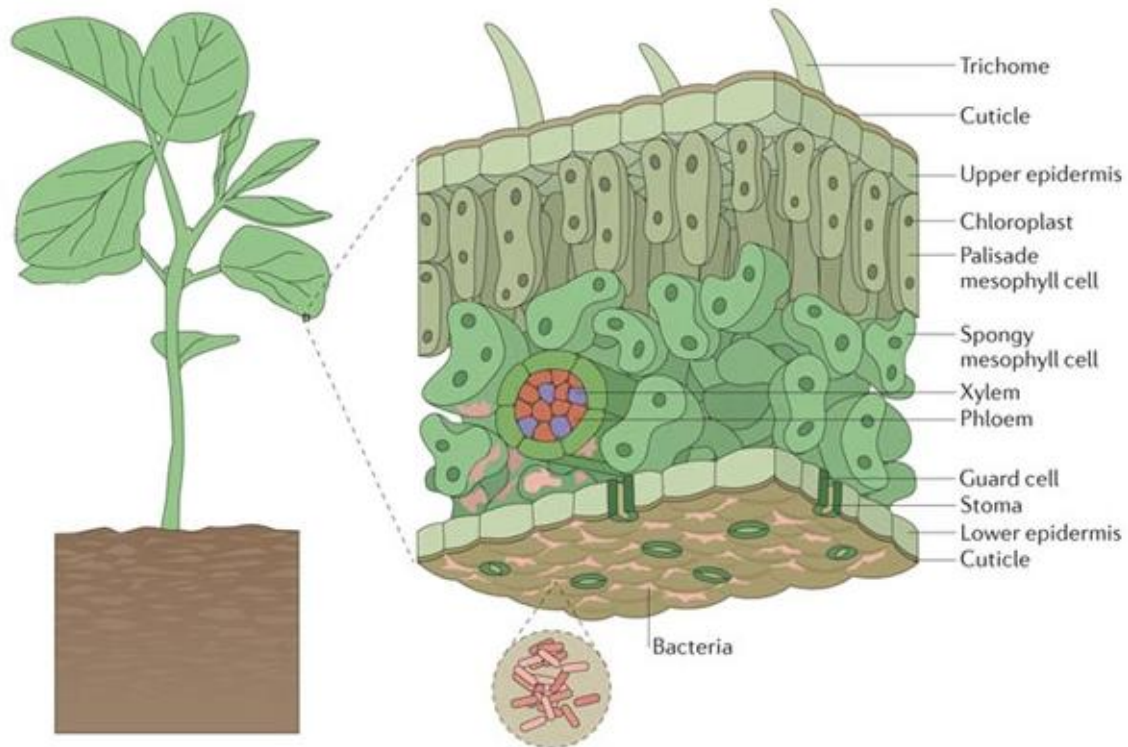


Figure 3: Structure of a plant leaf. A leaf can be divided in different compartments. The epidermis forms the outer boundary, the mesophyll is the main photosynthetic tissue, and the vascular tissue is important for water and nutrient transport. Compartments frequently colonized by microbes are the leaf surface and the apoplast. Figure modified from (Vorholt, 2012).

For long time, the leaf surface has been considered a hostile environment for microbial colonists, as it is an environment in which moisture, UV- and temperature levels can change rapidly (Hirsch & Fujishige, 2008). It remains a nutrient-poor environment which limits the growth of microorganisms and makes it necessary to develop new strategies to acquire nutrients (Stone et al.; Mercier & Lindow, 2000). The dominant microorganisms that can be found in the phyllosphere are non-pathogenic bacteria belonging to the phyla of Proteobacteria, mainly Alpha- and Gammaproteobacteria, Bacteroidetes and Actinobacteria. Examples for bacterial genera that can be frequently found in phyllosphere communities are *Methylobacterium*, *Sphingomonas* and *Pseudomonas* (Vorholt, 2012). Those bacteria are specifically adapted to the phyllosphere environment. An example are *Pseudomonas sp.*, which benefit from their flagellar motility to reach more favorable sites on the plant leaf (Haefele & Lindow, 1987) and are able to increase the water availability on the leaf by secreting the biosurfactant syringafactin (Burch et al., 2014; Hernandez & Lindow, 2019). Moreover, *Pseudomonas syringae* secretes the type-III effector protein HopM1, which helps to leak water from the plant cell into the apoplast (Xin et al., 2016). Similar to nitrogen fixation in leguminous plants via the symbiosis with rhizobia, also phyllosphere bacteria can play a role in nitrogen cycling. In the tropical rain forests, leaf

surfaces can be colonized by diazotrophic bacteria which are able to fix atmospheric nitrogen (N₂) at the phyllosphere-atmosphere interface (Abril et al., 2005).

An example for the use of typical phyllosphere bacteria as commercial biocontrol agents is the product BlightBan® A506 distributed by the US company NuFarm (Burr Ridge, IL). The active ingredient is the epiphytic bacterium *Pseudomonas fluorescens* strain A506, which can be used against the bacterial pathogen *Erwinia amylovora*, causing the fire blight disease on pear and apple flowers (Burrill, 1883; Eden-Green & Billing, 1974). The pathogen itself colonizes the stigmas of flowers as an epiphyte, then migrates to the nectary where it invades the host tissues and causes wilt and necrosis of infected floral tissues and branches (Eastgate, 2000). The mechanism of biocontrol was elucidated in studies by Wilson and Lindow (1993), in which they demonstrated that A506 is a good colonizer of floral tissues. As it is not known to produce specific antibiotics and its biocontrol ability is only achieved when pre-inoculated in large populations, it was hypothesized that the primary mechanism of control of fire blight is competitive exclusion.

In addition to bacteria, also fungi, including yeasts, are frequently colonizing the phyllosphere and have been described to have a high antagonistic potential against various plant pathogens (Freimoser et al., 2019). These antagonistic activities rely on the competition for nutrients, as well as on the synthesis of antimicrobial compounds, so called killer toxins. Those possess a large spectrum of activity against food spoilage microorganisms, but also against several pathogens (Muccilli & Restuccia, 2015). As many of those yeasts are already known from biotechnological applications, are easy to cultivate and have strong antifungal properties, they are an emerging option in biocontrol of fruits and vegetables (Guinebretiere et al., 2000). Some of those yeasts like *Candida oleophila* and *Pseudozyma flocculosa* have been commercialized and are known as the available products Aspire® and Sporodex® (Droby et al., 1998; Punja & Utkhede, 2003). Yeast biocontrol mechanisms thus represent a largely unexplored field of research and plentiful opportunities for the development of commercial, yeast-based applications for plant protection exist (Freimoser et al., 2019).

1.3 Basidiomycete yeasts as drivers of community structure

Agler et al. (2016) performed a scale-free correlation network analysis of the *A. thaliana* microbial leaf population and pointed out that the majority of interkingdom interactions (i.e., between bacteria and fungi) are found to be negative, as mainly antagonistic interactions stabilize microbial communities (Coyte et al., 2015). Furthermore, they identified a small number of hub organisms, which are highly connected in the network and have a severe effect on the community structure. In the *Arabidopsis* phyllosphere, the oomycete pathogen *Albugo laibachii* turned out to be a key microbe in shaping the microbial community structure, as it significantly reduces the bacterial diversity and stabilizes the community. *A. laibachii* itself is an eukaryotic organism belonging to the group of Stramenopiles (Cavalier-Smith & Chao, 2006). It is an obligate biotrophic pathogen causing white rust on the model plant *A. thaliana* (Kemen & Jones, 2012).

Furthermore, a small subset of bacteria and fungi was detected, which are frequently colonizing *A. thaliana* together with *A. laibachii* and could be used in gnotobiotic plate experiments. The most prominent fungi found in the dataset had been basidiomycete yeasts, belonging to the genus of *Dioszegia* and *Pseudozyma* (Agler et al., 2016).

1.3.1 Biology of Ustilaginomycetes

Pseudozyma yeasts belong to the order of Ustilaginales, which is a large group of mainly biotrophic plant pathogens that mostly infect grasses, including several important crop plants such as maize, wheat, barley and sugar cane (Agrios, 2005). Those infections can lead to drastic crop damage and loss in crop yield. As Ustilaginomycetes are typically dimorphic plant pathogens, their lifecycle can be characterized by a saprophytic haploid yeast phase until mating of two sporidia leads to a dikaryotic filamentous phase, what can be seen in Figure 4A (Brefort et al., 2009).

For mating, which in fungi is controlled by discrete mating loci, two compatible sporidia need to first recognize each other and then undergo cell fusion. Genomes of Ustilaginomycetes contain two mating loci. The a-locus, coding for an α -pheromone (Mfa) and a pheromone-receptor (Pra), as well as the b-locus, which encodes a heterodimeric homeodomain transcription factor. The a-locus is mainly important for cell-cell recognition between haploid sporidia and the fusion of those cells to a dikaryotic cell (Bölker et al., 1992). When one cell recognizes the pheromone in addition to other environmental signals, cAMP dependent protein kinase A (cAMP-PKA) and MAPK pathways are going to be activated (García-Pedrajas et al., 2008).

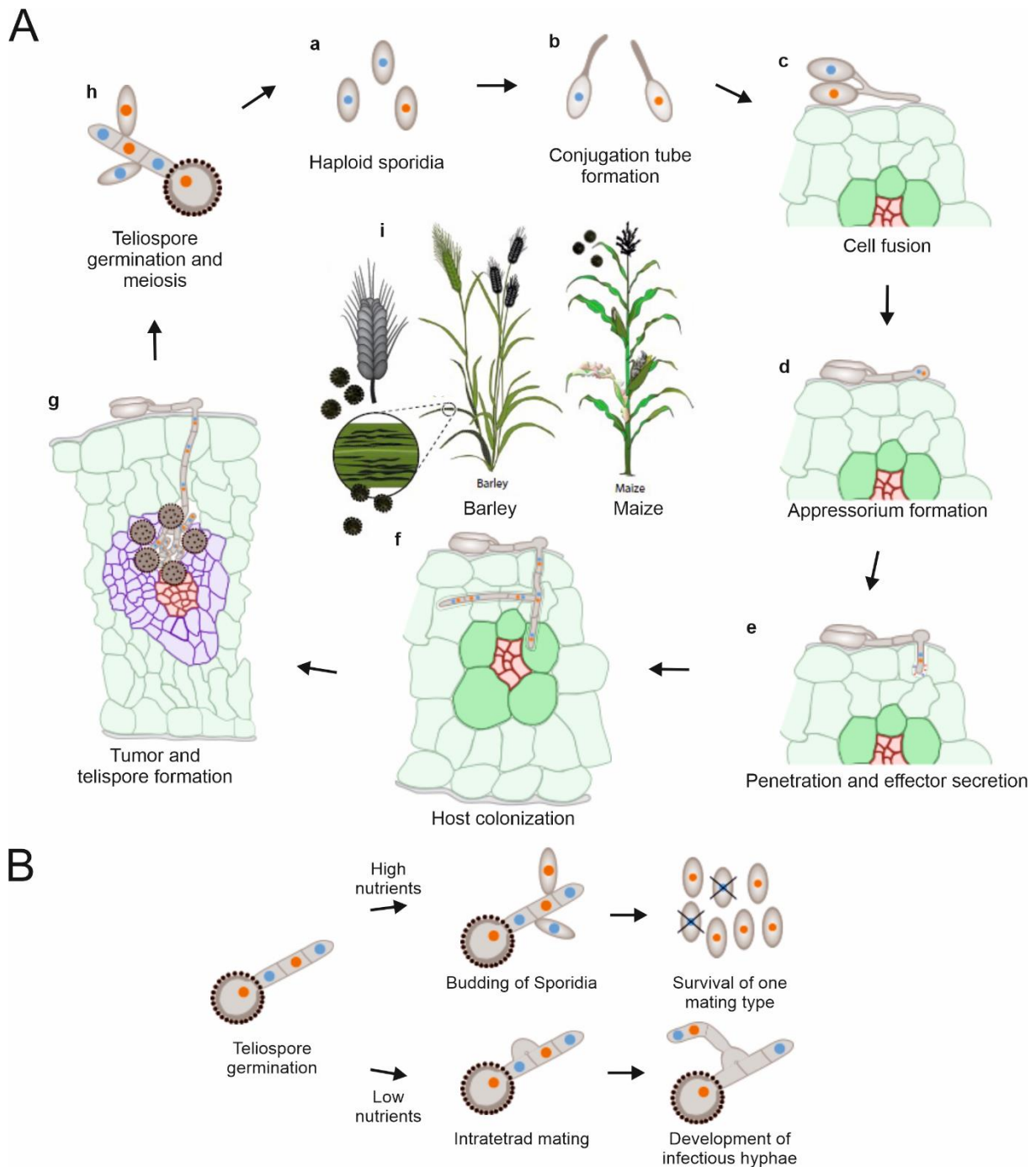


Figure 4: Lifecycle of Ustilaginomycetes. (A) Haploid sporidia on the plant start to recognize different mating types (a – blue and orange), which leads to the formation of conjugation tubes (b). Those tubes fuse on the plant surface (c) start a septated growth which leads to appressoria formation (d). By the help of this infection structure the plant gets penetrated and effector proteins are released to suppress the plants immune system and to guarantee a sufficient infection (e). Ustilaginomycetes are colonizing the plant by migrating to the vacuolar system (f). In most cases they colonize the plant almost symptomless until reaching the inflorescence (i), where they start karyogamy and form black teliospores. In case of the corn smut *U. maydis*, tumors and teliospores can also be formed in maize leaves (g,i). When teliospores germinate, they undergo meiosis and form a tetrad, consisting of four haploid cells (h). Each cell forms again haploid sporidia, that colonize the plant surface saprophytically until reentering the pathogenic cycle again. **(B)** An existing mating type bias leads to two different scenarios. Under high nutrient conditions haploid sporidia start to bud from the tetrad, but only one mating type is viable. Sporidia can't enter the pathogenic cycle until finding a mating partner without mating type bias and will live as saprophytes on the plant surface. Under nutrient limitations an intratetrad mating event can rescue the entry into the pathogenic cycle. Mating in here happens between to cells of the promycelium and lead to filamentous growth. Figure modified from (Zuo et al., 2019)

This leads to the activation of an HMG transcription factor named Prf1, which causes a higher expression of *a* and *b* mating type genes and by this generates a positive feedback loop to promote the mating between compatible partners and to initiate the formation of conjugation tubes by stimulating the MAPK cascade (Kaffarnik et al., 2003). The *b*-locus instead acts as a multiallelic recognition function. For this, the two transcription factor domains, *b*East (*bE*) and *b*West (*bW*), need to be expressed from different alleles to form a heterodimer after mating (Kämper et al., 1995). The active *b*-heterodimer controls the expression of genes involved in pathogenicity, like *clampless1* (*clp1*) which encodes for a protein important for in planta proliferation. *Clp1* mutants will still penetrate the plant cuticle but stop prior the first mitotic division and will not form clamp-like structures important for nuclei distribution (Scherer et al., 2006). Another gene controlled by the *bE/bW* heterodimer is *regulator of b-filament* (*rbf1*), encoding for a zincfinger transcription factor important for pathogenic development. It is a master regulator controlling for example appressoria formation and plant penetration via the transcription factor Biz1 and the MAPK Kpp6 or the G2 cell cycle arrest via the transcription factors Biz1 and Hdp1 (Heimel et al., 2010). The two mating loci are either located on different chromosomes, or on one chromosome linked to each other, resulting in a tetrapolar or bipolar mating type system, respectively (Bakkeren et al., 2008). After mating of two compatible cells, the resulting dikaryotic filament can form a hyphal tip swelling, the appressorium (Figure 4A), which initiates penetration of the host plant and subsequent intracellular growth. Most smut fungi, like *Ustilago hordei* or *Sporisorium reilianum* will spread systemically, largely without symptoms through their host's vascular system, to reach the plant inflorescence. In here they replace flowers by producing sori, filled with black teliospores.

Infections with some smut fungi like *Ustilago maydis* or *Melanopsichium pennsylvanicum* can lead to the formation of local tumors. The maize smut fungus *U. maydis* can directly penetrate the leaf, where it grows to the bundle sheath cells. Here, it initiates the reprogramming of bundle sheath cells into hypertrophic tumor cells, while mesophyll cells are formed into hypertrophic mesophyll tumor cells (Figure 4A; (Matei et al., 2018)). Afterwards *U. maydis* proliferates in apoplastic cavities, where the hyphae undergo fragmentation and start to form teliospores (Christensen, 1963; Martínez-Espinoza et al., 2002). The lifecycle starts again with release of teliospores from the host plant, which will germinate and give rise to a four-celled basidium with haploid basidiospores.

1.3.2 Special features of anamorphic Ustilaginomycete strains

In addition to the pathogenic smuts, Ustilaginomycetes that were found exclusively as haploid, anamorphic yeasts, were named *Pseudozyma* species (Boekhout, 1995). These species are found as epiphytic colonizers in a wide range of habitats. This phenomenon often occurs when a mating type bias is present. In here only one mating type is viable after teliospore germination (Figure 4B; (Hood & Antonovics, 2000)). Under high nutrient conditions, sporidia of one mating type are going to live as saprophytes on the plant surface and cannot undergo mating until finding a non-biased mating partner. Due to this sexual recombination is an event that only occurs infrequently and haploid sporidia need to be highly competitive to survive without mating and a pathogenic stage (Figure 4B; (Kruse et al., 2017)). Under low nutrient conditions the mating type bias can be bypassed by an intratetrad mating event. In here two cells of the promycelium mate with each other by forming a cytoplasmic bridge, to start the formation of infectious hyphae and to enter the pathogenic stage again (Figure 4B; (Hood & Antonovics, 2000)).

Further phylogenetic reconstructions (Begerow et al., 2000; Begerow et al., 2006; Wang et al., 2015; Kruse et al., 2017) showed that four *Pseudozyma* species, namely *P. antarctica*, *P. aphidis*, *P. parantarctica* and *P. rugulosa*, form a monophyletic group together with the smut pathogen of millet *Moesziomyces bullatus*. Based on this finding all strains had been renamed to *Moesziomyces* and can be divided into four subgroups: *M. bullatus*, *M. antarcticus*, *M. paraantarcticus* and *M. penicillariae* (Figure 5). Species formerly classified as *Pseudozyma* have been mainly studied for their biodegradative abilities (Middelhoven, 1997), or their activity against industrially and medically important yeasts like *Candida* spp. or *Yarrowia* spp. (Buzzini & Martini, 2000). Some anamorphic species became of great interest for biotechnological processes. *P. brasiliensis* for example serves as a producer of xylanases in bioethanol production (Kaupert Neto et al., 2016), while *M. antarcticus* has been utilized for the production of glycolipid biosurfactants like mannosylerythritol lipids (MEL) (Konishi et al., 2007). Those are extracellular amphiphilic compounds, which consist of mannose and erythritol as hydrophilic moieties and fatty acids and acetyl groups as hydrophobic moieties. Compared to synthetic surfactants they have a higher biodegradability, low toxicity, and excellent surface-activity, what made them attractive for several industrial applications. Until now four different MELs are known, referred to as MEL-A, MEL-B, MEL-C and MEL-D. In addition to its industrial function MEL-A and -B are also known to have strong antimicrobial activity against gram⁺ bacteria and weak activity against gram⁻ bacteria (Arutchelvi et al., 2008).

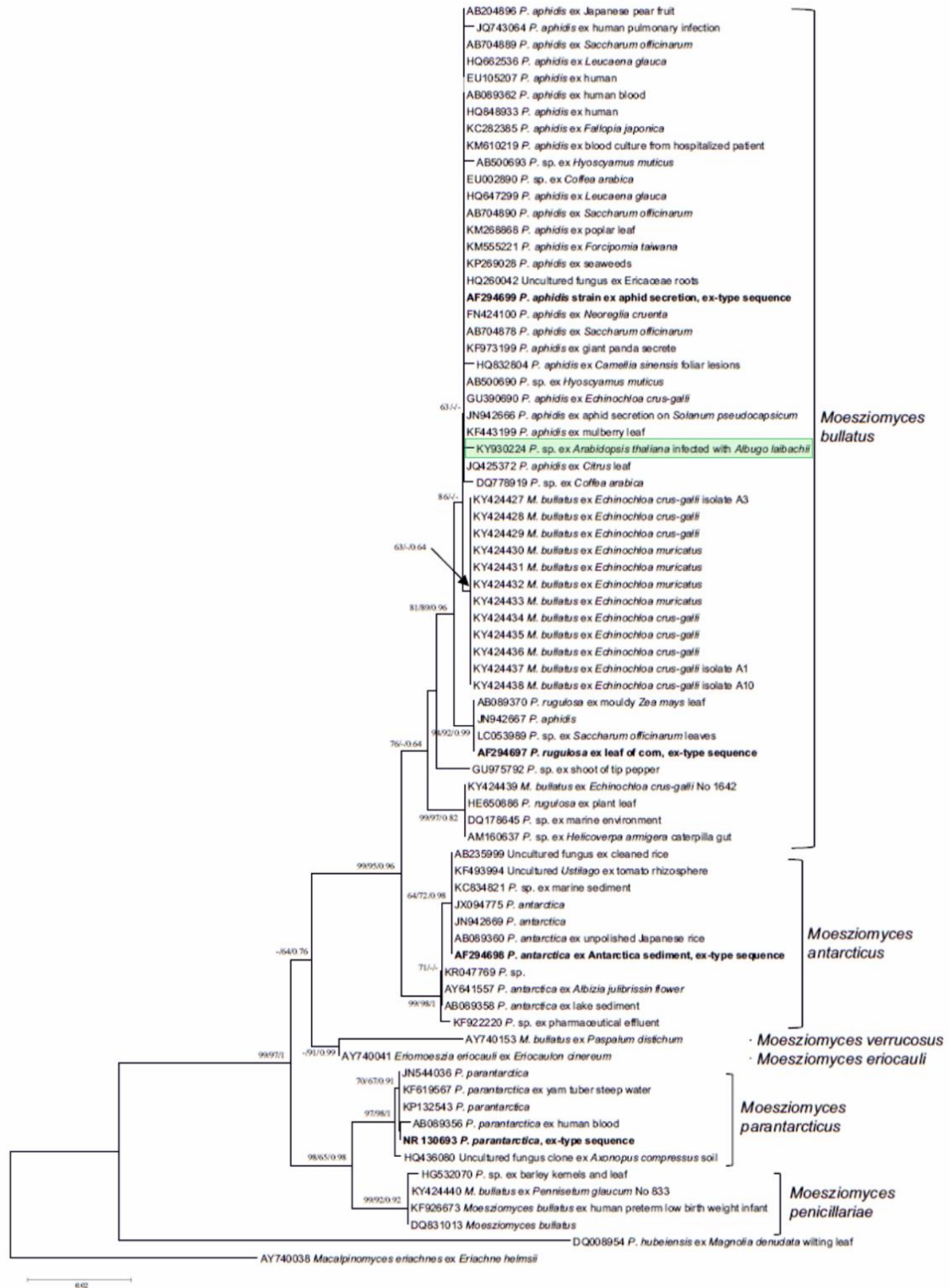


Figure 5: Phylogenetic tree of *Moesziomyces* spp. nrITS sequences based on Minimum Evolution analyses. The tree is rooted with the species *Macalpinomyces eriachnes* and the numbers on branches denote bootstrap support in Minimum Evolution, Maximum Likelihood and a posteriori probability from Bayesian Analyses (Values below 55 % are not shown). GenBank numbers precede taxon names and are followed by the name of the host or isolation source of the fungus. modified from (Kruse et al., 2017)

In the last decade, *Pseudozyma* species are more and more studied because of their potential as microbial antagonists (Avis & Bélanger, 2002). *P. flocculosa*, now renamed to *Anthracoystis flocculosa* (Piątek et al., 2015), was extensively studied for its potential as a bio-fungicide against powdery mildews (Bélanger et al., 2012). Its direct antibiotic properties based on the secondary metabolite “Flocculosin” have been studied for its mode of action in antibiosis. Recently it could be shown in a tripartite system of *A. flocculosa*, *Blumeria graminis* f. sp. *hordei* and *Hordeum vulgare*, that Flocculosin only plays a minor role in antagonism against powdery mildew.

Instead, fungal antagonism has been explained by the newly observed phenomenon of hyperbiotrophy (Laur et al., 2018), which is a special type of biotrophic mycoparasitism. *A. flocculosa* exploits nutrients from the plant which had been harvested before by the phytopathogen. Proteins involved in this process still need to be identified, but it becomes obvious that biocontrol activity of anamorphic Ustilaginomycetes is a complex trait, which is mainly directed by secreted molecules or proteins that have a function as antibiotics, effectors, elicitors or degrading enzymes (Srivastava et al., 2021). *M. bullatus* (formerly named *P. aphidis*) for example can induce a SA-independent resistance pathway by secreting extracellular metabolites that activate *PR1a*-expression in tomato plants. By this it triggers an induced-resistance response in *A. thaliana* against the bacterial pathogen *Clavibacter michiganensis* or the fungal pathogen *Botrytis cinerea* (Buxdorf et al., 2013; Barda et al., 2015; Gafni et al., 2015). In addition, *M. bullatus* was found to directly secrete molecules of yet unknown nature, that can activate ROS production and programmed cell death in *B. cinerea* hyphal cells (Calderón et al., 2019).

1.4 Aim of this study

Basidiomycete yeasts are proposed to be important members of the *A. thaliana* phyllosphere. They possess the ability to regulate growth of the oomycete pathogen *A. laibachii*, the major microbial hub in the *Arabidopsis* phyllosphere. By using the antagonistic yeast *M. bullatus ex Albugo* (*Mba*) as a model, this project aimed to identify the molecular mechanisms of basidiomycete antagonism in the *A. thaliana* phyllosphere. To test this hypothesis three main objectives should be achieved:

1. A high-quality genome sequence of *Mba* should be generated, and standard molecular techniques should be established. This will allow the generation of marker strains as well as deletion and over-expression mutants.
2. An RNA-sequencing experiment of *Mba* during interkingdom interactions should help to identify secondary metabolite clusters or secretory proteins which are upregulated in microbe-microbe interactions and important for its antagonistic mechanisms.
3. Candidate genes identified before should be tested in a reverse genetic approach which aims to validate crucial factors that determine antagonism of *Mba* against the oomycete *A. laibachii* and how this can be used to shape complex phyllosphere microbial communities

To understand these interactions on the molecular level and to study potential effector proteins in microbe – microbe interactions is important to transfer basic research to agricultural relevant systems. It will help to develop stable synthetic communities that can increase plant fitness and to understand the interactions of pathogens with their community.

2 Results

2.1 Morphology of *Mba*

Based on the phylogeny made by Kruse et al. (2017) the isolated *Pseudozyma* strain from *A. laibachii* infected *A. thaliana* leaves groups together with the millet pathogen *M. bullatus* (Figure 5 – highlighted). Its teleomorph was first described by Vánky (1977) and is known to produce sori in the ovaries of the barnyard grass (*Echinochloa crus-galli* (L.) P. Beauv.). However, several non-pathogenic forms are isolated from plants throughout the world, and some were even found in clinical samples. On PD-agar plates the yeast cells of *Mba* are beige colored and have a creamy texture (Figure 6A). When examined under the microscope differences to the model smut pathogen *U. maydis* are obvious.

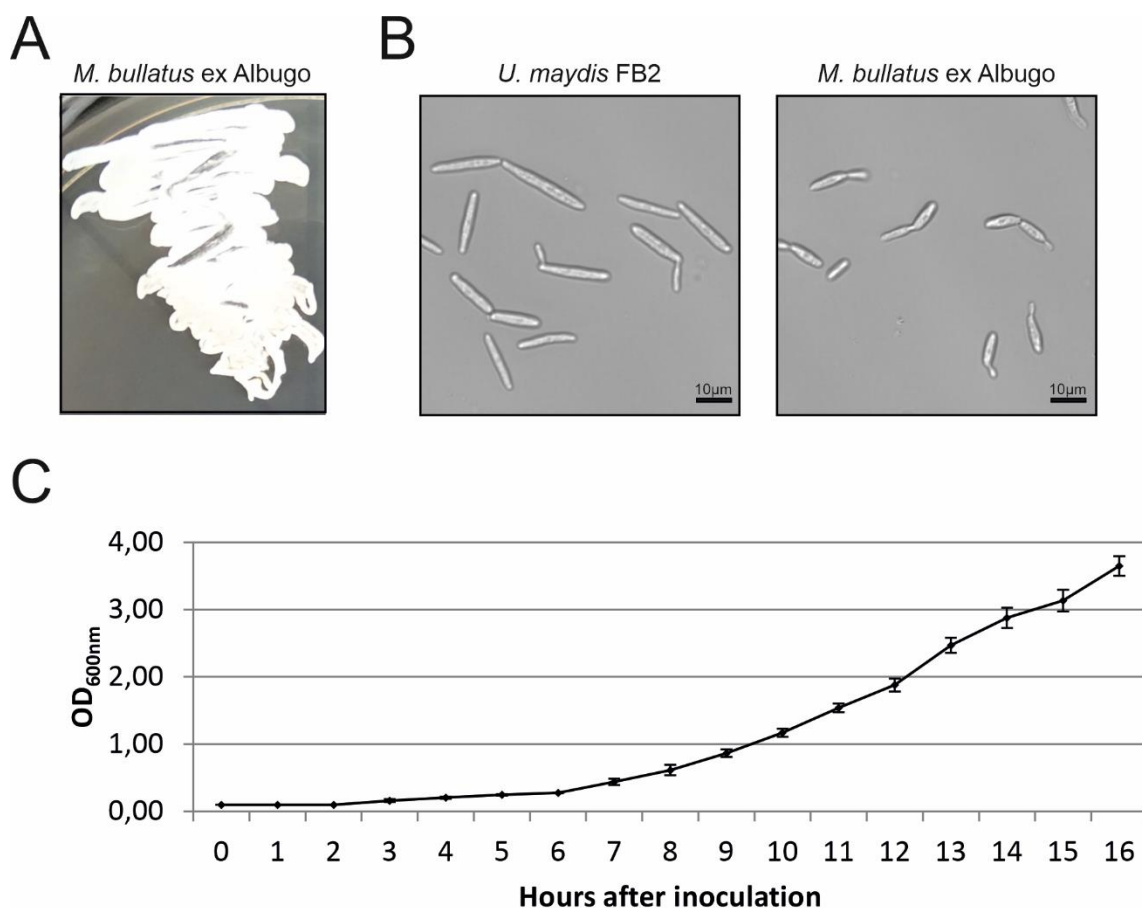


Figure 6: Growth aspects of *Mba*. On solid PD-agar media *Mba* colonies are beige colored and have a creamy appearance (**A**). Microscopically, *Mba* cells are smaller than *U. maydis* FB2 cells and have a more roundish shape (**B**). Growth of *Mba* in liquid YEPSL media at 22 °C leads to a doubling time of around 3 h. Experiments were performed in 3 biological replicates and error bars indicate standard error (**C**).

2. Results

Cells of *Mba* have a size around 10 μm and a more roundish shape, while cells of the haploid *U. maydis* strain FB2 are bigger than 10 μm and have an elongated, cigar-like shape (Figure 6B). As growth conditions at 28 $^{\circ}\text{C}$, like it is usual for *U. maydis*, led to microscopically stressed cells, *Mba* growth temperature was lowered to 22 $^{\circ}\text{C}$. By measuring the optical density of a *Mba* culture in liquid YEPSL media at 22 $^{\circ}\text{C}$ over 16 hours, a doubling time of around 3 h during exponential phase was calculated (Figure 6C).

To gain more information on *Mba*'s morphology, cell growth was examined microscopically on parafilm, which was used as an artificial leaf surface and on *A. thaliana* leaves. On parafilm, *Mba* can be found in three different morphological forms. First, most of the cells were found as yeast-like sporidia (Figure A), what is the typical growth of those haploid cells and comparable to their growth in liquid cultures. Second, cells can be found as pseudohyphae, which are mainly haploid cells not separated from each other after cell division (Figure 7A).

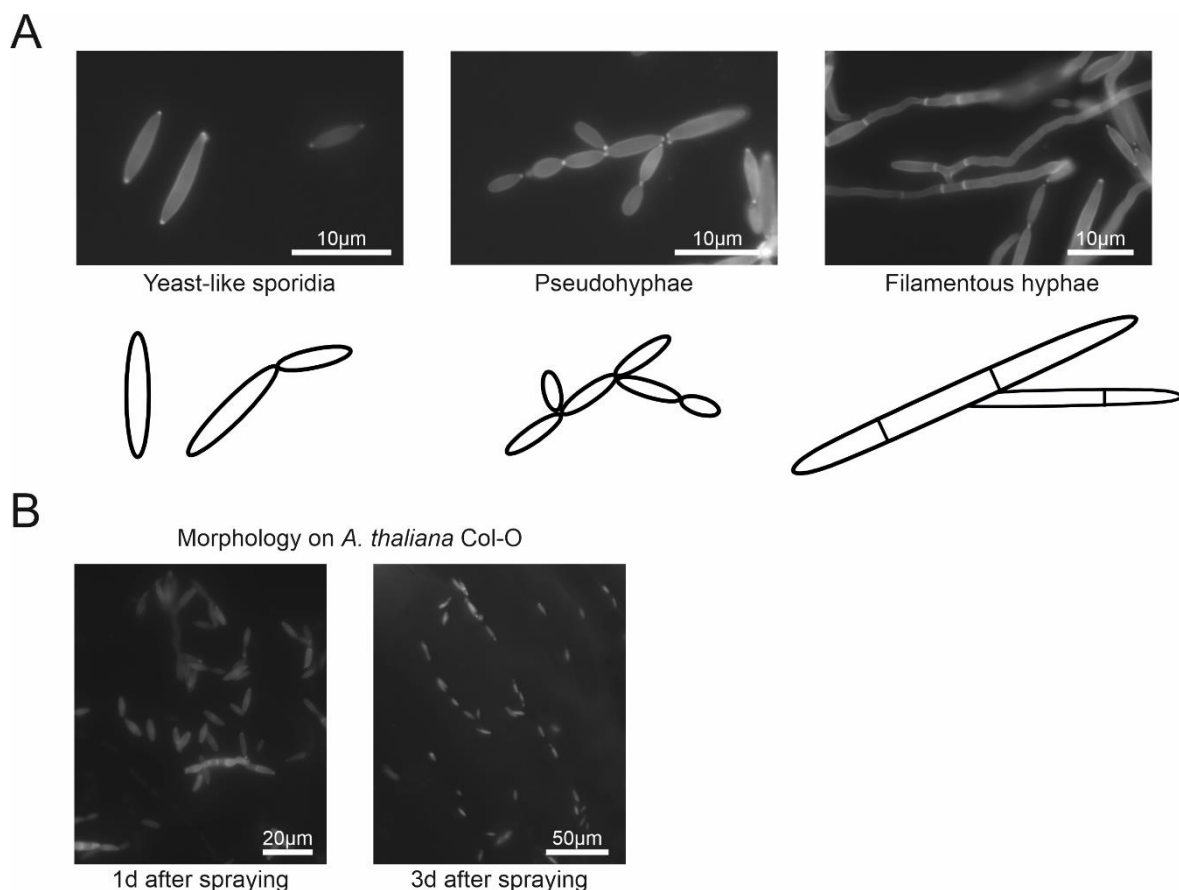


Figure 7: Morphology of *Mba* on parafilm and *A. thaliana*. Typical forms of *Mba* seen on parafilm are yeast-like sporidia, pseudo hyphae and filamentous hyphae (**A**). On the *A. thaliana* leaf surface, *Mba* appears mainly as yeast-like sporidia and can be found in aggregated forms (**B**). In all pictures cells have been stained with Calcofluor White.

Last some filamentous hyphae could be found, but only at spots with high cell density due to drop spraying (Figure 7**Figure A**). On the *A. thaliana* leaf surface, which is *Mba*'s natural habitat, fungal cells can be mainly found as Yeast-like sporidia. Interestingly, after three days of incubation they were often found in aggregates at the depressions which are formed at the junctions of epidermal cells or along the veins (Figure 7**Figure B**).

As *Mba* was identified by Agler et al. (2016) to have a significant effect on bacterial diversity in the *Arabidopsis* phyllosphere, its interaction with 30 bacterial strains from 17 different species of a bacterial SynCom (Table 6) of *Arabidopsis* leaves was tested in one-to-one plate assays. In this experiment seven strains inhibited by *Mba*, as indicated by halo formation after 7 days of co-cultivation, could be identified (Figure 8A). This halo formation is independent from bacterial cell wall composition, as *Pseudomonas* and *Xanthomonas* are classified as gram⁺-bacteria, while *Arthrobacter*, *Bacillus*, *Brochotrix* and *Rhodococcus* are gram⁻-bacteria. Interestingly, this bacterial inhibitory effect could not be seen in interactions with the phytopathogenic fungus *U. maydis*. This indicates a species-specific inhibition of the bacteria by *Mba*. Nevertheless, the primary hub microbe in the *Arabidopsis* phyllosphere is the pathogenic oomycete *A. laibachii* (Agler et al., 2016). As *Mba* was found to be directly associated with *Albugo* spore propagation, it was tested if both species interfere with each other. For this a gnotobiotic plate assay was performed (chapter 4.7.3) and *A. laibachii* infection symptoms on *Arabidopsis* were quantified. In control experiments, in which *A. laibachii* spores were sprayed alone on *Arabidopsis* leaves, about 33 % of the leaves showed infection symptoms at 14 dpi (Figure 8B). A significant reduction of *A. laibachii* infection by about 50 % could be observed when the bacterial SynCom was pre-inoculated on the leaves two days before *A. laibachii* spray inoculation (Figure 8**Figure B**). However, in case of *Mba* pre-inoculation together with the bacterial SynCom, *A. laibachii* infection was almost completely blocked (Figure 8**Figure B**). Similarly, the pre-inoculation of only *Mba* without the bacterial SynCom resulted in an almost complete loss of *A. laibachii* spore production (Figure 8B). In contrast to the prior experiment, this interaction is not species-specific as spray inoculation with *U. maydis* leads to the same inhibitory effect, although spore production is not completely abolished (Figure 8B). Both experiments demonstrate a strong antagonistic activity of *Mba* towards *A. laibachii* and SynCom bacteria, which results in efficient biocontrol of pathogen infection. To enable a molecular understanding of how *Mba* acts on the members of the *Arabidopsis* phyllosphere community, it was necessary to sequence its genome and to establish molecular tools, including a protocol for stable genomic transformation. This will enable the implementation of functional genomics approaches to determine proteins involved in multitrophic plant-microbe-microbe interactions.

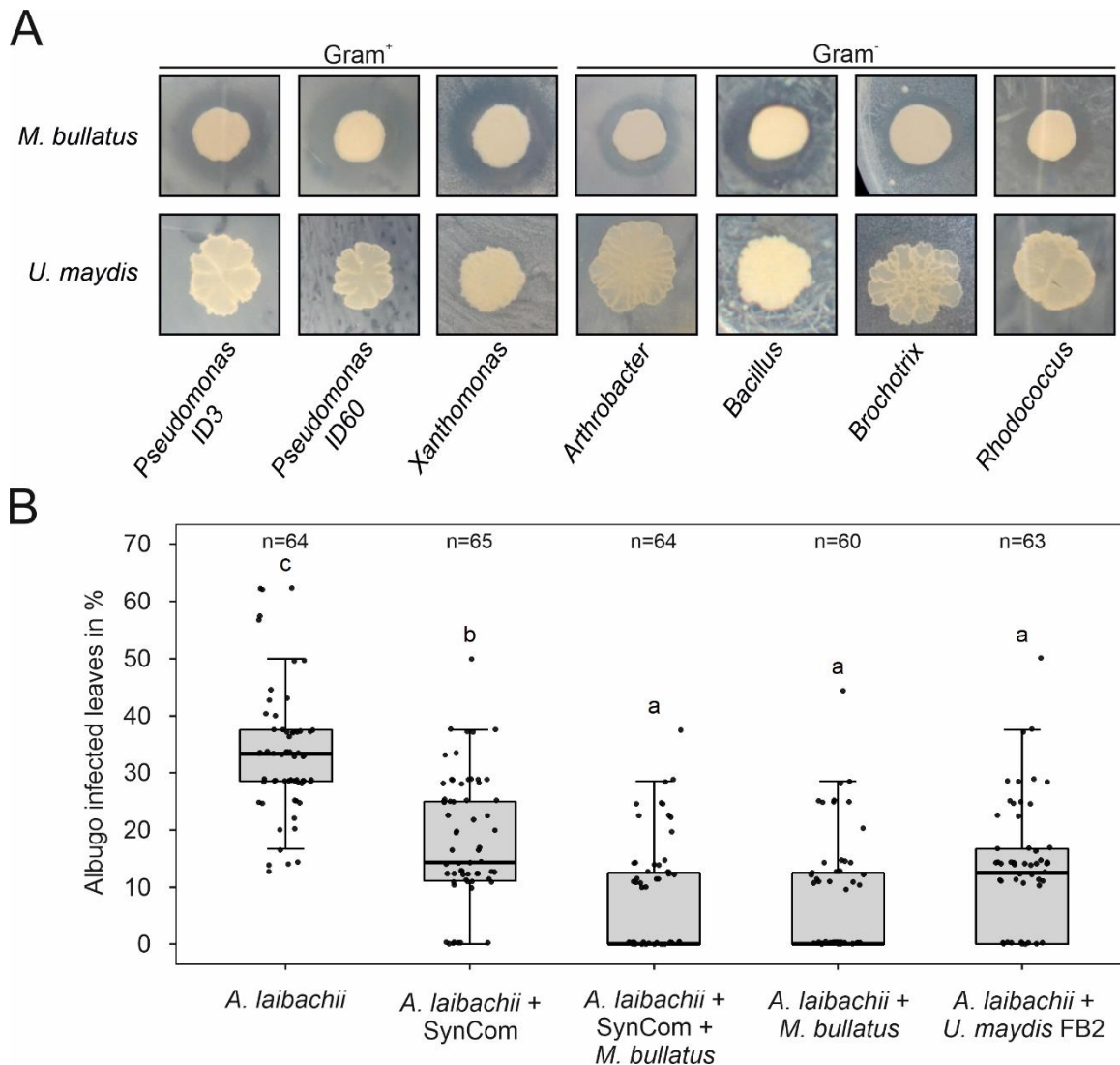


Figure 8: Antagonistic activity of *Mba* against bacteria and *A. laibachii*. One-to-one interaction assays on PD-Agar plates show a high antagonistic potential of *Mba* against seven members of a bacterial SynCom (**A**). This effect cannot be seen in interactions with *U. maydis*. In addition, a strong antagonism can also be seen in interactions of *Mba* with the oomycete pathogen *A. laibachii* (**B**). While already the addition of a bacterial SynCom prior to *A. laibachii* infection reduces the infection symptoms scored at 14dpi, spraying of *Mba* almost completely blocks spore production of *A. laibachii*. This antagonism is independent from the presence of the bacterial community. *U. maydis* is also able to block *A. laibachii* infection symptoms, but not as strong as *Mba*. Infections were performed in six individual replicates with 12 technical replicates. N indicates the number of infected plants that were scored for symptoms. An analysis of variance (ANOVA) model was used for pairwise comparison of the conditions, with Tukey's HSD test to determine differences among them. Different letters indicate significant differences (P values < 0.05).

2.2 The genome of *Mba*

The genome of *Mba* was sequenced by using Single Molecule Real-Time sequencing (Pacific Biosciences, Menlo Park, CA), which lead to 69674 mapped reads with an accuracy of 87.3 % and 8596 bp sub-read length. The achieved sequences were assembled by using the HGAP-pipeline (Pacific Biosciences) which resulted in 31 Contigs with a N₅₀Contig Length of 705 kb (Table 1). The total length of all contigs resulted in a predicted genome

size of 18.3 Mb, which is a bit smaller compared to the *U. maydis* genome size of 19.7 Mb ((Dutheil et al., 2016); Table 1). The predicted *Mba* genome has a relatively high GC-content of 60.9 %, with an even higher GC-content (62.8 %) in its coding sequences. Compared to other pathogenic smut fungi, only *S. reilianum* has similar GC-contents, while all others show values around 53 % (55 % in coding regions). Even higher GC-contents can be found only in the genome of the anamorphic fungus *A. flocculosa* (Table 1). Gene prediction with Augustus identified 6653 protein coding genes with an average gene size of 1935 bp. The high number of coding genes in combination with its small genome size results in a compact genome structure with 69.5 % of the DNA-sequences being coding sequences and only small intergenic regions of around 769 bp (Table 1). This is comparable to other pathogenic smut fungi such as *U. maydis* and *U. hordei*. In contrast to those, *Mba* exhibits a significantly higher rate of introns (9333 introns) what was only observed in the other anamorphic and nonpathogenic yeast, *A. flocculosa* (Table 1).

Table 1: Comparison of genomes and genomic features of known pathogenic and anamorphic Ustilaginomycetes.¹(Rabe et al., 2016), ²(Dutheil et al., 2016), ³(Schirawski et al., 2010), ⁴(Kämper et al., 2006), ⁵(Laurie et al., 2012), ⁶(Sharma et al., 2014), ⁷(Lefebvre et al., 2013)

	<i>M. bullatus</i>	<i>U. bromivora</i> ¹	<i>S. scitamineum</i> ²	<i>S. reilianum</i> ³	<i>U. maydis</i> ⁴	<i>U. hordei</i> ⁵	<i>M. pennsylvanicum</i> ⁶	<i>A. flocculosa</i> ⁷
Assembly statistics								
Total contig length (Mb)	18.3		19.5	18.2	19.7	20.7	19.2	23.2
Total scaffold length (Mb)		20.5	19.6	18.4	19.8	21.15	19.2	23.3
Average base coverage	50x	154x	30x	20x	10x	25x	339x	28x
N50 contig (kb)	705.1		37.6	50.3	127.4	48.7	43.4	38.6
N50 scaffold length (kb)		877	759.2	738.5	817.8	307.7	121.7	919.9
Chromosomes	21	23		23	23	23		
GC-content (%)	60.9	52.4	54.4	59.7	54	52	50.9	65.1
Coding (%)	62.8	54.4	57.8	62.6	56.3	54.3	54	66.3
Coding Sequence								
Percentage CDS (%)	69.5	59.8	62	65.9	61.1	57.5	56.6	54.3
Average gene size (bp)	1935	1699	1819	1858	1836	1708	1734	2097
Average gene density (gene/kb)	0.36	0.35	0.34	0.37	0.34	0.34	0.33	0.30
Protein-coding genes	6653	7233	6693	6648	6786	7113	6279	6877
Exons	11645	11154	10214	9776	9783	10907	9278	19318
Average exon size (bp)	1091	1101	1191	1221	1230	1107	527	658
Exons/gene	1.75	1.5	1.5	1.47	1.44	1.53	1.48	2.8
tRNA genes	150	133	116	96	111	110	126	176
Noncoding sequence								
Introns	9333	3921	3521	3103	2997	3161	2999	12427
Introns/gene	1.40	0.54	0.53	0.47	0.44	0.44	0.48	1.81
Average intron length (base)	163	163	130.1	144	142	141	191.4	141
Average intergenic distance (bp)	769	1054	1114	929	1127	1186	1328	1273
Secretome								
Protein with signal peptide	559		622	632	625	538	419	622
Secreted without TMD	380				467			737
- with known domain	260				264			554

2. Results

Out of its 6653 protein coding genes, 559 are potentially secreted proteins as a signal peptide was predicted by SignalP (Petersen et al., 2011). From those, 380 are expected to be secreted extracellularly, what means they do not carry a predicted transmembrane-domain or cell-wall anchors (Table 1; (Krogh et al., 2001)).

According to the classifications made by Zhao et al. (2013) 40 plant cell wall degrading enzymes (PCWDE) could be identified in *Mba* (Figure 9; Table 15). Compared to other Ustilaginomycetes, *Mba* possesses a higher number of enzymes degrading hemicellulose (H) and pectin (P), with the biggest differences in enzymes carrying the GH terms 36, 39, 43 or 88 (Table 15). Other main categories like fungal cell wall degrading enzymes (FCWDE) or enzymes involved in energy storage are nearly similar in all compared species (Figure 9). Enzymes involved in the cleavage of bacterial peptidoglycan (BPG), or bacterial extracellular polysaccharides (BEPS) are present in all species except of the anamorphic fungus *A. flocculosa* (Figure 9; Table 15).

In the following the *Mba* genome structure was compared to the *U. maydis* genome, a manually annotated high-quality reference genome for smut fungi (Kämper et al., 2006). Out of the 31 assembled *Mba* contigs, 21 have telomeric repeat structures at both ends and can be mapped to chromosomes of *U. maydis* (Table 1; Figure 10A). By comparing the genome to the *U. maydis* genome structure, two major recombination events could be found in the genome of *Mba* (Figure 10B). The *Moesziomyces* contig 2, contains parts of three different *U. maydis* chromosomes, namely chromosome 2, 5 & 20.

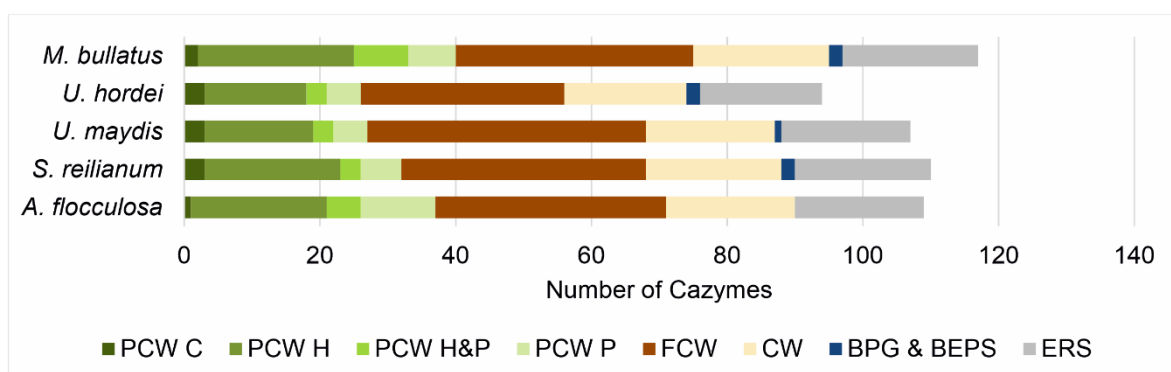


Figure 9: Comparative analysis of Cazymes in pathogenic and anamorphic Ustilaginomycetes. Cazymes are grouped based on their most common substrate (Zhao et al., 2013). PCW C: Plant cell wall - Cellulose; PCW H: Plant cell wall – Hemicellulose; PCW H&P: Plant cell wall – Hemicellulose & Pectin; PCW P: Plant cell wall – Pectin; FCW: Fungal cell wall; CW: Cell wall; BPG: Bacterial peptidoglycan; BEPS: Bacterial exopolysaccharides; ESR, energy storage and recovery.

Interestingly on this chromosome also homologs to pathogenic loci like the *U. maydis* virulence cluster 2A can be found (Figure 22; (Kämper et al., 2006)). Even more chromosomal crossover of *Mba* contig 2 and Contig 6 changes also the genomic context of genes encoding for essential virulence factors in *U. maydis* (*stp1* & *pit1/2*), as well as the A-mating type locus, which is important for pheromone perception and recognition of mating partners (Figure 10A&B; (Bölker et al., 1992; Doehlemann et al., 2011)). A second recombination event can be found on contig 8 and was also found in the genome of the maize head smut *S. reilianum*.

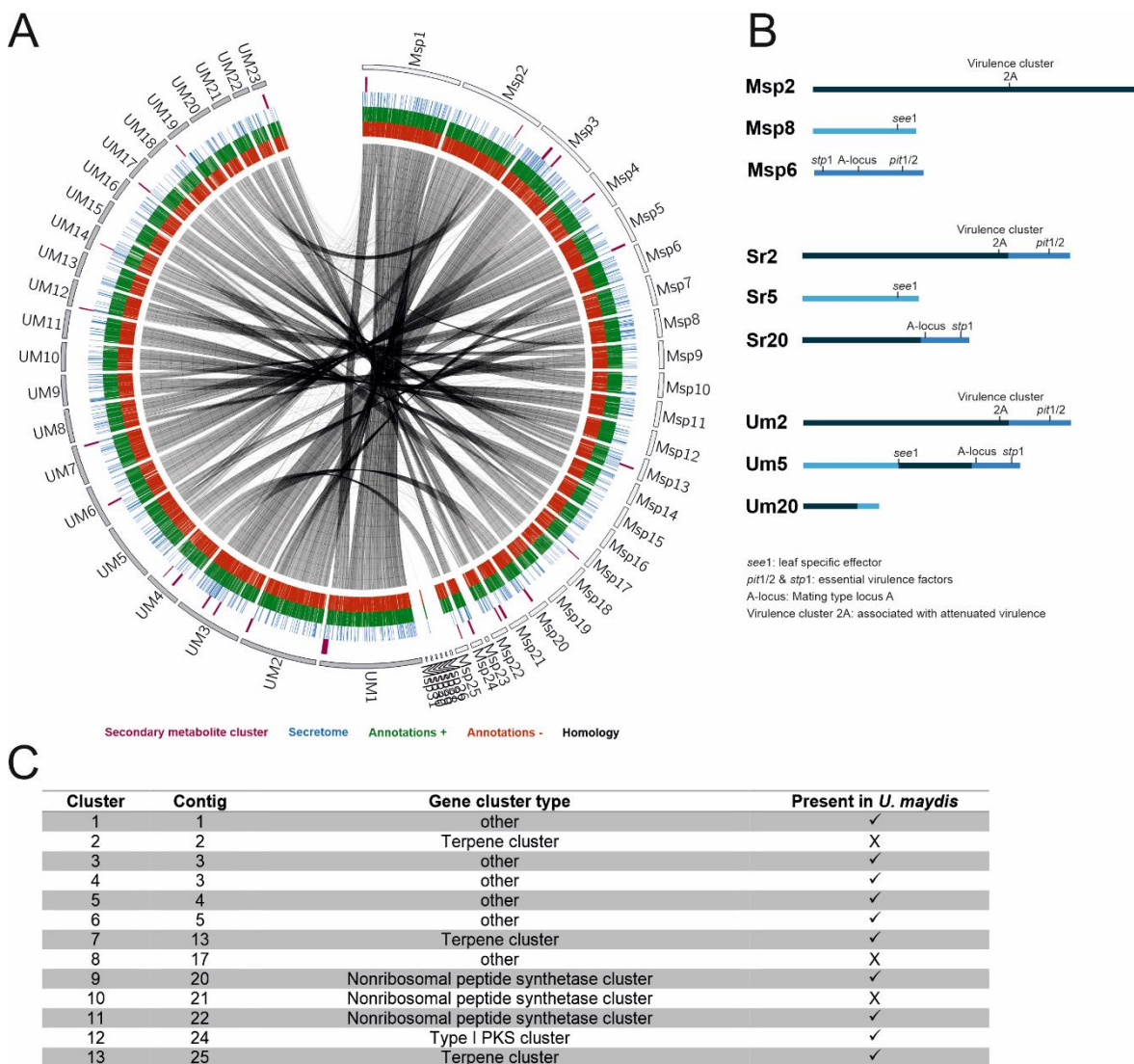


Figure 10: Chromosomal structure and secondary metabolite clusters of *Mba*. Synteny of *U. maydis* and *Mba* genomes visualized by Circos plot identified three major chromosomal rearrangements (**A**). In addition, potential secondary metabolite clusters, secreted proteins, and gene predictions on both strands (\pm) are highlighted. More detailed visualization of those chromosomal breaks showed that mainly regions important for virulence or mating are located close to the breakages (**B**). By comparing predicted *M. bullatus* secondary metabolite clusters to known clusters in *U. maydis*, three unique *Mba* secondary metabolite clusters were identified, which can have a function in its antagonistic behavior (**C**).

2. Results

The *S. reilianum* chromosomes 5 and 20 recombined in the promoter region of the *see1* gene, which is a leaf-specific effector protein and required for leaf tumor formation in *U. maydis* (Figure 10A&B; (Redkar et al., 2015)). To proof correctness of those recombination events, the genomic structure of *Mba* was compared to the best available genome sequence of a closely related species, *M. antarcticus* T-34 (Figure 23). In here all three contigs show a high synteny to the reference genome, which supports the correctness of the *Mba* genome assembly.

Because of its strong antagonistic activity against bacteria the genome of *Mba* was screened for the presence of secondary metabolite gene clusters by using AntiSMASH (Blin et al., 2017). By this, 13 potential clusters could be predicted, of which three can be assigned to terpene synthesis, three contain nonribosomal peptide synthetases and one cluster has a polyketide synthase backbone gene (Figure 10C). Unexpectedly, the ustilagic acid secondary metabolite cluster, which is known to be involved in the production of an antimicrobial metabolite, is completely absent in *Mba* (Figure 24A, (Teichmann et al., 2007)). On the contrary, three *Mba* specific metabolite clusters were identified, which could potentially be involved in the antagonistic activity of *Mba* against bacteria (Figure 24B).

Lefebvre et al. (2013) already concluded by genome comparison that the anamorphic yeast *A. flocculosa* had lost most of its effector genes, what reflects the absence of a pathogenic stage in this organism (Lefebvre et al., 2013). In contrast, *Mba* contains 1:1 homologs of several known effectors with a known virulence function in *U. maydis* (Table 2), for example Pep1, the core virulence effector of *U. maydis* (Doehlemann et al., 2009).

Table 2: *Mba* proteins homologous to *U. maydis* effector genes with known virulence function.

Name	Homologue	Query cover	E-value	Identity (%)	Expressed in axenic culture	Expressed on <i>A. thaliana</i>	<i>U. maydis</i> knockout phenotype	Reference
g1653	UMAG_01987 (Pep1)	82%	3-e56	60.96	×	×	complete loss of tumor formation - blocked in early stages of infection	(Doehlemann et al., 2009)
g1828	UMAG_01829 (Afu1)	99%	0.0	71.57	✓	✓	organ specific effector - reduced virulence in seedling leaves	(Schilling et al., 2014)
g2626	UMAG_12197 (Cce1)	98%	2e-48	60.16	×	×	complete loss of tumor formation - blocked in early stages of infection	(Seitner et al., 2018)
g2765	UMAG_11938 (Scp2)	100%	1e-73	93.44	✓	✓	Reduced in virulence	(Krombach et al., 2018)
g2910	UMAG_02475 (Stp1)	32%	3e-42	60.71	×	×	complete loss of tumor formation - blocked in early stages of infection	(Schipper, 2009)
g3652	UMAG_02239 (See1)	43%	9e-11	54.90	×	×	organ specific effector - reduced virulence in seedling leaves	(Redkar et al., 2015)
g3113	UMAG_01375 (Pit2)	-	-	-	×	×	complete loss of tumor formation - blocked in early stages of infection	(Doehlemann et al., 2011)
g3279	UMAG_03274 (Rsp3)	10%	5e-20	70.11	×	×	strong attenuation of virulence – reduced tumor size and number	(Ma et al., 2018)
g5296	UMAG_05731 (Cmu1)	98%	3e-70	43.84	×	×	Reduced in virulence	(Djamei et al., 2011)
g6183	UMAG_06098 (Fly1)	100%	0.0	81.85	✓	✓	Reduced in virulence	(Okmen et al., 2018)
g5835	UMAG_05302 (Tin2)	87%	8e-24	37.81	×	×	Minor impact on tumor formation – reduced anthocyanin biosynthesis	(Brefort et al., 2014)

In addition Sharma et al. (2019) showed, that several former *Pseudozyma* strains, like *M. antarctica* or *Kalmanozyma brasiliensis*, possess functional homologues of the *pep1* gene. This strengthened the hypothesis that such anamorphic yeasts still have the potential to form infectious hyphae (Kruse et al., 2017).

To proof the functionality of those effector homologues, the homolog of Pep1 was identified in the genome of *Mba*. The gene *Mb_1653* is located on contig 2 and encodes for a protein with 177 amino acids. Protein alignment of *Mb_1653* with Pep1 homologues showed, that like in *U. maydis* Pep1, a putative secretion signal, a conserved region with four important cysteine residues in the middle of the protein and a terminal glycine rich region could be identified (Figure 11A). To assess its functionality, *Mb_1653* was expressed in an *U. maydis* *pep1* deletion strain (SG200 Δ 01987). By this the deletion phenotype, which shows complete loss of virulence, could be fully restored. This demonstrates that *Mb_1653* encodes for a functional Pep1 effector protein (Figure 11B).

A unique feature in the genome of *U. maydis* is the presence of large effector gene clusters. They mainly arose through gene duplication and their expression depends on dikaryon formation during plant infection (Kämper et al., 2006).

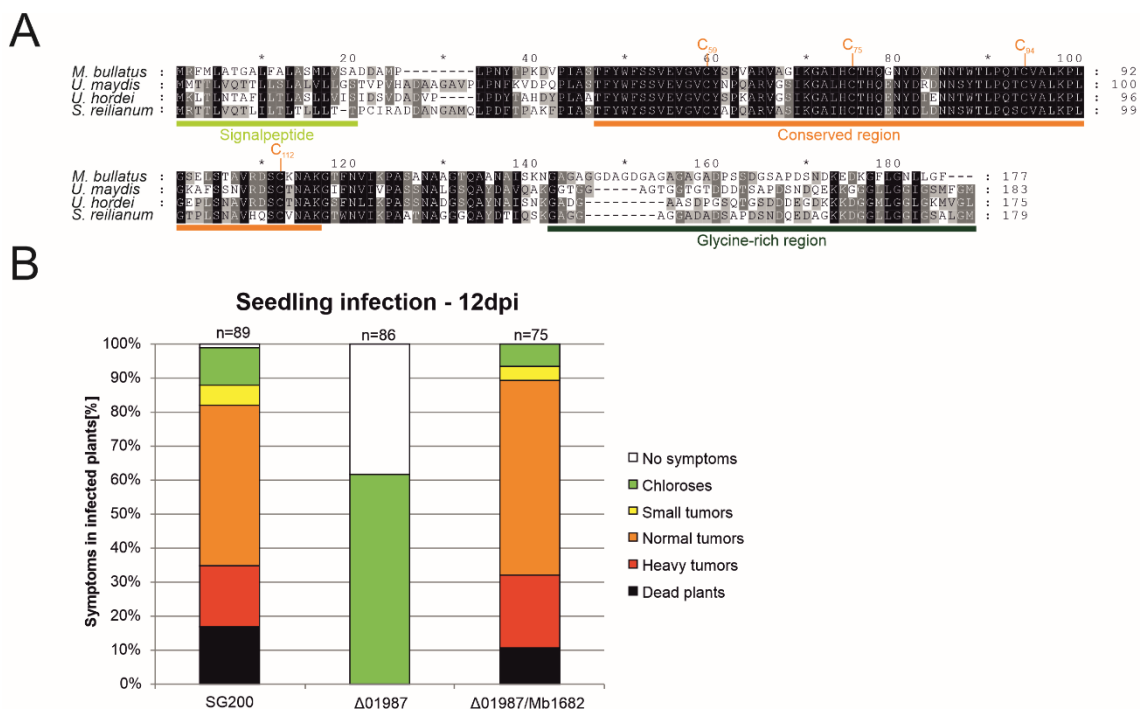


Figure 11: Function of *Mba* Pep1. Based on sequence homology, all characteristic regions of Pep1 (Signal peptide, conserved cysteine residues and a glycine-rich region) can be found in the *Mba* homologue (A). Complementation of the *U. maydis* *pep1* deletion mutant (Δ 01987) with the *Mba* homologue leads to full restoration of virulence 12 days post infection (B).

As *Mba* is a non-pathogenic fungus, potential virulence clusters in its genome were identified based on homology to already known virulence clusters in *U. maydis*. This revealed that all twelve effector clusters of *U. maydis* are present in *Mba*, but in several cases it carries only a single copy of each effector gene, which results in minimalistic versions of the *U. maydis* effector clusters (Figure 22). A suitable example for this is the biggest and most intensively studied virulence cluster of smut fungi, the effector cluster 19A (Schirawski et al., 2010; Brefort et al., 2014; Dutheil et al., 2016). In *Mba*, only five out of the 24 effector genes present in *U. maydis* are conserved in this cluster (Figure 12). Interestingly, some anamorphic yeasts like *K. brasiliensis* and *A. flocculosa* completely lost some virulence clusters, while another non-pathogenic member of the Ustilaginales, *Kalmanozyma hubeiensis*, shows an almost complete set of effectors when compared to *U. maydis* (Figure 12).

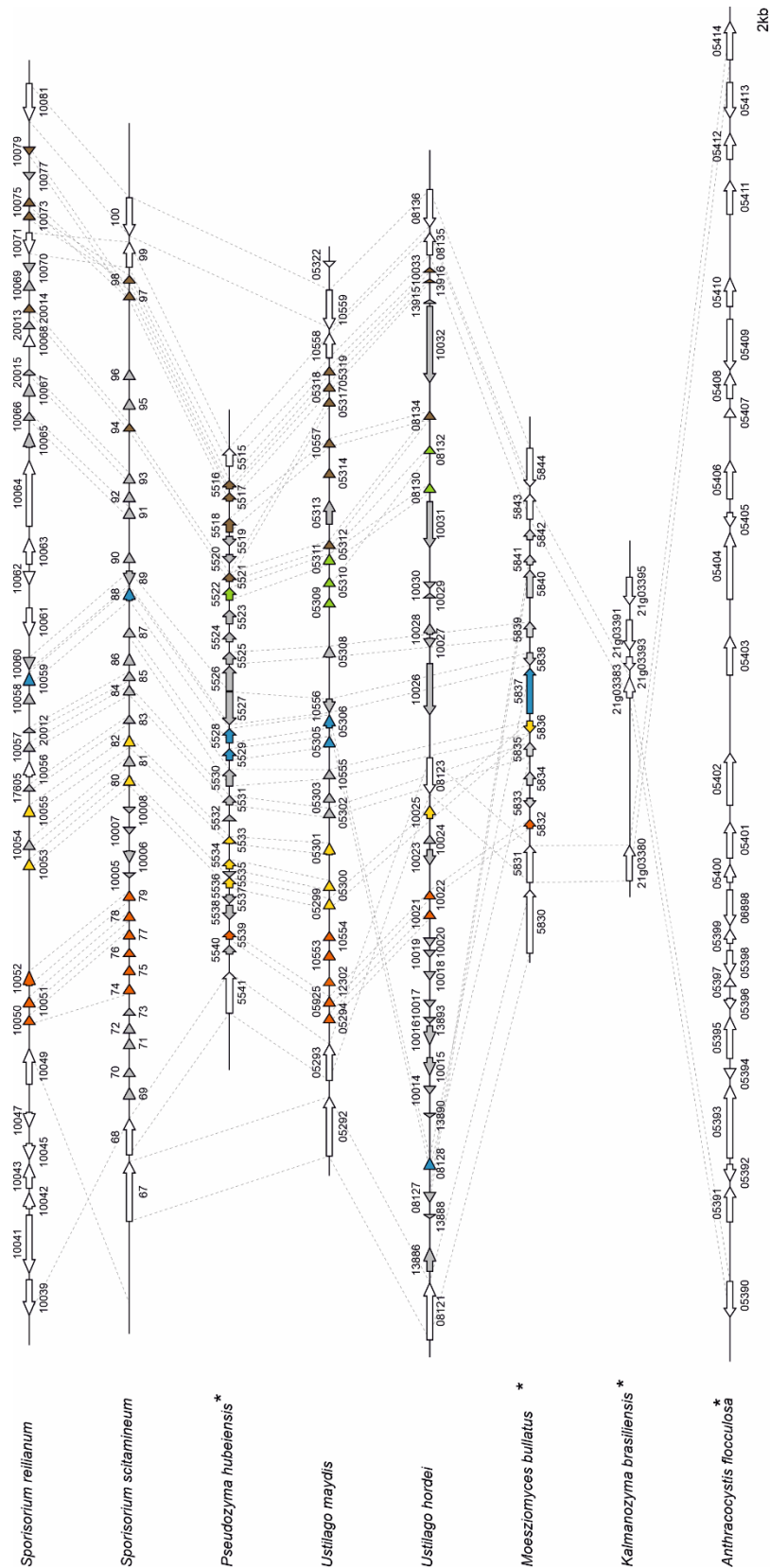


Figure 12: Comparison of the largest virulence cluster (Cluster 19A) in different pathogenic and anamorphic (marked with*) Ustilaginomycetes. Arrows indicate open reading frames (ORFs) and are labeled by the respective gene numbers. Related gene families are indicated in different colors, while unique effector genes are shown in grey. White arrows indicate genes encoding proteins without a predicted secretion signal (Brefort et al., 2014).

2.3 Generation of a transformation system for *Mba*

By sequencing the *Mba* genome the first step to establish the molecular work with this *Moesziomyces* strain was made. In the following the generation of a transformation system was needed. For this, the method of polyethylene glycol (PEG) - mediated protoplast transformation was adapted from the model fungus *U. maydis* (Figure 13A; (Bösch et al., 2016)). Prior to protoplast preparation, *Mba* cells were harvested from liquid culture by centrifugation. To guarantee the use of healthy and fit cells, cultures were harvested before reaching the exponential growth phase. The enzymatic digest of *Mba* cell walls was achieved by treating them with 2 % Glucanex[®] for 20 minutes. Afterwards linearized DNA was transferred into the protoplasts by using PEG and cell walls were regenerated by embedding the fungal culture in regeneration agar. The highest number of regenerated cells had been achieved by using sucrose as an osmotic stabilizer. Suitable selection markers tested in transformations were Hygromycin, Nourseothricin, Phleomycin and Carboxin (Table 5).

A first transformation assay of *Mba* was performed to express a cytosolic GFP reporter-gene under control of the constitutive *o2tef*-Promoter (Figure 13B). Those transformations have been performed with *U. maydis* as a positive control in parallel. Although integration was supposed to be guided via homologous recombination at the *cbx*-locus (Kojic & Holloman, 2000), a Southern-Blot analysis verified only ectopic integrations into the genome of *U. maydis* and *Mba*. Hybridization with an hygromycin probe led to signals bigger than 7,2 kb, what corresponds to the size of the linearized vector cut with *PvuII* (Figure 21 **Figure 25**). As ectopic integrations into the *Mba* genome seemed to be favored, a split-marker approach was used in the following to facilitate a side-directed transfer of DNA-fragments into the genome (Figure 13C; (Goswami, 2012)). In here two individual fragments need to recombine at the desired locus to generate antibiotic resistant strains. Strains carrying only ectopically integrated fragments do not possess a functional copy of the resistance gene and will not be viable on selection media. Additionally, as the number of available selection markers for *Mba* is limited, a selection marker recycling system (FLP/FRT system) was introduced, which allows selection marker excision (Figure 13C; (Khrunyk et al., 2010)). The resistance cassette is flanked by FRT-sites which function as recognition sites for a FLP-recombinase, which is brought into the cells on an autonomously replicating plasmid. Growth of cells on arabinose containing media will induce *flp*-expression and excision of the resistance cassette. This will allow the easy generation of multiple knockouts in *Mba*.

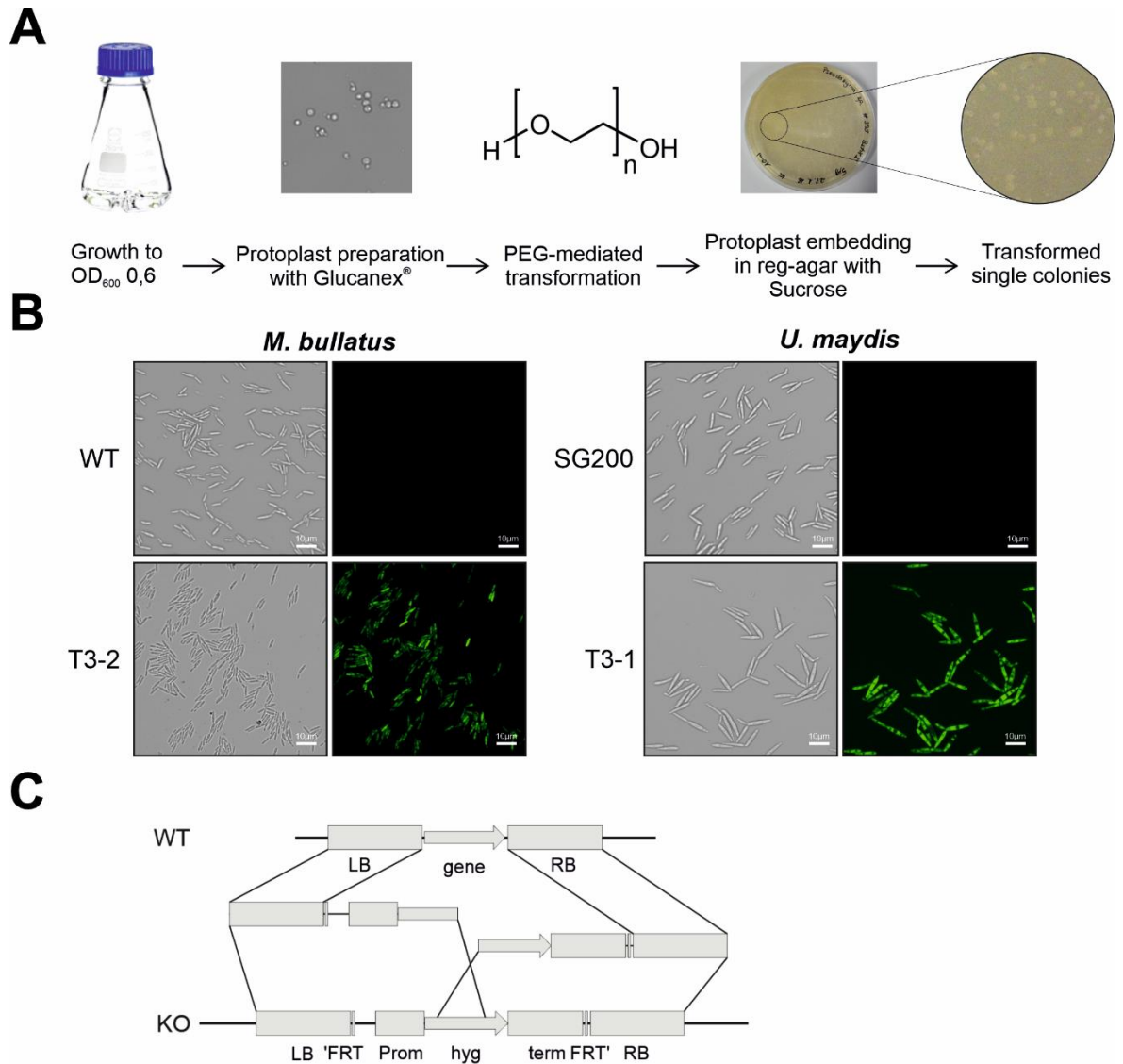


Figure 13: Transformation of *Mba*. Foreign DNA-fragments can be transferred into *Mba* cells by PEG-mediated transformation of protoplasts (**A**). A first trial of this method yielded into Hygromycin resistant *Mba* (KL14) and *U. maydis* (T3-1) transformants, showing a cytoplasmic GFP-signal after ectopic integration of linearized plasmid-DNA (**B**). Wildtype strains in comparison show no GFP-expression. To delete specific regions in the genome of *Mba* a split-marker approach was used (**C**). In here two individual fragments need to recombine at a specific locus to form a functional copy of a resistance protein. Cells, in which only one fragment integrated randomly into the genome are not viable under selection pressure. Knockout cassettes are suitable for marker recycling, as FLP-recombinases can recognize the integrated FRT-sites and by this cut the resistance marker out of the genome.

2.3.1 The Self-compatible *Mba* strain CB1

The successful establishment of molecular tools offers the possibility to study the cause of *Mba*'s anamorphic lifestyle in more detail. The mating process in Ustilaginomycetes is mainly controlled by two mating type loci. (Figure 14A; (Bakkeren et al., 2008)). Although *Mba* is phylogenetically closely related to *U. hordei*, which has a bipolar mating system, *Mba* owns a tetrapolar mating system. This situation is comparable to the mating type structure that can be found in the pathogenic smut *U. maydis* (Figure 14A). Recombination events on the *Mba* contig 6 mentioned already before, may led to a rearrangement of genes at the a-locus. In here three additional genes (g3026, g3027, g3028) can be found inside of the locus. The b-locus instead can be found on contig 1 and has a structure comparable to the *U. maydis* and *U. hordei* B-locus. Since the *Mba* genome is completely equipped with mating type genes, a screen for potential mating partners was performed, in which ten wild *Mba* strains isolated from *Echinochloa crus-galli* (A1-A10) were used to find a suitable mating partner. For this the haploid strains were grown in liquid cultures, mixed and as drops arranged on PD-plates with charcoal to visualize filament formation after mating. Figure 14B shows the mating plate with the haploid *Ustilago* strains FB1 and FB2 and the solopathogenic strain SG200 as an internal control. After mixing strains of different mating types together the growth shows the typical "fluffy" phenotype. Unfortunately for no combination of *Moesziomyces* strains a mating event could be observed (Figure 14B).

To test if *Mba* is still able to undergo pathogenic differentiation in the absence of a mating partner, a self-compatible strain (CB1) which carries compatible b-mating alleles was generated (Figure 15A). For this strain, compatible alleles of the *b-East* and *b-West* genes of the barley smut *U. hordei* were used. This decision was made as *U. hordei* is phylogenetically the closest relative in which reverse genetics have been applied. Via PCR the complete B-locus of the self-compatible *U. hordei* strain DS200 (6.6 kb) was amplified and via homologous recombination integrated at the native *Mba* B-locus (Figure 15A; (Ökmen et al., 2021)). The resulting strain "compatible B-1" (CB1) was tested on different media to exclude growth defects due to B-locus integration, where it behaved like the wildtype strain (Figure 25). Incubation of the *Mba* CB1 strain on charcoal plates led to the formation of aerial hyphae with the characteristic fluffy phenotype of filamentous strains like the self-compatible, solopathogenic *U. maydis* SG200 strain (Figure 15B). An additional method to artificially induce filament formation in smuts is the cultivation of cells on hydrophobic surfaces, like parafilm (Mendoza-Mendoza et al., 2009). Incubation of *Mba* CB1 on parafilm for 18 hours resulted in the formation of filaments comparable to those of the *U. maydis* SG200 strain (Figure 15C).

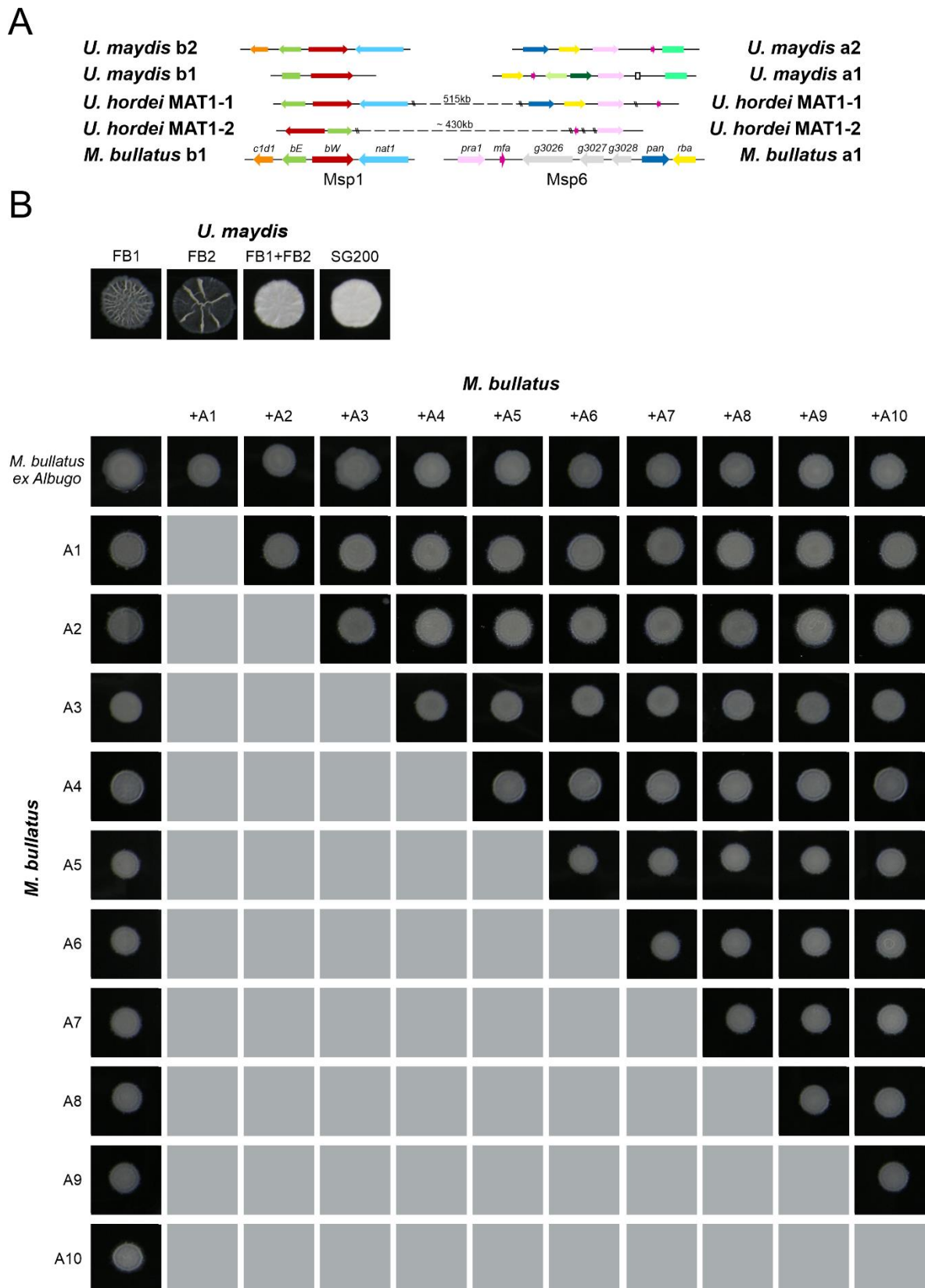


Figure 14: Mating tests of *M. bullatus*. Mating type systems in Ustilaginomycetes can be tetrapolar, in which the two mating loci, termed *a* and *b*, are unlinked from each other (*U. maydis*/*M. bullatus*) or bipolar, in which both loci are coupled to each other on one chromosome (*U. hordei*) (A). Mating of two haploid *U. maydis* strains (FB1 & FB2) leads to the formation of aerial hyphae on PD-charcoal plates, similar to the self-compatible strain SG200. Mixing of 11 different *M. bullatus* strains did not lead to mating of haploid strains, as no aerial hyphae formation could be seen on plate and via stereomicroscope (B).

2. Results

While about 17% of *Mba* wild type cells showed filaments, the CB1 cells with compatible *U. hordei* b-genes showed 38 % filamentous growth. While the switch from yeast-like growth to filamentous development is the first step in the pathogenic development of smut fungi, host penetration is accompanied by the formation of a terminal swelling of infectious hyphae, called “appressoria”. Appressoria-formation can be induced *in vitro* by adding 100 μ M of the cutin monomer 16-Hydroxyhexadecanoic acid (HDD) to the fungal cells prior to spraying the cells onto a hydrophobic surface (Mendoza-Mendoza et al., 2009). In absence of HDD, only about 8 % of the *U. maydis* SG200 cells and 14 % of the *Mba* cells formed appressoria on parafilm 24 hours after spraying (Figure 15D).

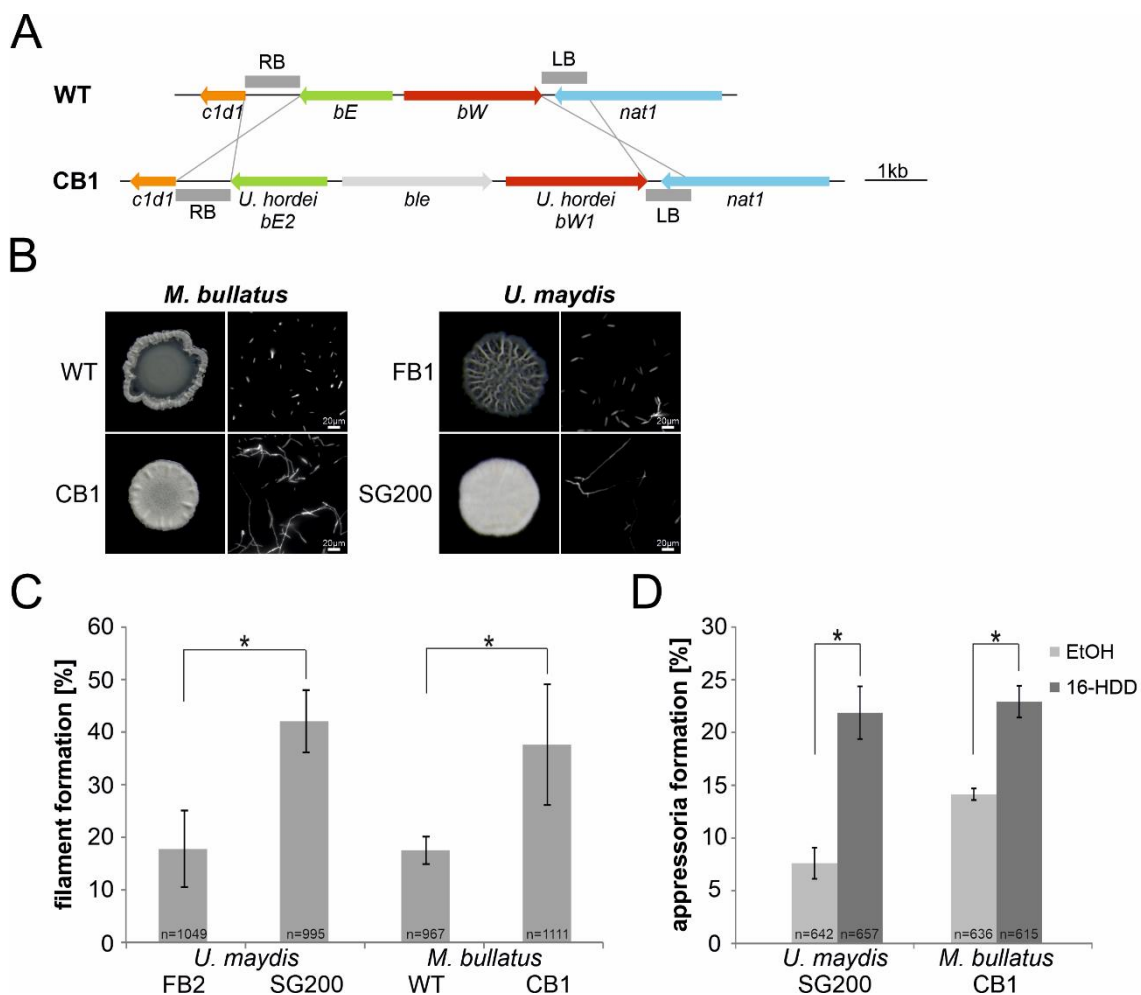


Figure 15: Phenotype of the self-compatible *Mba* strain CB1. To generate a self-compatible strain of *Mba* its B-locus was exchanged via homologous recombination with the complete B-locus of the self-compatible *U. hordei* strain DS200 (A). In those self-compatible strains (CB1 & SG200) filament formation can be artificially induced on PD-agar plates supplemented with charcoal and on a hydrophobic surface like parafilm (B). A “fluffy” appearance on charcoal plates indicates the formation of aerial hyphae. Quantification of filament formation (C) and appressoria formation (D) was studied in three independent experiments. Around 1000 cells for filament formation and around 600 cells for appressoria formation were analyzed and error bars indicate standard error. After incubation on a hydrophobic surface, both, filament and appressoria formation in strain CB1, were significantly different (*chi-squared test for Independence – $\alpha = 0.0001$) when compared to the wild type strain and similar to the level of the self-compatible *U. maydis* strain SG00. *U. maydis* haploid F2 strain was used as negative control. Scale bar: 20 μ m.

Addition of 100 μ M HDD resulted in a significant induction of appressoria in both *U. maydis* SG200 and *Mba* CB1, demonstrating that *Mba* does hold the genetic repertoire to form infection structures *in-vitro*. Together, the analysis of the recombinant CB1 strain indicates that *Mba* can still sense pathogenesis-related surface cues and produce penetration structures to a similar level as that seen for the pathogenic model organism *U. maydis*.

As *in-vitro* experiments with the self-compatible *Mba* strain CB1 led to filament and appressoria formation it was exciting to see, whether this strain is also able to infect plants. Different methods for plant infections had been established. Ustilaginomycetes mainly infect grasses, but natural host jumps to dicotyledonous plants are also known (Halisky & Barbe, 1962; Sharma et al., 2014). So, it was first hypothesized that *Mba*, in addition to its biocontrol function, can be a pathogen of *A. thaliana*. To infect *Arabidopsis* plants, liquid fungal cultures were sprayed onto the leaf surface and fungal growth was assessed two days after spray inoculation by calcofluor staining. While the wildtype strain can only be found as haploid sporidia or as pseudohyphae, the self-compatible strain shows clear filament formation (Figure 16). Nevertheless, no appressoria formation or infection attempts could be visualized in case of *A. thaliana* plants.

In the following it was tried to infect natural hosts of *Moesziomyces spp.* like perl millet (*Pennisetum glaucum*) or barnyard grass (*Echinochloa crus-galli*). As a first trial a protocol for *U. maydis* seedling infections had been adapted for *Mba* (Redkar & Doehlemann, 2016). Both plants have been grown at 22 °C until reaching the three-leaf stage (Perl millet after ~7 d; Barnyard grass after ~10 d) and inoculated with a liquid culture of *Mba* WT or CB1 ($OD_{600} = 3$) into the interior of the leaf whorl by using a syringe. The third and fourth leaves, showing an infection mark, were harvested two days after inoculation and subjected to microscopy. As seen in Figure 16 *Mba* WT strains showed typical haploid growth on the surface of perl millet while the self-compatible strain CB1 started to grow filamentous (Barnyard grass is not shown as the results were similar to perl millet microscopy). Some spots, possibly being appressoria formations, could be detected, but a verification with an appressoria marker strain is needed.

As perl millet and barnyard grass plants are quite thin and inoculation with a syringe is quite complicated and time consuming, it was tried to infect coleoptiles after seed germination. For this, recently germinated seeds had been inoculated with a liquid culture ($OD_{600} = 3$) supplemented with 10 % Tween20 and incubated on a rotary shaker for 45 minutes. Seedlings have been transferred to the soil and grown for 10 days at 22 °C in the greenhouse. Proliferated hyphae in planta were visualized by using a co-staining with Wheat Germ Agglutinin-Alexa Fluor 488 (WGA) conjugate and propidium iodide. Nevertheless, in those infection assays no fungal material could be detected.

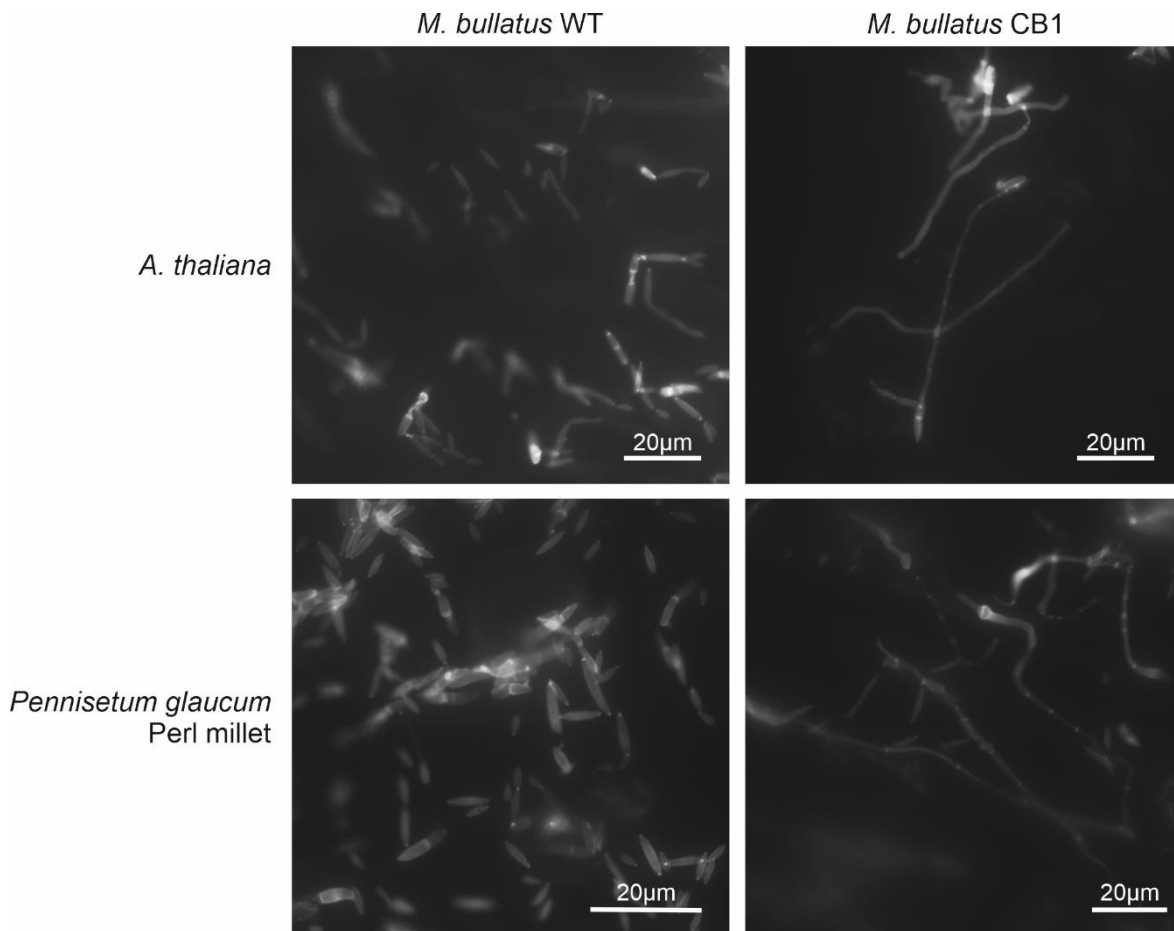


Figure 16: Morphology of *Mba* WT and CB1 strains on potential host plants. The haploid wildtype grows on all leaf surfaces as sporidia, while the self-compatible strain CB1 starts a filamentous growth. The potential formation of appressoria can be seen on perl millet surfaces, but in all cases the fungus was only found to be growing extracellular.

2.3.2 The influence of Mannosylerythritol lipids on microbial community members

Ustilaginomycetes are known to produce biosurfactants, like Mannosylerythritol lipids. They are amphiphilic molecules and able to lower the surface tension. As those compounds are known to have antimicrobial activities, the biosynthetic gene cluster involved in MEL-production (SM6) was deleted from the genome of *Mba* by homologous recombination (Figure 17A). The cluster itself consists out of 6 genes, 5 of them having an assigned function in MEL production and has a length of roundabout 15 kb. As the cluster is quite big and deletion via homologous recombination error-prone, the knockout of SM6 was verified by PCR, southern blot, and amplification of cDNA (Figure 26). All three methods confirmed the deletion of genes involved in MEL production. The loss of MEL production could be already seen by eye as it affected culture supernatant appearance. While the liquid has a

turbid appearance for wildtype strains, the supernatant of Δ SM6 strains looks noticeably clearer (Figure 17B).

When subjected to a microbial inhibition assay the Δ SM6 strain shows the formation of a more precise halo compared to the wildtype strain (Figure 17C). Nevertheless, when tested in interactions with *A. laibachii* on *A. thaliana* plants no changes in biocontrol activity could be seen (Figure 17D).

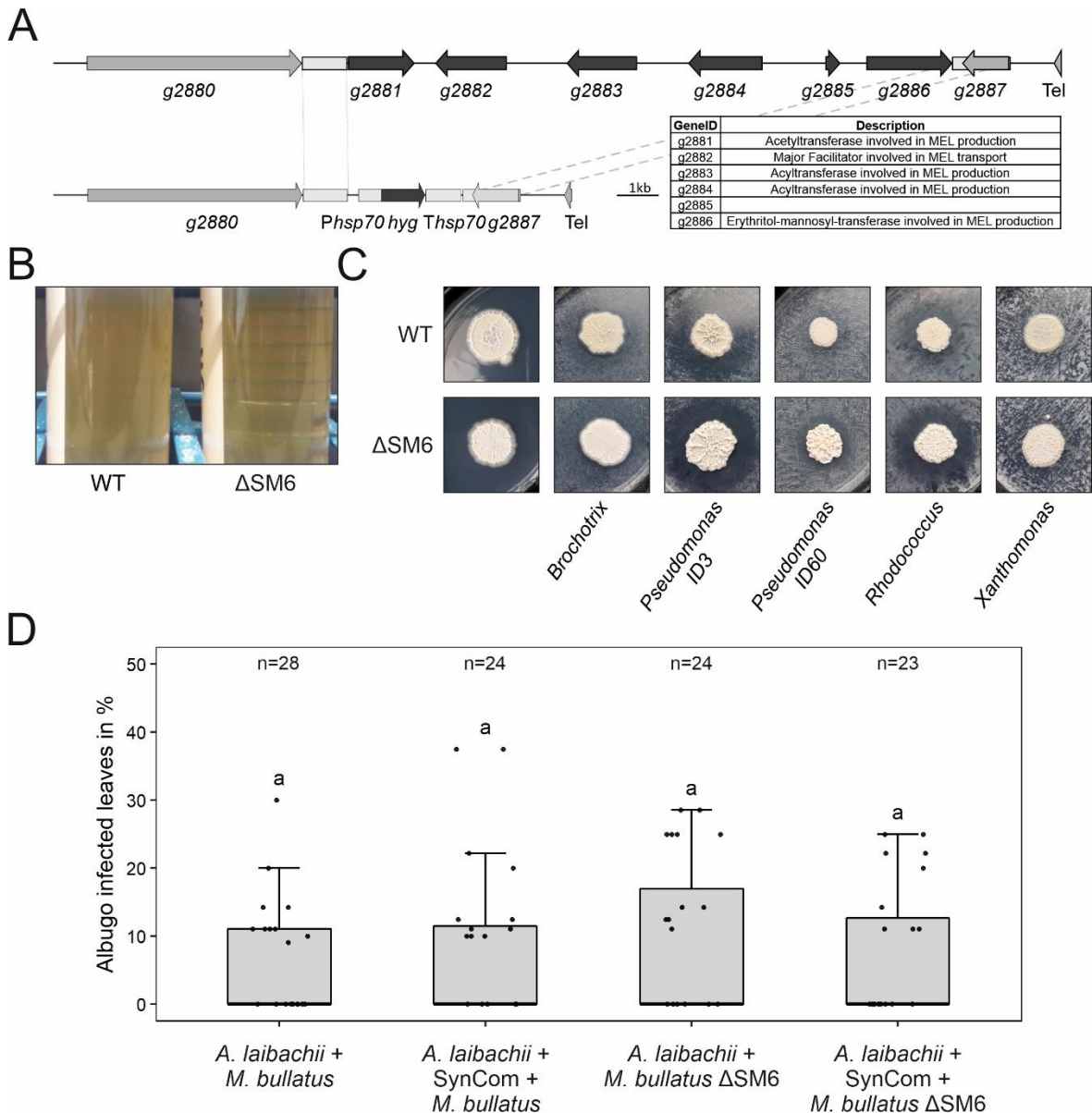


Figure 17: Knockout of *Mba* Secondary Metabolite Cluster 6. This cluster is important to produce mannosylethritol lipids and comprises of five biosynthetic genes and one gene with unknown function (**A**). When deleted, microbial inhibitory effects of *Mba* seen on plate are more intense (**B**) and culture supernatant has a clearer appearance (**C**). Deletion of the MEL-cluster in *Mba* does not change its biocontrol activity on *A. laibachii* (**D**). Infections were performed with 12 plants in three individual replicates. N indicates the number of infected plants that were scored for symptoms. Different letters indicate significant differences (p -values < 0.05 ; ANOVA model for pairwise comparison with Tukey's HSD test).

2.4 Identification of microbe-microbe effector genes by RNA-Seq

To study the transcriptomic response of *Mba* to different biotic interactions, RNA sequencing was performed. For this the *Mba* transcriptome was profiled in five different conditions (Figure 18A; cells in axenic culture versus cells on-planta, on-planta + SynCom, on-planta + *A. laibachii*, on-planta + SynCom + *A. laibachii*). Inoculations of *A. thaliana* leaves were performed as described before for *A. laibachii* infection assays (chapter 4.7.3). For *Mba* RNA preparation, the epiphytic microbes were peeled from the plant surface by using liquid latex (chapter 4.5.1.3). The libraries of 15 different samples (5 conditions in 3 biological replicates) were generated at the Cologne Center for Genomics (CCG) by using a poly-A enrichment, to exclude bacterial RNA, and sequenced on an Illumina HiSeq4000 platform. The achieved paired end reads were mapped to the *Mba* genome by using Tophat2 (Kim et al., 2013). As the data showed high variations in plant conditions differentially expressed genes were determined with the "limma"-package in R on "voom" transformed data (Figure 27) using a False discovery rate threshold of 0.05 and $\log_2FC > 0$. The analysis revealed that *Mba* cells on *A. thaliana* leaves (on-planta) showed 1300 downregulated and 1580 upregulated genes compared to cells in axenic culture (Figure 18B). Among the downregulated genes, a GO-terms analysis revealed that 50 % of those genes were associated with primary metabolism (Figure 28). In the two conditions in which *A. laibachii* was present, upregulation of 801 genes could be observed. Among these genes, 411 genes were specific to co-incubation of *Mba* with *A. laibachii* and SynCom while 174 were specific to incubation with *A. laibachii* only. A set of 216 genes could be found upregulated in both conditions (Figure 18B). In presence of *A. laibachii*, mainly metabolism- and translation-dependent genes were upregulated, which might indicate that *Mba* can access a new nutrient source in presence of *A. laibachii* (Figure 28). Among all *A. laibachii* induced *Mba* genes, 18 genes encode proteins carrying a secretion signal peptide and having no predicted transmembrane domain (Figure 18C). After excluding proteins being predicted to be located in intracellular organelles, nine candidate genes remained as potential microbe-microbe dependent effectors, i.e., *Mba* genes which are induced by *A. laibachii*, show no or low expression in axenic culture and encode for putative secreted proteins (Figure 18C – bold proteins). Interestingly, four of these genes encode putative glycoside hydrolases (*g5*, *g879*, *g3161*, *g2490*). Furthermore, two genes encode putative peptidases (*g6152* & *g4482*), one gene likely encodes an alkaline phosphatase (*g1798*) and two encode uncharacterized proteins (*g3657* & *g5755*) (Figure 18C).

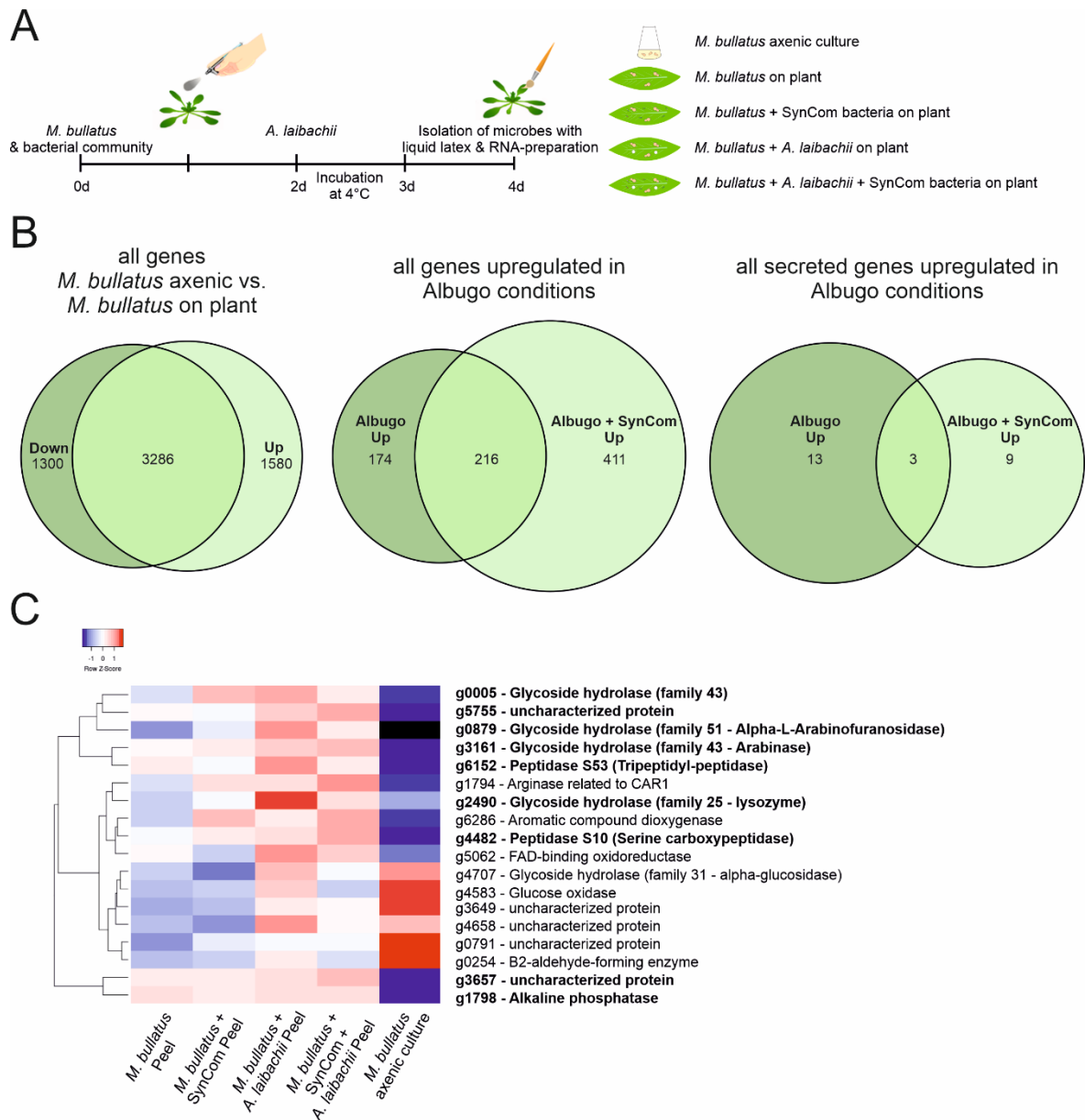


Figure 18: Transcriptome analysis of *Mba*. Experimental setup used for the RNA-Sequencing experiment (A). Microbes were sprayed onto the leaf surface as described in *A. laibachii* infection assays. Four days after *Mba* inoculation, microbes were peeled from the leaf with liquid latex and subjected to RNA-extraction. Five different conditions were used to determine transcriptional differences in *Mba* in response to different biotic stimuli. Venn diagrams showing differential regulated *Mba* genes after spraying haploid cells onto the *A. thaliana* leaf surface. The first diagram shows the *Mba* response to *A. thaliana*, with downregulation of 1300 and upregulation of 1580 genes. A total number of 801 genes were upregulated in response to *A. laibachii*, independently from presence or absence of a bacterial SynCom. Out of those 801 genes, 216 were upregulated in both conditions. Taking a closer look on those 801 genes, 25 are predicted to be secreted outside of the cell (B) Hierarchical clustering of 18 *A. laibachii*-induced *Mba* genes that are predicted to encode secreted proteins. Of these genes, nine were selected as candidate microbe–microbe effector genes, based on their transcriptional upregulation and prediction to encode for extracellularly localized proteins (C).

2. Results

To directly test the eventual antagonistic function of those genes towards *A. laibachii*, two predicted glycoside hydrolases-encoding genes *g5* & *g2490* (GH43 & GH25) and one gene encoding the uncharacterized protein *g5755* could be deleted in *Mba*. The deletion of all three genes was verified via PCR-amplification of knockout-regions (Figure 29). The respective mutant strains were tested in stress assays on different media to assess, whether the gene deletions resulted in general growth defects. Different stress conditions had been osmotic stress (sorbitol, NaCl), cell wall stress (calcofluor, congoled) and oxidative stress (H₂O₂). In all tested conditions the deletion mutants behaved comparable to the wild type and a growth defect due to gene deletions could be excluded (Figure 30). To test an eventual impact of the deleted genes in the antagonism of *Mba* against *A. laibachii*, the deletion strains were each pre-inoculated on *A. thaliana* leaves prior to *A. laibachii* infection (Figure 19A). Deletion of *g5* resulted in a significant but yet marginal increase of *A. laibachii* disease symptoms, while deletion of *g5755* had no effect on *A. laibachii*. Therefore, these two genes were considered to not being important for the antagonistic activity of *Mba*. Strikingly, the *Mba* Δ *g2490* strain almost completely lost its biocontrol activity towards *A. laibachii*. This phenotype was reproduced by two independent *g2490* deletion strains (Figure 19A). To check if this dramatic loss of microbial antagonism is specific to the deletion of *g2490*, *in-locus* genetic complementation of strain Δ *g2490_1* was performed via homologous recombination. The resulting *Mba* strain Δ *g2490/compl* regained the ability to suppress *A. laibachii* infection, confirming that the observed phenotype specifically resulted from the deletion of the *g2490* gene (Figure 19B). In addition, although *U. maydis* did not showed a strong antagonism against *A. laibachii*, deletion of the *g2490* homologue in *U. maydis* (UMAG02727) led to the same results as in *Mba* (Figure 19B).

This deletion strain showed no antagonistic activity against the oomycete pathogen and pre-inoculation led to disease symptoms like inoculation of *A. laibachii* alone. Together, these results demonstrate that biocontrol of the pathogenic oomycete *A. laibachii* by the basidiomycete yeast *Mba* is determined by the secretion of a previously uncharacterized GH25 enzyme, which is transcriptionally activated specifically when both microbes are co-colonizing the *A. thaliana* leaf surface.

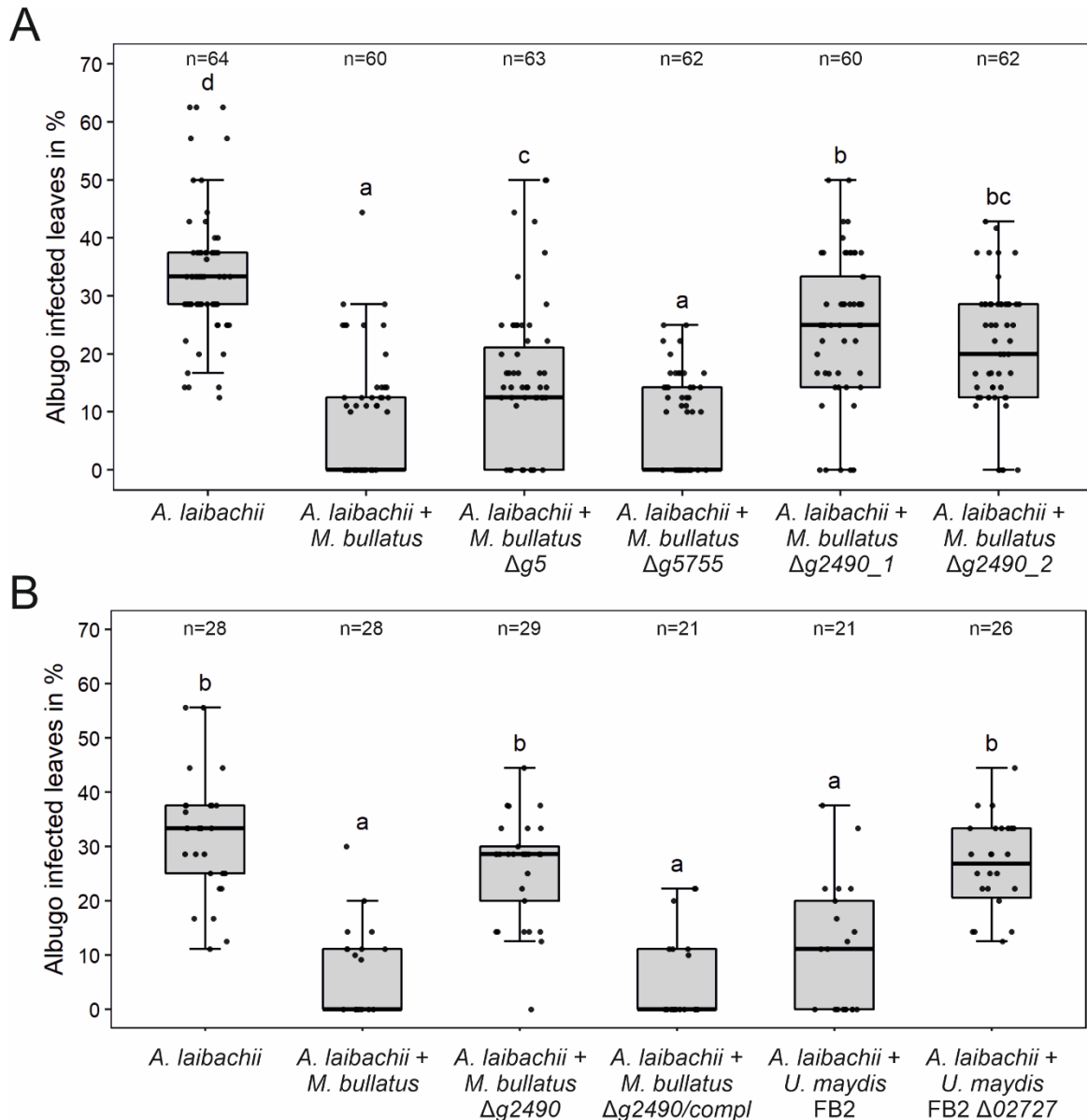


Figure 19: Reverse-genetics approach to identify the *Mba* gene responsible for antagonism against *A. laibachii*. Based on the transcriptomics approach three candidate microbe–microbe effector genes (*g5*, *g5755*, and *g2490*) were deleted in *Mba* and deletion strains were individually inoculated on *A. thaliana* seedlings together with *A. laibachii* (A). Inoculation of two independent *g2490* deletion strains (Δ *g2490_1*; Δ *g2490_2*) resulted in significant loss of the biocontrol activity of *Mba*. In contrast to this deletion of *g5* resulted only in a small reduction of disease symptoms at 14 days post infection, while deletion of *g5755* had no effect on *A. laibachii*. Genetic complementation of the *g2490* deletion restores the biocontrol activity to wild-type levels (B). Also, deletion of the *g2490* homologue in *U. maydis* (UMAG_02727) leads to the same loss of biocontrol activity, although *U. maydis* does not show an antagonistic activity as strong as *Mba*. Infections in (A) were performed in six, in (B) in three individual replicates. In each replicate 12 plants were infected. N indicates the number of infected plants that were scored for symptoms. Different letters indicate significant differences (p -values < 0.05 ; ANOVA model for pairwise comparison with Tukey’s HSD test).

2.5 Heterologous expression of a secreted *Mba* glycoside hydrolase

As seen before, the *Mba g2490* encodes for a glycoside hydrolase being important for its biocontrol activity against *A. laibachii*. It belongs to the family of GH25 lysozymes, which are also known as the Chalaropsis (CH) type of lysozymes (Hash & Rothlauf, 1967). In the CAZY database 13568 entries can be found for GH25 enzymes and out of those most enzymes originate from bacterial or viral (phage) genomes. They are known to mainly cleave the β -1,4-glycosidic bond between N-acetylmuramic acid (NAM) and N-acetylglucosamine (NAG) in the carbohydrate backbone of bacterial peptidoglycan (Figure 20A).

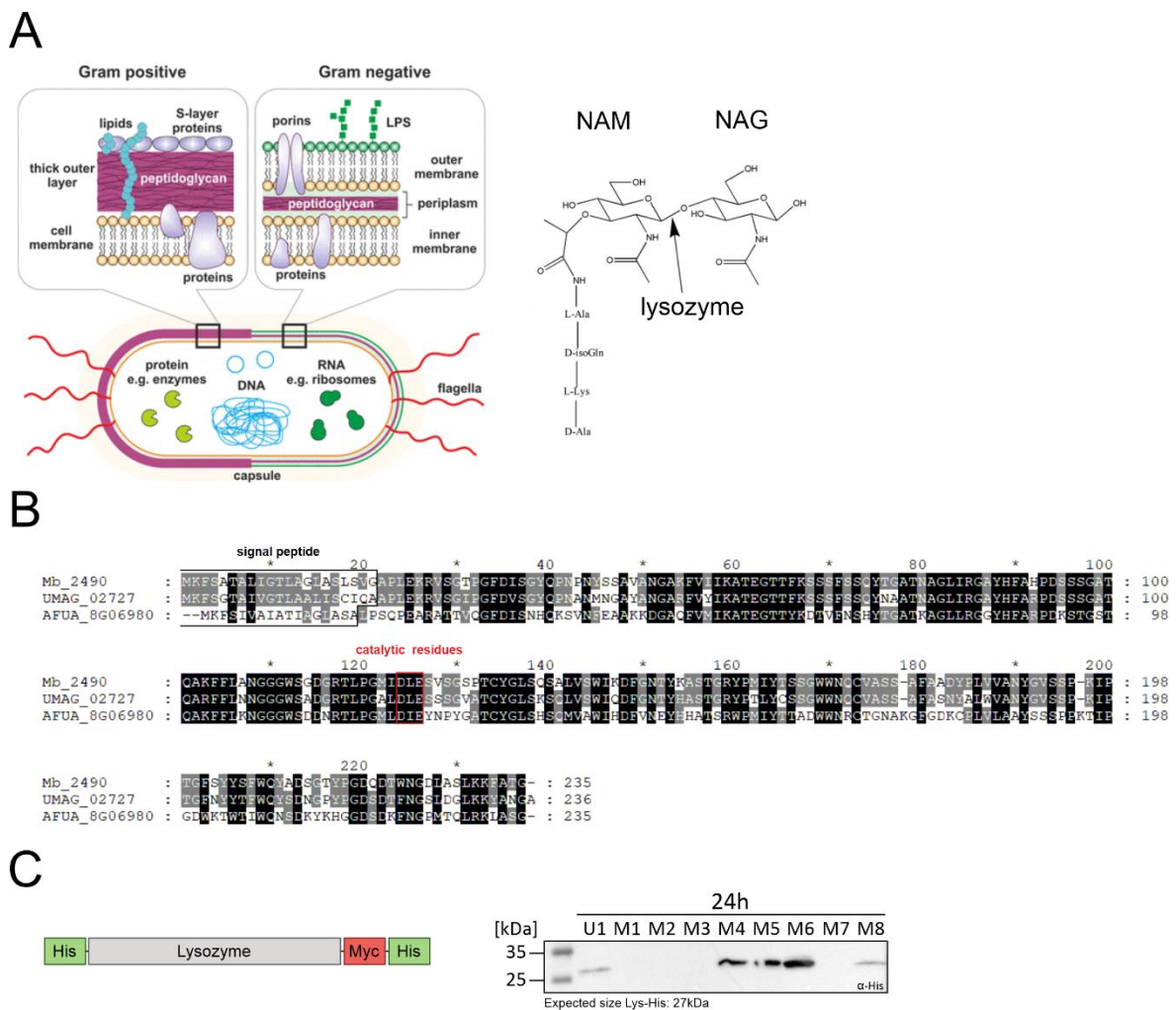


Figure 20: Recombinant production of *Mba g2490* lysozyme. GH25-lysozymes are predicted to cleave the β -1,4-glycosidic bond between N-acetylmuramic acid (NAM) and N-acetylglucosamine (NAG) in bacterial peptidoglycan, which is a polymer forming the bacterial cell wall. While Gram⁺ bacteria have a thick peptidoglycan layer, gram⁻ bacteria only possess a small layer surrounded from outer and inner cell membrane. Modified from (Ahmed et al., 2014) (A). The *Mba* lysozyme has a high synteny to the *U. maydis* and *A. fumigatus* homologues, with all of them carrying a secretion signal and a catalytic DXE motif (B). For recombinant protein production in *P. pastoris* the *Mba* and *U. maydis* lysozymes were tagged with a N- and C-terminal polyhistidine tag and a C-terminal myc-epitope. Best expression of the protein in the supernatant could be detected after 24 hours of incubation (C).

Because of this the main activities of GH25 lysozymes seem to be the re-modelling of peptidoglycan in cellular processes and the release of phages progeny by lysis of bacterial cell walls. However, there are a few eukaryotic representatives, which are so far restricted to the fungal kingdom, but their function is still unknown.

Protein alignment of *Mba* g2490 shows high synteny to the *U. maydis* homologue UMAG_02727 and to the structurally characterized *Aspergillus fumigatus* protein AFUA_8G06980 (Figure 20B; (Korczyńska et al., 2010)). All proteins share a signal peptide at the beginning and a typical DXE catalytic motif, which promotes a double-displacement mechanism in which the nucleophile is typically provided by the substrate (Vocadlo & Davies, 2008). To functionally characterize the function of this putative GH25 lysozyme a heterologous expression system in *Pichia pastoris* was established. The *Mb_g2490* and *UMAG_02727* coding sequence was cloned without secretion signal into the pGAPZ α vector. The protein is going to be expressed with an N- and C-terminal polyhistidine tag and a C-terminal Myc-epitope. Furthermore, it's going to be N-terminally fused to a peptide encoding the *Saccharomyces cerevisiae* α -factor as a secretion signal. This enables nickel-nitrilotriacetic acid (Ni-NTA) affinity purification of the recombinant protein from the culture supernatant. Test-expressions in *P. pastoris* showed a production of the recombinant protein with an expected size around 25 kDa after 24 hours of incubation (Figure 20C).

3 Discussion

The phyllosphere represents a diverse microbial habitat, which is extensively colonized by various microbes. With $10^6 - 10^7$ cells/cm², bacteria are the most prominent microbes on the leaf surface (Lindow & Brandl, 2003; Vorholt, 2012). Phyllosphere yeasts on the other hand, whose titer range from $10 - 10^4$ cells/cm², receive increasing attention in recent years (Shivas & Brown, 1984). They can be strong drivers of microbial community structure, reflecting their numerous ways of microbial antagonism. Some yeasts have plant protective functions and therefore they hold a great potential for pest control in agricultural systems. In this thesis, I studied the role of the anamorphic basidiomycetous yeast *Mba*, which was isolated from the *A. thaliana* phyllosphere together with the phytopathogenic oomycete *A. laibachii*. In *in-vitro* experiments, *Mba* inhibits the growth of seven members of a bacterial *A. thaliana* leaf SynCom. Most strikingly, it strongly suppresses disease progression and reproduction of *A. laibachii* on *A. thaliana* Col-0 accessions. Deletion of a GH25 hydrolase in *Mba* almost completely abolishes this antagonistic activity. This thesis provides new insights into the evolution of anamorphic Ustilaginomycetes and how this led to the identification of new antagonistic interactions of basidiomycete yeasts with bacteria and oomycetes in the *A. thaliana* leaf phyllosphere.

3.1 Genetic repertoire of anamorphic Ustilaginomycetes

3.1.1 *Mba* still carries the genetic prerequisites for mating

Microscopy of *Mba* showed that it grows predominantly as haploid yeast, and it will not enter its pathogenic stage, neither on *A. thaliana*, nor on pearl millet or barnyard grass plants (chapter 2.1 & 2.3.1). *Mba* stays strictly asexual, as a compatible mating partner is needed to complete its lifecycle and to infect a host plant. Essential prerequisite for mating is a complete set of mating type genes. In the genome analysis of *Mba*, all components of a tetrapolar mating system were identified (chapter 2.3.1). In addition, the transcriptome data revealed that all genes important for mating are expressed in axenic culture (data not shown). Therefore, the characterized strain holds the genetic potential for mating, but however this requires a compatible mating partner. To find such a strain, 10 different *M. bullatus* isolates from infected barnyard grass plants had been used in mating assays together with *Mba* in all possible combinations, but no mating event could be identified (chapter 2.3.1). Rabe et al. (2016) proposed that an occurring mating type bias after spore germination is the main cause of anamorphism in Ustilaginomycetes. In case of *Ustilago*

bromivora it is only possible to detect both mating types immediately after spore germination. Afterwards, a putative haplo-lethal allele restricts lifetime of one mating type and in this consequence causes anamorphism. This mating type bias can only be overcome in nature by an initiation of mating directly after spore germination, or an intratetrad mating event. In both cases, mating of spore progeny is mainly an inbreeding mode.

It is striking that, compared to other non-pathogenic Ustilaginomycetes, *Moesziomyces* strains can be found in their anamorphic form all over the world and on several non-host plants (Kruse et al., 2017). This suggests that they are good colonizers which in their saprophytic stage are highly competitive against other microbes. Thus, they can occupy new ecological niches and rapidly spread to new environments. Although asexual reproduction is fast and cost-effective, it has major disadvantages. Asexual colonies show a decreased genetic variation among their offspring and progenies tend to accumulate deleterious mutations. This theory is also known as “Muller’s ratchet”, and it is a likely reason why sexual reproduction is favored in many organisms. At this point it is conceivable that many *M. bullatus* strains will never be able to find a suitable mating partner and will stay mainly asexual, as they are well adapted to this lifestyle. In worst case, this situation could lead to extinction of anamorphic lineages over time. But it should not be ruled out that compatible mating partners could meet on a suitable host surface from time to time and by sexual reproduction revitalize their gene pool.

3.1.2 Anamorphic strains tend to have a higher intron number

Genome sequencing of *Mba* revealed several similarities between pathogenic and non-pathogenic Ustilaginomycetes. All strains, that have been analyzed in genome studies share a similar genome size around 20 kb and a highly compact genome organization (Kämper et al., 2006; Schirawski et al., 2010; Laurie et al., 2012; Lefebvre et al., 2013; Sharma et al., 2014; Dutheil et al., 2016; Rabe et al., 2016). A striking feature of the non-pathogenic strains *Mba* and *A. flocculosa* is the high number of introns in their genomes. Compared to the pathogenic species *U. maydis*, the number of introns in *Mba* is three times higher (Table 1). Until now it is not fully understood whether introns accumulate in anamorphic species or get lost in phytopathogens. But as many eukaryotic ancestors seemed to have intron rich genomes, the loss of introns seems to be more likely (Csuros et al., 2011). Lefebvre et al. (2013) speculated that smut fungi lost many introns due to a mechanism of reverse transcriptase-mediated intron loss (RTMIL; (William Roy & Gilbert, 2006; Lim et al., 2021)). By this process a reverse-transcribed copy of a spliced mRNA transcript (RT-mRNA) is reintegrated into the genome by homologous recombination.

Prerequisites of this process are RT-like enzymes, most likely originated from retrotransposons or viruses, a highly efficient homologous recombination system. As those recombination events are favored and implemented during meiosis, RTMIL is prevalent in fungi that undergo sexual reproduction (Gladyshev & Arkhipova, 2011). Another hint for the occurrence of RTMIL is the biased distribution of introns at the 5' end, which is present in some Ustilaginomycetes (Lefebvre et al., 2013). As the reverse transcriptase reads from the 3' end to the 5' end, integration of incomplete products will mainly lead to intron loss at the 3' end (William Roy & Gilbert, 2006). It would be interesting to compare genomes of other non-pathogenic strains in this analysis. When considering intron-loss rate to correspond to the number of meioses per time, a lower number of introns would strengthen the hypothesis of RTMIL in teleomorphic species. Nevertheless, *Mba* might still have the potential to enter the pathogenic phase, for example due to intratetrad mating processes, and thus the higher number of introns would correspond to infrequent meiosis events.

3.1.3 Chromosomal recombination in *Mba* affects genes important for virulence and mating

Smut genomes typically consist of 23 chromosomes (Kämper et al., 2006; Schirawski et al., 2010; Laurie et al., 2012; Rabe et al., 2016). SMRT sequencing, a third-generation sequencing technique which leads to the generation of long read fragments, enabled the full assembly of 21 chromosomes for *Mba*. Furthermore, it was possible to identify three contigs with telomeric repeats on only one side of the contig. When mapping all *Mba* contigs to the reference genome of *U. maydis*, few assembly gaps have been identified. As the gaps are only minor, they still should be manually assembled to generate a full high-quality reference genome of *Mba* with 23 assembled chromosomes.

Comparisons to other smut fungi revealed two major recombination events in the *Mba* genome. Interestingly, one of them affects genes involved in virulence, while the other one led to changes in A-mating locus architecture. As those events in *Mba* affected long regions until the end of chromosomes, they are most likely the result of chromosomal crossover during meiosis and a remainder of its pathogenic lifetime. Nevertheless, chromosomal restructuring can also be observed in asexual organisms. One example for this is the pathogenic fungus *Verticillium dahliae* (de Jonge et al., 2013). Although being strictly asexual, it is known to be a devastating plant pathogen that can quickly adapt to their host. Chromosomal rearrangements in this fungus are mainly a result of homologous recombination between copies of retrotransposons, leading to mitotic crossover and the creation of new genetic variations (de Jonge et al., 2013).

Based on comparative chromosome analysis between *U. hordei*, *S. reilianum* and *U. maydis*, Laurie et al. (2012) introduced *S. reilianum*'s genome organization as the ancestral genome form of all three mentioned smuts. As *Mba* is a close relative of those smut fungi, it seemed reasonable to compare its chromosomal organization to those results. Except from *U. maydis* all before mentioned fungi share one chromosome (Msp8, Sr5, Uh5), while a recombination event with chromosome 20 led to a partition of this chromosome in *U. maydis*. Interestingly this recombination event in *U. maydis* leads to changes in the promoter region of the effector *see1*. Strikingly, Redkar (2015) showed in his doctoral thesis that a *U. maydis see1* deletion strain can be complemented with a *S. reilianum see1* homologue, but only under control of the *U. maydis see1* promoter. Considering that *U. maydis* is one of few smuts able to cause tumors on the leaf and that expression of *see1* is leaf-specific it is tempting to speculate that this chromosomal recombination led to changes in the *see1* expression pattern, resulting in the formation of leaf tumors.

In contrast to all three genomes, *Mba* and other closely related anamorphic fungi like *M. aphidis* or *M. antarcticus* are the only fungi showing a different chromosomal organization of their chromosome 2. It is likely that it recombined with chromosome 6, leading to the chromosome structure that can be found in other pathogenic smut fungi (Figure 10). With *Mba* having the highest synteny to *S. reilianum* and a completely different organization of its chromosome 2, one could speculate that *Mba*'s genome reflects the ancestral chromosomal organization of all before mentioned smuts. Nevertheless, additional genome analyses of Ustilaginomycetes are needed to strengthen this hypothesis.

3.1.4 *Mba* possess effector genes important for pathogenicity

Schuster et al. (2018) pointed out that two anamorphic fungi, *M. antarcticus* and *A. flocculosa*, share a similar secretome with other pathogenic smut fungi. This analysis revealed that also *Mba* has a comparable number of potentially secreted proteins. Many of those secreted proteins in smut fungi are important for plant infection, microbial competition, or nutrient acquisition and due to this, they are under a strong selection pressure. In case of a host jump event, diversification and, due to this, loss or gain of effector genes is supposed to be an important determinant of host specificity (Sharma et al., 2014; Benevenuto et al., 2018). As anamorphic smut fungi do not infect plants, one can hypothesize that the genetic prerequisites for plant infections are lost over several generations, as spontaneous mutations tend to accumulate in genes that are not subjected to any selection pressure. This can be observed in *A. flocculosa*, which lost several

important effector proteins like *see1*, *pit2* or *tin2*. In contrast, *Mba* still possess homologues of these effector genes and many of those effector genes are still associated in cluster like structures. This structured organization most likely evolved through gene duplication events in association to host specialization (Dutheil et al., 2016). Genome comparisons in case of *Mba* revealed small effector clusters, in which a reduced set of effector genes is present. It is still debatable whether *Mba* has an ancestral form of clusters or lost many duplicated genes as they are not needed in microbial antagonism.

To test if *Mba* effector genes are functional, the homologue of Pep1 was used to complement the *U. maydis pep1* deletion mutant. This led to full virulence restoration in case of *Mba*, but also for other nonpathogenic yeasts (Sharma et al., 2019). This suggests that this core effector is functional in anamorphic smuts. One could also hypothesize whether Pep1 owns additional functions besides the suppression of PAMP-triggered ROS generation during plant. However, transcriptomic data of *Mba* revealed that several known effector genes like *pep1* are not expressed in this anamorphic yeast, neither in axenic culture nor on plant surfaces (Table 2). In *U. maydis*, many effector genes are only induced after mating, due to activation of the b-gene encoded heterodimeric transcription factor. Therefore, the CB1 strain was generated which, similarly to the solopathogenic *U. maydis* strain SG200, contains compatible b-genes. To test an effect of pathogenic effector genes on microbial antagonism this strain was tested in *A. laibachii* competition assays by my colleague Priyamedha Sengupta. But the presence of a filamentous *Mba* strain, having the potential to express pathogenic effector proteins, does not alter its antagonistic activity against *A. laibachii* (personal communication Priyamedha Sengupta). Based on those results it is more likely that effector genes in *Mba* are still needed for infrequent plant infections as sexual reproduction possibly occurs from time to time.

3.1.5 Integration of self-compatible mating genes enables pathogenic development of *Mba*.

In nature *Mba* is known to be a mainly anamorphic organism, but still a pathogenic relative is known (Kruse et al., 2017). To enable reverse genetics, I established a transformation system for *Mba* and generated the self-compatible strain CB1 to study pathogenic development in haploid strains. Since none of the 10 *M. bullatus* wild type isolates had the ability to mate with each or with *Mba* (chapter 2.3.1), the *U. hordei* b-genes were chosen to generate a self-compatible strain. *U. hordei* is the phylogenetically closest relative in which reverse genetics have been applied and could be adapted. The entire b-locus of the self-compatible *U. hordei* strain DS200 was amplified and integrated in-locus in *Mba* to replace

its native *b*-locus. The resulting strain CB1 did not show growth differences in axenic culture. Even more, the *U. hordei* *b*-alleles seemed to be functional in *Mba*, as CB1 showed filamentous growth on charcoal plates, as well as on hydrophobic surfaces. Moreover, treatment with the cutin monomer 16-HDD induced appressoria formation in CB1 similarly to *U. maydis* strain SG200. This demonstrates that *Mba* senses plant surface cues and forms infection structures similarly to pathogenic smuts.

Although the induction of *b*-gene dependent genes, like the master regulator *rbf1* and other effector genes like *pep1*, could be assessed in qRT-PCR experiments (Bachelor thesis Franca Arndt), successful infections were neither seen on *A. thaliana*, nor on millet plants (perl millet or barnyard grass).

In this study, I tested syringe infections of the outgrowing third and fourth leaf, a method typically used to infect maize plants with *U. maydis*. As this did not lead to successful infections, it is important to consider that leaf infections are a phenomenon only present in few smut fungi. Most other smuts need to infect plants in early stages of growths, for example during seed germination. As they need to reach the meristematic tissue, also coleoptile infections had been performed. However, also these infection methods did not lead to successful plant infections with endophytically growing fungal hyphae. While syringe infection only showed epiphytic hyphae with few appressoria formations, coleoptile infections resulted in no fungal colonization at all (chapter 2.3.1). As a perspective for following experiments coleoptile infections could be improved by using vacuum infiltration of seeds, as it is usually done for *U. hordei* infections (Ali et al., 2014). Instead of only wetting the seed surface, cells would directly reach the outgrowing coleoptile and infect immediately after seed germination, comparable to natural infections.

As most smuts have a narrow host range it is still imaginable that the used plant accessions are resistant to *Mba* infections. Based on the phylogeny, barnyard grass is most likely *Mba*'s host plant (Kruse et al., 2017), but with the current knowledge it remains unclear whether *Mba* can infect millet plants.

3.2 Mechanisms of biocontrol in *Mba*

3.2.1 Secondary metabolites and their function in biocontrol

Secondary metabolites are structurally diverse chemical compounds and not directly involved in primary metabolism. They are produced by bacteria, fungi or plants and often mediate ecological interactions. In *Mba* thirteen different secondary metabolite clusters could be identified, three of them being not present in the smut fungus *U. maydis* (chapter 2.2). Since secondary metabolites often mediate antagonistic interactions, I hypothesized that *Mba*'s biocontrol function against bacteria and *A. laibachii* might be based on the production of such compounds. One possible candidate for this are MELs, as the purified glycolipids MEL-A and MEL-B from *M. antarcticus* are already known to have antimicrobial activities (Kitamoto et al., 1993). They are supposed to damage the bilayer cell membranes of other microorganisms and due to this, they have a high activity against gram⁺ bacteria. A MEL-deficient strain of *Mba* was successfully generated in this thesis. Unexpectedly, deletion of the MEL secondary metabolite cluster led to even stronger biocontrol activities against some bacteria and had no influence on *A. laibachii* colonization (chapter 2.3.2). As MELs are known to be amphiphilic products and play a role in biofilm formation, it is imaginable that their absence leads to changes in diffusion properties of other compounds and due to this to stronger halo formations. Also, it is possible that metabolites used for MEL production can be used for other products and by this led to stronger production of other metabolites with activity against SynCom bacteria. In general, it needs to be considered that *Mba*'s biocontrol activity might be based on multiple traits. In competition assays on planta antagonism against *Albugo* is the dominant trait, but still SynCom members are antagonized in vitro and the RNA-Seq experiment revealed several hydrolases to be upregulated.

3.2.2 Transcriptional reprogramming points to changes in nutrient acquisition

Transcriptome analysis of *Mba* on *A. thaliana* showed that the epiphytic growth on the plant surface leads to massive transcriptional changes compared to axenic cultures. Those differences particularly concern genes involved in primary metabolism, which might reflect adaptation to the nutritional situation on the plant surface. Moreover, *Mba* showed specific transcriptional responses to presence of bacterial SynCom members, as well as to *A. laibachii* when being co-inoculated on plant leaves. The presence of *A. laibachii* mainly resulted in the induction of primary metabolism and biosynthesis pathways. This might

reflect enhanced growth of *Mba* in the presence of *A. laibachii* caused by the acquisition of new nutrient sources.

3.2.3 GH43 enzymes could give an advantage in nutrient acquisition

Analysis of CAZymes in *Mba* revealed a similar repertoire of carbohydrate degrading enzymes as in other smut fungi. This correlates with a previous analysis performed on the secretome of *A. flocculosa* (Lefebvre et al., 2013). It remains unclear, why smuts generally own a reduced repertoire of CAZymes. In case of the anamorphic species it can be suggested that the present set of enzymes is sufficient for an epiphytic life style and biocontrol activity towards competing microbes (Avis & Bélanger, 2002). Minor differences in *Mba* compared to other smut fungi can only be found in the number of CAZymes carrying the GH terms 36, 39, 43 or 88 (chapter 2.2), which are specific for the cleavage of hemicellulose or pectin. As these are mainly plant cell wall degrading enzymes, it can be speculated that those enzymes were needed in pathogenic ancestors due to different cell wall compositions of their host plants. Nevertheless, it is still conceivable that those enzymes have additional uncharacterized functions in microbial competition. Transcriptomic analysis of *Mba* (chapter 2.4) showed that several potentially secreted glycoside hydrolases and peptidase are activated during interaction with *A. laibachii*.

Interestingly, expression of two GH43 hydrolase genes, namely *g5* and *g3161*, was induced when *Mba* was cultivated on planta together with *A. laibachii* (chapter 2.4). The GH43 family is one of the largest GH families, and only 4 % of all sequences have a eukaryotic origin. So far, the known enzymatic activities are β -d-xylosidase (EC 3.2.1.37), α -l-arabinofuranosidase (EC 3.2.1.55), endo- α -l-arabinanase (EC 3.2.1.99), and 1,3- β -galactosidase (EC 3.2.1.145). In summary, their main function can be described as the degradation of hemicellulose, particularly arabinoxylans, and pectin.

Deletion of *g5* in *Mba* led to a slight, but significant, decrease of biocontrol activity against *A. laibachii* (chapter 2.4). Its homologue in *U. maydis* is named *UMAG_03416* (*crg1*) and is known to be regulated by carbon-source-dependency, in particular arabinose (Bottin et al., 1996). One can hypothesize that infection of *Arabidopsis* by *A. laibachii* could release arabinose from the cell walls, which would lead to *g5* induction in *Mba*. Deletion of *g5* on the other hand could lead to less acquired nutrients and consequently reduced growth of *Moesziomyces* biomass on the plant surface. But still a direct effect on *A. laibachii* cannot be ruled out. In addition to *g5*, two additional homologous genes could be identified in *M. bullatus*, resulting in the higher number of GH43 enzymes compared to other Ustilaginomycetes. While *g3922* is also expressed on the plant surface but not significantly

changed in its expression, *g4173* seems to be a pseudogene being not expressed in any of the tested condition.

Although knockouts of other GH43 enzymes could not be generated in this study, it would be interesting to see whether a double knockout of both expressed arabinose regulated enzymes (*g5* & *g3922*) or even a triple knockout of *g5*, *g3922* and *g3161* would have an additive effect on *Mba*'s growth on *A. thaliana* and its biocontrol activity against *A. laibachii*.

3.2.4 GH25 hydrolases are important for biocontrol activity of *Mba* against *A. laibachii*

In addition to plant cell wall degrading enzymes, one *Albugo*-induced gene was predicted to encode a putative GH25 hydrolase of the Chalaropsis type lysozymes. Strikingly, deletion of this single gene almost completely abolished the antagonistic activity of *Mba* against *A. laibachii*. Like other muramidases, GH25 is predicted to cleave the β -1,4-glycosidic bond between N-acetylmuramic acid and N-acetylglucosamine units in the bacterial peptidoglycan. Specific for GH25 hydrolases is an additional β -1,4-N,6-O-diacetylmuramidase activity, which allows degradation of the cell wall of *Staphylococcus aureus* (Rau et al., 2001). Although this type of enzymes was initially discovered in the fungus *Chalaropsis sp.*, the majority of GH25 muramidases can be found in bacteria, where they function in cell division and cell wall remodeling (Vollmer et al., 2008), or in bacteriophages, to lyse bacterial peptidoglycan at the end of its lytic cycle (Fastrez, 1996). Furthermore GH25 muramidase genes have been found in plants, insects, many species of fungi, and archaea, where they were integrated independently via horizontal gene transfer from bacteria to all domains of life (Metcalf et al., 2014). An alignment of 86 GH25 muramidases revealed highly conserved sites, which can be structurally mapped to the identified active site pocket (Martinez-Fleites et al., 2009; Metcalf et al., 2014). The presence of an N-terminal signal peptide was considered to indicate an extracellular secretion of the protein which can be linked to possible antimicrobial properties (Korczynska et al., 2010).

After test expressions of the *Mba* GH25 lysozyme in *P. pastoris* were sufficient (chapter 2.5), large-scale productions have been performed. The recombinant protein was detected via western blot after Ni-NTA affinity purification at an expected size of 27 kDa. In addition, a mutated version of the protein was generated (Eitzen et al., 2021). After the enzymatic activity of the GH25 was confirmed by cleavage of a fluorogenic substrate (*Micrococcus lysodeikticus* cell walls labeled with fluorescein), its biological function in the *M. bullatus* - *A. laibachii* interaction was investigated (Eitzen et al., 2021). A quantitative experiment was

performed by Priyamedha Sengupta, which showed a significant reduction of *A. laibachii* colonization to about 50 % after treating the leaves with the active GH25 lysozyme (Eitzen et al., 2021).

Regarding the fact that GH25 muramidases are present in all kingdoms, it is possible that they help to defend against niche competitors. This is often accompanied by an upregulation of the corresponding gene in presence of the competitor, what can be seen in case of *Mba*, but also for other organisms like the aphid *Acyrtosiphon pisum* that shows a differential tissue expression of its GH25 muramidase (Nikoh et al., 2010) or the archaea *Aciduliprofundum boonei* which upregulates the expression of its lysozyme in presence of bacterial competitors (Metcalf et al., 2014).

In addition to an antibacterial function, a function in hyperparasitism can be hypothesized. Herein this scenario, secreted glycoside hydrolases are proposed to be important for fungi parasitizing fungi (Hyde et al., 2019) or oomycetes parasitizing oomycetes (Horner et al., 2012). The results of this study might therefore indicate a cross kingdom hyperparasitism event between a fungus and an oomycete. As Coyte et al. (2015) already indicated, negative interactions are the main drivers to stabilize microbial communities, hyperparasitism can be such a negative interaction with a strong evolutionary effect on pathogen–host interactions and therefore on community stability (Parratt & Laine, 2016). The quantification of oomycete biomass by qPCR performed by my colleague Priyamedha Sengupta points towards the idea that *A. laibachii* can be a direct target of *M. bullatus* GH25 lysozyme, but until now no other substrate than bacterial cell walls could be identified (Eitzen et al., 2021). Based on current knowledge, cell walls of oomycetes are mainly composed of β -1,3, and β -1,6 glucans (Aronson et al., 1967), which cannot be cleaved by muramidases. Nevertheless, Mélida et al. (2013) showed that oomycete cell walls are indeed more diverse than it was thought and proposed a cell wall paradigm which is primarily based on *N*-acetylglucosamine (NAG) content: While in cell walls of type I NAG is completely absent, type II oomycetes exhibit up to 5 % NAG and type III has the highest content with more than 5 % NAG. As NAG is also a component of bacterial peptidoglycan it would be interesting to know whether GH25 muramidases can cleave unknown substrates in oomycete cell walls. This cleavage of oomycete cell walls by GH25 lysozymes could lead to changes in cell wall integrity or signal perception and by this block the infection process.

Also, an indirect effect of *Mba* on *A. laibachii*'s infection efficiency cannot be ruled out. Since oomycetes can be found in close association with bacteria, one could even speculate that the GH25 targets *Albugo*-associated bacteria, which might be necessary for virulence of the oomycete. Such a tempting scenario would be in line with findings of endosymbiotic bacteria in mycorrhizal fungi but should still be interpreted with caution (Pawlowska et al., 2018).

No matter which substrate is cleaved by GH25 hydrolases, microbial cell wall components could also trigger plant defense mechanisms in *A. thaliana*. The activated immune responses would transfer the plant into a state of emergency and block the infection of *A. laibachii*. This could result in the observed biocontrol phenotype caused by *Mba*.

3.3 Conclusion and future perspectives

Plants are known to have the ability to manipulate their host microbiome under stress conditions and to protect themselves from pathogenic invaders (Trivedi et al., 2020). Many of those protective microbes have the potential to be used as biocontrol fungi in agricultural systems. The basis of this thesis is a non-pathogenic Ustilaginomycete which was found to be important for microbial community stabilization, by strongly antagonizing other community members like oomycetes and bacteria. As Ustilaginomycetes possess a great effector repertoire important for plant infection we raised the question whether those effector genes gained additional functions in microbial competition to counteract the plants acquisition of beneficial microbes. This thesis showed that rather hydrolytic enzymes belonging to the classes of GH43 or GH25 than small-secreted effector proteins are important for biocontrol function of this anamorphic *M. bullatus* strain. They are expressed in early stages of colonization prior to infection, most likely leading to an advantage in nutrient acquisition or competition in microbial communities. As the secretion of hydrolases seems to be the dominant trait of *Mba*'s biocontrol activity, their deletion in the self-compatible CB1 strain could lead to the identification of additional proteins important for microbial antagonism.

The biggest challenge of future research is to identify the substrates of GH43 and GH25 hydrolases and to unravel their mode of action in biocontrol. On the one hand a direct antagonism against *A. laibachii* is possible, leading to death of the plant pathogen. In this context it will be interesting to see, whether this biocontrol activity is a general mechanism of *Mba* against several oomycetes like *Hyaloperonospora spp.* or *Phytophthora spp.* On the other hand, an indirect effect of *Mba* on plant pathogens via plant defense responses is still conceivable. Indirect mechanisms could be demonstrated by checking the expression patterns of pathogenesis related (PR)- or WRKY-genes upon treatment with purified GH25 protein in presence and absence of *A. laibachii*. Nevertheless, the role of secreted hydrolases in the fungal kingdom is still not fully explored yet and will be an interesting research field in the following years.

4 Material and Methods

4.1 Material

4.1.1 Chemicals

All chemicals used in this study were purchased from Biozym (Hessisch Oldendorf, Germany), Becton Dickinson (Heidelberg, Germany), GE Healthcare (Munich, Germany), Invitrogen (Darmstadt, Germany), Merck (Darmstadt, Germany), Roche Diagnostics (Mannheim, Germany), Roth (Karlsruhe, Germany), and Sigma-Aldrich (Deisenhofen, Germany) unless otherwise stated.

4.1.2 Buffers and solutions

Buffers and solutions were prepared according to (Sambrook et al., 1989; Ausubel, 2002) if not otherwise stated in the respective method description. Sterilization of buffers and solutions was done at 121 °C, 5 min or via a sterile filter, if solution was heat sensitive (Pore size 0.2 µm, Merck, Darmstadt, Germany).

4.1.3 Enzymes and antibodies

The restriction enzymes used in this study were purchased from New England Biolabs (NEB, Frankfurt/Main, Germany), or Thermo (Thermo Fisher Scientific Inc., Bonn, Germany). DNA polymerases used in this study were Phusion® Hot Start High-Fidelity DNA-Polymerase (Thermo Fisher Scientific Inc., Bonn, Germany), KOD Xtreme™ Hot Start DNA Polymerase (Novagen®/Merck Millipore, Darmstadt, Germany), or GoTaq® Green Master Mix (Promega, Walldorf, Germany). Ligation of DNA molecules was done by using the T4 DNA ligase (NEB, Frankfurt/Main, Germany). The enzymatic degradation of RNA was done with RNaseA (Serva, Heidelberg, Germany) and enzymatic degradation of DNA was done with the TURBO DNA-free™ Kit (Ambion®/ Thermo Fisher Scientific Inc., Bonn, Germany). For the enzymatic degradation of fungal cell walls Novozyme234 (Novo Nodisk, Copenhagen, Denmark) and Lysing enzymes from *Trichoderma harzianum*/ Glucanex® (Sigma-Aldrich, Deisenhofen, Germany) was used. Antibodies were obtained from Thermo Fisher Scientific (Bonn, Germany) or Sigma-Aldrich (Deisenhofen, Germany). For further information concerning antibodies used in this study see Table 11.

4. Material & Methods

4.1.4 Commercial kits

Plasmid DNA extraction was done using the QIAprep® Mini Plasmid Kit (Qiagen, Hilden, Germany). The NucleoSpin gel and PCR Clean-up kit (Machery-Nagel, Düren, Germany) was used to purify PCR products or to extract nucleic acids from agarose gels. The DIG High Prime Kit (Roche, Mannheim, Germany) was used for the digoxigenin labeling of PCR products for southern blots. cDNA was synthesized by using the RevertAid H Minus First Strand cDNA Synthesis Kit (Thermo Fisher Scientific Inc., Bonn, Germany). Direct ligation of PCR products into the pGEM®-T vector was done by using the pGEM®-T easy kit (Promega, Walldorf, Germany). For Gibson assembly cloning reactions, the 2x Hifi DNA assembly mix (NEB, Frankfurt/Main, Germany) was used. To remove or to add restriction sites in a plasmid, single mutations were induced with the Quickchange (Multi) Kit (Agilent Technologies, Santa Clara, USA).

4.2 Media and growth conditions for microorganisms

4.2.1 Media

The recipes for media used to cultivate gnotobiotic plants or microorganisms in this study are listed in Table 3. The media was autoclaved at 121 °C for 5 min before use, unless otherwise stated.

Table 3: Media for cultivation of microorganisms

Name	Composition	Remarks
1/2 Murashige and Skoog (MS)	0.2 % (w/v) MS basal salt mixture 0.8 % (w/v) Agar	in H ₂ O _{bid.} pH 5.7
Potato-Dextrose (PD)-Agar	2.4 % (w/v) PD broth 2.0 % (w/v) Agar	in H ₂ O _{bid.}
PDA-Charcoal	Addition of 1 % (w/v) Charcoal to PD-Agar media	in H ₂ O _{bid.}
YEPSL	1.0 % (w/v) Yeast extract 0.4 % (w/v) Peptone 0.4 % (w/v) Sucrose	in H ₂ O _{bid.}
Regeneration Agar	1.0 % (w/v) Yeast extract 0.4 % (w/v) Peptone 0.4 % (w/v) Sucrose 18.22 % (w/v) Sorbitol 1.5 % (w/v) Agar	in H ₂ O _{bid.}
dYT	1.6 % (w/v) Tryptone 1.0 % (w/v) Yeast extract 0.5 % (w/v) NaCl	in H ₂ O _{bid.}
YT-Agar	0.8 % (w/v) Tryptone 0.5 % (w/v) Yeast extract 0.5 % (w/v) NaCl 1.3 % (w/v) Agar	in H ₂ O _{bid.}
Low salt LB	1 % (w/v) Tryptone 0.5 % (w/v) NaCl 0.5 % (w/v) Yeast Extract	In H ₂ O _{bid.} pH to 7.5 with 1N NaOH
Low salt LB-Agar	Addition of 1.5 % (w/v) Agar to low salt LB medium	

YPD	1 % (w/v) Yeast Extract 2 % (w/v) Peptone 2 % (w/v) Dextrose	in H ₂ O _{bid} . Add 100 ml of 20 % (w/v) Dextrose after autoclaving!
YPD-Agar	Addition of 2.0 % (w/v) Agar to YPD medium	
YPDS-Agar	Addition of 1 M sorbitol to YPDA medium	
Kings-B	2.0 % (w/v) Peptone 0.15 % (w/v) K ₂ HPO ₄ 0.5 % (v/v) 1M MgSO ₄ 1.5 % (w/v) Glycerol	in H ₂ O _{bid} . pH to 7.2 with HCl (If MgSO ₄ is added before autoclaving, the medium becomes cloudy!)
Kings-B-Agar	Addition of 1.5 % (w/v) Agar to Kings-B medium	

4.2.2 Propagation of *A. laibachii*

Due to its obligate biotrophy *A. laibachii* was maintained on *A. thaliana* Ws-O plants and reinoculated every 2 weeks. For this 10-12 infected leaves were harvested in 20 ml H₂O_{bid} and incubated on ice for 1 h with (vigorous shaking is needed to dissolve the spores). Afterwards plant parts were filtered by using Miracloth (Millipore/ Merck, Darmstadt, Germany) and spun down at 2000 x g for 10 min. The pellet was washed with sterile water and sprayed again onto uninfected *A. thaliana* seedlings. Plants were incubated at 4 °C and high humidity (inside a plastic bag) over night and afterwards transferred to the growth chamber. To maintain a high humidity, plants were left inside the plastic bag for one additional day.

4.2.3 Cultivation of *E. coli*

E. coli cultures were cultivated at 37 °C on a rotary shaker at 200 rpm in dYT liquid media or on YT-Agar plates (Table 3 and (Sambrook et al., 1989)). For selection of transformed strains both media were supplied with the appropriate antibiotics (Table 4). For long term storage 25 % f.c. (v/v) dYT-glycerol was added to a thickly grown overnight culture in a total volume of 2 ml and stored in a screw cap vial at -80 °C. Strains were streaked out on YT-Agar plates to be reused after long term storage. To cultivate Zeocin™ resistant strains Low salt LB liquid and agar medium was used, as high salt concentrations deactivate the antibiotic.

Table 4: Antibiotic concentrations *E. coli*

Antibiotic	Working concentration [µg/ml]
Ampicillin (Amp)	100
Carbenicillin (Carb)	100
Kanamycin (Kan)	50
Zeocin	25

4.2.4 Cultivation of SynCom Bacteria

Bacterial strains were cultivated at 22 °C on a rotary shaker at 200 rpm in KingsB liquid media or on KingsB-Agar plates. For long term storage 25 % f.c. (v/v) KingsB-glycerol was added to a thickly grown overnight culture in a total volume of 2 ml and stored in a screw cap vial at -80 °C. Strains were streaked out on KingsB-Agar plates to be reused after long term storage.

4.2.5 Cultivation of *M. bullatus* and *U. maydis*

M. bullatus and *U. maydis* cultures were grown on a rotary shaker at 22 °C/28 °C and 200 rpm in liquid YEPSL medium. For long term storage 25 % f.c. (v/v) YEPSL-glycerol was added to a thickly grown overnight culture in a total volume of 2 ml and stored in a screw cap vial at -80 °C. Strains were streaked out on PD-agar plates to be reused after long term storage. For selection of transformed strains regeneration agar (Table 3 and Schulz et al. 1990) plates were supplied with the appropriate antibiotics (Table 5).

Table 5: Antibiotic concentrations used for fungi

Antibiotic	Working concentration [µg/ml] <i>M. bullatus</i> / <i>U. maydis</i>
Hygromycin	400/ 400
Nourseothricin	300/ -
Carboxin	8/ 2
Phleomycin	80/ -

4.2.6 Cultivation of *Pichia pastoris*

P. pastoris cultures were grown on a rotary shaker at 30 °C and 200 rpm in liquid YPD medium (Table 3). For long term storage 25 % f.c. (v/v) YPD-glycerol was added to a thickly grown overnight culture in a total volume of 2 ml and stored in a screw cap vial at -80 °C. Strains were streaked out on YPD-agar plates to be reused after long term storage. For selection of transformed strains YPD-agar plates were supplemented with 100 µg/ml Zeocin.

4.2.7 Determination of cell density

The cell density was determined by measuring the absorption at 600 nm (OD₆₀₀) in a Genesis 10S VIS spectrophotometer (Thermo Fisher Scientific Inc., Bonn, Germany) and taking the corresponding culture medium as reference value. Cultures were diluted to absorption values below 0.8 to ensure a linear dependence of the measurements.

4.3 Microbial strains, oligonucleotides, and vectors

4.3.1 *A. laibachii* strain

All multipartite experiments were performed with the *A. laibachii* Isolate Nc14 which was isolated in Norwich, UK and kindly provided by the Group of E. Kemen at the University of Tübingen.

4.3.2 *E. coli* strains

For plasmid amplification during normal cloning procedures *E. coli* K-12 Top10 [F⁻ *mcrA* Δ(*mrr-hsdRMS-mcrBC*) φ80*lacZ*ΔM15 Δ*lacX74 recA1 araD139 Δ(ara-leu)*7697 *galU galK* λ⁻ *rpsL(Str^R) endA1 nupG*] ((Grant et al. 1990)/ Invitrogen Karlsruhe) and *E. coli* K-12 DH5α [F⁻ φ80*lacZ*ΔM15 Δ(*lacZYA-argF*)U169 *recA1 endA1 hsdR17(r_K⁻, m_K⁺) phoA supE44* λ⁻ *thi-1 gyrA96 relA1*] ((Glover 1985)/ Gibco/BRL Eggenstein) were used.

4.3.3 SynCom bacteria

The used synthetic community consists of 30 bacteria (Table 6;(Agler et al. 2016)) isolated usually together with *A. laibachii*.

Table 6: SynCom bacteria

Species	Isolated from	Source
<i>Pseudomonas</i> sp. (ID3)	<i>A. thaliana</i> leaf	Group Kemen
<i>Pseudomonas</i> sp. (ID4)	<i>A. thaliana</i> leaf	Group Kemen
<i>Flavobacterium</i> sp. (ID9)	<i>A. thaliana</i> leaf	Group Kemen
<i>Xanthomonas</i> sp. (ID10)	<i>A. thaliana</i> leaf	Group Kemen
<i>Xenophilus</i> or <i>Variovorax</i> sp. (ID18)	<i>A. thaliana</i> leaf	Group Kemen
<i>Brochotrix</i> sp. (ID20)	<i>A. thaliana</i> leaf	Group Kemen
<i>Bacillus</i> sp. (ID21)	<i>A. thaliana</i> leaf	Group Kemen
<i>Agrobacterium</i> or <i>Rhizobium</i> sp. (ID24)	<i>A. thaliana</i> leaf	Group Kemen
<i>Xylophilus</i> or <i>Variovorax</i> sp. (ID25)	<i>A. thaliana</i> leaf	Group Kemen
<i>Pseudomonas</i> sp. (ID26)	<i>A. thaliana</i> leaf	Group Kemen
<i>Flavobacterium</i> sp. (ID28)	<i>A. thaliana</i> leaf	Group Kemen
<i>Acinetobacter</i> sp. (ID32)	<i>A. thaliana</i> leaf	Group Kemen
<i>Microbacterium</i> sp. (ID35)	<i>A. thaliana</i> leaf	Group Kemen
<i>Agreia</i> or <i>Herbiconiux</i> sp. (ID36)	<i>A. thaliana</i> leaf	Group Kemen
<i>Xanthomonas</i> sp. (ID38)	<i>A. thaliana</i> leaf	Group Kemen
<i>Agreia</i> or <i>Herbiconiux</i> sp. (ID40)	<i>A. thaliana</i> leaf	Group Kemen
<i>Bacillus</i> sp. (ID45)	<i>A. thaliana</i> leaf	Group Kemen
<i>Streptomyces</i> sp. (ID46)	<i>A. thaliana</i> leaf	Group Kemen
<i>Arthrobacter</i> sp. (ID52)	<i>A. thaliana</i> leaf	Group Kemen

4. Material & Methods

<i>Arthrobacter</i> sp. (ID53)	<i>A. thaliana</i> leaf	Group Kemen
<i>Curtobacterium</i> sp. (ID54)	<i>A. thaliana</i> leaf	Group Kemen
<i>Pseudomonas</i> sp. (ID60)	<i>A. thaliana</i> leaf	Group Kemen
<i>Microbacterium</i> sp. (ID62)	<i>A. thaliana</i> leaf	Group Kemen
<i>Bacillus</i> sp. (ID63)	<i>A. thaliana</i> leaf	Group Kemen
<i>Bacillus</i> or <i>Brevibacterium</i> sp. (ID75)	<i>A. thaliana</i> leaf	Group Kemen
<i>Pseudomonas viridiflava</i> strain ATCC 13223 (ID76)	<i>A. thaliana</i> leaf	Group Kemen
<i>Xanthomonas</i> sp. (ID77)	<i>A. thaliana</i> leaf	Group Kemen
<i>Pandoraea</i> sp. (ID79)	<i>A. thaliana</i> leaf	Group Kemen
<i>Rhodococcus</i> sp. (ID80)	<i>A. thaliana</i> leaf	Group Kemen
<i>Stenotrophomonas</i> sp. (ID81)	<i>A. thaliana</i> leaf	Group Kemen

4.3.4 *M. bullatus* and *U. maydis* strains

The *M. bullatus* wildtype strain (*a1mfa1bW1bE1*) was isolated from *A. laibachii* infected *A. thaliana* leaves. The *U. maydis* FB2 strain was used for all *U. maydis* experiments. All plasmids generated for transformation of this strain as well as the plasmids used for transformation of the knockout strains derived from this initial strain are listed in chapter 4.3.7.2. As a summary, all *M. bullatus* strains produced in this study are listed in Table 7 & Table 8.

Table 7: *Moesziomyces* strains used in this study

Name	Genotype	Resistance	Reference
WT	<i>a1mfa1</i> <i>bW1bE1</i>	-	(Agler et al., 2016)
CB1	<i>a1mfa1</i> <i>UhbW1</i> <i>UhbE2</i>	Phleomycin	This study
MspΔg2490	<i>a1mfa1</i> <i>bW1bE1</i> Δ Mspg2490:: <i>hph</i>	Hygromycin	This study
MspΔg5	<i>a1mfa1</i> <i>bW1bE1</i> Δ Mspg5:: <i>hph</i>	Hygromycin	This study
MspΔg5755	<i>a1mfa1</i> <i>bW1bE1</i> Δ Mspg5755:: <i>hph</i>	Hygromycin	This study
MspΔg2490c	<i>a1mfa1</i> <i>bW1bE1</i> Δ Mspg2490:: <i>P_{nativ}</i> <i>Mspg2490:Tnos:nat</i>	Nourseothricin	This study

Table 8: *Ustilago* strains used in this study

Name	Genotype	Resistance	Reference
FB2	<i>a2mfa2</i> <i>bW2bE2</i>	-	(Banuett und Herskowitz 1989)
FB2ΔUMAG 02727	<i>a2mfa2</i> <i>bW2bE2</i> ΔUMAG_02727:: <i>hph</i>	Hygromycin	This study
FB2ΔUMAG 02727_ Mspg2490	<i>a2mfa2</i> <i>bW2bE2</i> ΔUMAG_02727:: <i>P_{orf}:Mspg2490:T_{nos}:nat</i>	Nourseothricin	This study

4.3.5 *P. pastoris* strains

For protein expressions the *P. pastoris* strain KM71H (Invitrogen, Karlsruhe, Germany) was used, as it enables a selection of Zeocin-resistant expression vectors to generate strains with Mut^S phenotype. All plasmids generated for transformation of this strain are listed in chapter 4.3.7.3. As a summary, all *P. pastoris* strains produced in this study are listed in Table 9.

Table 9: *P. pastoris* strains used in this study

Name	Genotype	Resistance	Reference
KM71H	<i>aox1::ARG4, arg4</i>	-	
pGAPzA-His-g2490-His	<i>aox1::ARG4, arg4, pgap::Mspg2490</i>	Zeocin	This study
pGAPzA-His-UMAG_02727-His	<i>aox1::ARG4, arg4,</i> <i>pgap::UMAG_02727</i>	Zeocin	This study

4.3.6 Oligonucleotides

All oligonucleotides used in this study were purchased from Sigma-Aldrich (Deisenhofen, Germany). A list of the oligonucleotides can be found in Table 10.

Table 10: General oligonucleotides used in this study.

Name	Sequence	Use
Pseudoz_peg1_fw_XbaI	GCGTCTAGAATGAGGTTTCATGCTTGCCAC	U. MaydisΔpeg1 complementation
Pseudoz_peg1_rv_XmaI	GTGCCCCGGTTAAAAGCCAAGCAGATTAC	U. MaydisΔpeg1 complementation
P-CbxLocus_fw2_NruI	CCAATCTCGCGACAAGACGCCAATCAGAGAC	Amplification Cbx-Locus
P-CbxLocus_rv2_NdeI	GGCATGCATATGTGATGCCGACACAGACGTTTC	Amplification Cbx-Locus
M_cbx-mut_fw	CCTTCTCCCTCTACCGCTGCCTTACCATCATGAA CTGCTCC	Mutagenesis of cbx-gene in Moesziomyces
M_cbx-mut_rv	GGAGCAGTTCATGATGGTAAGGCAGCGGTAGAG GGAGAAGG	Mutagenesis of cbx-gene in Moesziomyces
HY-R	GTATTGACCGATTCTTGCGGTCCGAA	Split-marker Hyg
YG-F	GATGTAGGAGGGCGTGGATATGTCCT	Split-marker Hyg
PhleoP6f	AAGTTGACCAGTGCCGTTCC	Split-marker Phleo
PhleoP7r	CACGAAGTGCACGCAGTTG	Split-marker Phleo
NA-F	AAGGTGTTCCCCGACGACGAATCG	Split-marker Nat
AT-R	AACTCCGTCGCGAGCCCCATCAAC	Split-marker Nat
bE1_rv	TCAACCGAAAGCGGCAGAAAGGC	Amplification <i>Ustilago hordei</i> DS200 B-locus

4. Material & Methods

UhDS200_bW1_fw	TTATTCGAGGGAAAACATCTCCGGACC	Amplification Ustilago hordei DS200 B-locus
DS200_B-Loc_Seq1	CACCGTACTTGATCCAACCTG	sequencing of U. Hordei DS200 B-Locus in pGem-T
DS200_B-Loc_Seq2	GGAGGGTCTGAAAGCAAGAG	sequencing of U. Hordei DS200 B-Locus in pGem-T
DS200_B-Loc_Seq3	GAACGTGGTAACTACCAGCG	sequencing of U. Hordei DS200 B-Locus in pGem-T
DS200_B-Loc_Seq4	AGGTCGTGTCCACGAACTTCC	sequencing of U. Hordei DS200 B-Locus in pGem-T
DS200_B-Loc_Seq5	TACTAAGATGGTATAGCTTGGC	sequencing of U. Hordei DS200 B-Locus in pGem-T
DS200_B-Loc_Seq6	TTGCAGCACGTTGAGCAGAC	sequencing of U. Hordei DS200 B-Locus in pGem-T
DS200_B-Loc_Seq7	TCGACCAGCTCATCCTCTAC	sequencing of U. Hordei DS200 B-Locus in pGem-T
DS200_B-Loc_Seq8	ATACGCAAACCGCCTCTCCC	sequencing of U. Hordei DS200 B-Locus in pGem-T
P_LBblocus_fw_SpeI_2	GCATACTAGTGCCGATCCTCATGCACGCAAG	Generation of integration-construct
P_LBblocus_rv_SbfI_2	ATATCCTGCAGGCGTTCACATGGTGGTGCCTC	Generation of integration-construct
P_RBblocus_fw_SacII	CATACCGCGGGCTGTAGATCAAAGCGTCCG	Generation of integration-construct
P_RBblocus_rv_SacII	TATACCGCGGGCCCGCACTGTACATTCTTC	Generation of integration-construct
HR_BLoc_RB_F	TCTTCTTGGCCGGCGTTGAG	Verification of homologous recombination
HR_BLoc_RB_R	CGTGCCTAGAAGGGAGAATC	Verification of homologous recombination
HR_BLoc_LB_F	GGCCCGCACAGTTCTATTTG	Verification of homologous recombination
HR_BLoc_LB_R	GGGCTACGAGAACGTCATGC	Verification of homologous recombination
HR_BLoc_ble_F	GCAATCGAGCTGACAGTACG	Verification of homologous recombination
HR_BLoc_ble_R	CAGCTGGTACGCTGACAGAG	Verification of homologous recombination
HygFRT_Gibson_fw	GGCCTAGATGGCCAGAAGTTCC	Generation of KO-construct
HygFRT_Gibson_rv	CTCAGGCCAGAAGTTCTATAC	Generation of KO-construct
LBSM6_fw	TGCATGCCTGCAGGTCGACTCTGCTGCGAATGC CATAAAG	Generation of KO-construct
LBSM6_rv	AACTTCTGGCCATCTAGGCCAGCGGATGAGGTG GTGATTG	Generation of KO-construct
PHsp70-seq 1912	AGTTTGCAGAAGTCTGCTGGTAG CAGGAGGAGATGACTACC	Knockout verification
LBSM6_check	GCCGGACCTGTACTTTGTGG	Knockout verification
RBSM6_check	CGAGAGCGAGCATTGGTTTTG	Knockout verification
g2881fw_RT-PCR	CTTTGACGCCCCAACCACTAC	Knockout verification
g2881rv_RT-PCR	TGAACCCCGAGAACCACACACC	Knockout verification
Msp_ppi_RT_fw	GTTCTTCATCACCACCGTCCG	Amplification of ppi for qRT-PCR
Msp_ppi_RT_rv	CGATGGTGATGGTGCTCTTG	Amplification of ppi for qRT-PCR
g5KO_LBfw	TGCATGCCTGCAGGTCGACTGGTAAAGGCGCCG ATGTTTC	Generation of KO-construct
g5KO_LBrv	AACTTCTGGCCATCTAGGCCGAAGGGACGAAGG TAGATAG	Generation of KO-construct
g5KO_RBfw	ATAGGAACTTCTGGCCTGAGCGAGTCAGGCATA CGTACAC	Generation of KO-construct
g5KO_RBrv	AAAACGACGGCCAGTGAATTAAGATCTCGTTGC GGACTGC	Generation of KO-construct
g2490KO_LBfw	TGCATGCCTGCAGGTCGACTTCCGATTTCCCG ATCCCTC	Generation of KO-construct
g2490KO_LBrv	AACTTCTGGCCATCTAGGCCATGGGCAGATGTG ATGTGAG	Generation of KO-construct
g2490KO_RBfw	ATAGGAACTTCTGGCCTGAGAGTGCGCCCTCCT AGTAATC	Generation of KO-construct
g2490KO_RBrv	AAAACGACGGCCAGTGAATTTTGACCATAGGG CCTACCG	Generation of KO-construct
g5755KO_LBfw	TGCATGCCTGCAGGTCGACTTCCCGCGGATCG ACAAGAC	Generation of KO-construct
g5755KO_LBrv	AACTTCTGGCCATCTAGGCCCTGTCTCGTGCAA CTCCTTC	Generation of KO-construct
g5755KO_RBfw	ATAGGAACTTCTGGCCTGAGTTGAGGGTGTGAT TCCGAAGAG	Generation of KO-construct
g5755KO_RBrv	AAAACGACGGCCAGTGAATTTCTCGGGAGTATC GGAAATC	Generation of KO-construct
g5LB_HR_fw	AGGTACGGCAGGCATAGTTG	Knockout verification

g5RB_HR_rv	CGTGCAGATGAGACTTGAAC	Knockout verification
Mspg5_fw	GGATTGCCTGCGCCTGAAAC	Knockout verification
Mspg5_rv	GCTGCGGCGTGGTAAAGTTG	Knockout verification
g2490LB_HR_fw	GGAGTCCGAGGAGGAATACG	Knockout verification
g2490RB_HR_rv	GAAGTAAGTCGGCTTCACAG	Knockout verification
Mspg2490_fw	ACGCCCCGGTTTCGACATTAG	Knockout verification
Mspg2490_rv	CGTACTGCCAGAAGGAGTAG	Knockout verification
g5755LB_HR_fw	AGACAGCTCCAGAGTCAAAC	Knockout verification
g5755RB_HR_rv	TGAGGCAGGCATCCGTATTG	Knockout verification
Mspg5755_fw	GCCGTTACCGTTGATGTTAC	Knockout verification
Mspg5755_rv	GTTCTCCGCCGTTCTCATCG	Knockout verification
Pgapdh_fw	CGCACCTAGAAGTGATAAGC	Generation of compl-construct
Tnos_fw	GGCCGCCCGGCTGCAGATCGTTC	Generation of compl-construct
g2490RB_Pgapdh_fw	GCTTATCACTTCTAGGTGCGAGTGCGCCCTCCT AGTAATC	Generation of compl-construct
g2490ORF_Tnos_rv	GAACGATCTGCAGCCGGGCGGCCTCAGCCGGT GGCGAACTTCTTG	Generation of compl-construct
UMAG_02727_LB_fw	TGTCGGATTGAGCGCTAGGC	Generation of KO-construct
UMAG_02727_LB_rv	AACTTCTGGCCATCTAGGCCGTGGAGAGCGGAT CCTGATG	Generation of KO-construct
UMAG_02727_RB_fw	ATAGGAACTTCTGGCCTGAGTTCAAATTGCCGCT GTCTC	Generation of KO-construct
UMAG_02727_RB_rv	TTTGCGCCGCATTCTAGTCC	Generation of KO-construct
hygP9r	GGCGTCGGTTTCCACTATC	Complementation verification
hygP8f	AAAGTTCGACAGCGTCTCC	Complementation verification
Msp2490_fw_EcoRI_His Tag	GCAGCTGAATTCCATCATCATCATCATGCTC CCTTGAGAAGCGCGTG	Production of Msp Lysozyme in Pichia pastoris
Msp2490_Xbal	TTTTGTTCTAGACCGCCGGTGCGAACTTCTTG	Production of Msp Lysozyme in Pichia pastoris
UMAG_02727_fw_EcoRI HisTag	GCGGCCGAATTCCATCATCATCATCATGCTC CCCTTGAGAAGCG	Production of U. Maydis Lysozyme in Pichia pastoris
UMAG_02727_rv_Xbal	TTTTGTTCTAGACCAGCACCGTTGGCGTACTTC	Production of U. Maydis Lysozyme in Pichia pastoris

4.3.7 Plasmids

All plasmids used in this study were tested via restriction enzyme digest. In case of insertion of plasmid parts that were generated via PCR, the newly generated sequence was verified via sequencing.

4.3.7.1 Plasmid for Cloning of PCR Products

pGEM®-T Easy (Promega, Walldorf, Germany)

This plasmid was used for intermediate cloning steps during the generation of knockout constructs, especially for subcloning of left and right borders. This plasmid contains an ampicillin resistance and is suitable for Blue/White Selection.

4.3.7.2 Plasmids for *M. bullatus* and *U. maydis* transformation

#395 p123+uhcbx+Hyg

The plasmid was used to generate *M. bullatus* strains expressing the eGFP protein. It carries the bacterial gene for hygromycin-phosphotransferase (*hph*) under control of the *U. maydis hsp70* promoter (*Phsp70*). Termination is facilitated by the *Agrobacterium tumefaciens nos* terminator (*Tnos*). The enhanced GFP (eGFP) reporter gene, derived from *Aequorea victoria*, is under control of the *o2tef* promoter (*Po2tef*) and is terminated by the *Tnos* as well. It was originally used for *cbx*-locus integration in *U. hordei*, therefore the plasmid was cut inside the *cbx*-locus prior to transformation of *M. bullatus*. This should avoid additional *Cbx*-resistance. Selection of this plasmid in *E. coli* was based on Ampicillin resistance.

#1567 PInt_UhDS200BLoc

This plasmid was generated to exchange the native *M. bullatus* B-Locus with the artificial B-Locus of the solopathogenic *U. hordei* strain DS200. For this, the B-Locus region was amplified via PCR from genomic DNA with primer 457 & 3339 and the generated 6.6kb fragment was cloned into the pGEM®-T Easy plasmid. To insert the amplified fragment in the *M. bullatus* genome, 1 kb flanking regions of the *M. bullatus* B-Locus were integrated via restriction enzyme digest with *SacI* for the right border and with *SbfI* & *SpeI* for the left border. The *U. hordei* B-Locus carries a phleomycin resistance cassette, consisting of the *Streptoalloteichus hindustanus* phleomycin-resistance polypeptide (Sh-ble) under control of the *U. maydis Phsp70* and terminated by the *Aspergillus nidulans trpC* terminator (*TtrpC*). Due to its pGEM®-T Easy background *E. coli* transformants can be selected with Ampicillin.

pAGM1311

This *E. coli* plasmid served as a background to generate knockout plasmids for *M. bullatus*. It is suitable for Blue-white screening of transformants, and selection of this plasmid is based on the antibiotic Kanamycin.

pHwtFRT

pHwtFRT is an *E. coli* plasmid that was used to amplify the *hph* cassette flanked by FRT sites to generate deletion constructs. The *hph* gene is under control of the *U. maydis Phsp70* and termination is facilitated by the *A. tumefaciens Tnos*. For selection in *E. coli* this plasmid harbors a kanamycin as well as an ampicillin resistance gene. The addition of

FRT sites enables a FLP-mediated recombination system that allows repeated rounds of gene deletion using a single selectable marker (Hyg^R).

PKO_g5

This plasmid was generated in this study via Gibson Assembly to delete the *M. bullatus* gene 5. It carries 1 kb left (LB) and right (RB) flanking regions of the gene 5 and a hygromycin resistance cassette with flanking FRT sites. Due to its pAGM1311 background *E. coli* transformants can be selected with Kanamycin.

PKO_g5755

This plasmid was generated in this study via Gibson Assembly to delete the *M. bullatus* gene 5755. It carries 1 kb LB and RB flanking regions of the gene 5755 and a hygromycin resistance cassette with flanking FRT sites. Due to its pAGM1311 background *E. coli* transformants can be selected with Kanamycin.

PKO_g2490

This plasmid was generated in this study via Gibson Assembly to delete the *M. bullatus* gene 2490. It carries 1 kb LB and RB flanking regions of the gene 2490 and a hygromycin resistance cassette with flanking FRT sites. Due to its pAGM1311 background *E. coli* transformants can be selected with Kanamycin.

pStorI-1n

pStorI-1n is an *E. coli* plasmid that was used to amplify the *nat* cassette to generate complementation constructs. The bacterial gene for nourseothricin N-acetyl transferase (*nat*) is under control of the *U. maydis gapd* promoter (*Pgapd*); termination is facilitated by the *S. cerevisiae cyc1* terminator (*Tcyc1*). For selection in *E. coli* this plasmid harbors a gentamycin resistance gene.

PC_g2490

This plasmid was generated in this study via Gibson Assembly to complement the *g2490* deletion in *M. bullatus*. It carries 1 kb LB and RB flanking regions of the gene 2490, the *g2490* coding sequence under control of its native promoter and a *nat* resistance cassette. Due to its pAGM1311 background *E. coli* transformants can be selected with Kanamycin.

PKO_UMAG02727

This plasmid was generated in this study via Gibson Assembly to delete the *U. maydis* gene 02727. It carries 1 kb LB and RB flanking regions of the gene 02727 and a hygromycin resistance cassette with flanking FRT sites. Due to its pAGM1311 background *E. coli* transformants can be selected with Kanamycin.

4.3.7.3 Plasmids for the expression of recombinant proteins in *P. pastoris*

pGAPZ α (Thermo Fisher Scientific Inc., Bonn, Germany)

This plasmid was used to constitutively express recombinant proteins under control of the GAP promoter. It carries the *S. cerevisiae* α -factor secretion signal, which is fused N-terminally to the recombinant protein, to secrete the protein into the supernatant. Recombinant proteins are C-terminally fused to a Myc epitope and a Polyhistidine-Tag, which can be visualized by western blot. Selection of this plasmid is based on the selectable marker Zeocin™.

pGAPZ α -His-Msp2490-Myc-His

This plasmid contains the *M. bullatus* gene 2490 without secretion signal amplified using the primers 5166 and 5167 and cloned via *EcoRI* and *XbaI* into the empty pGAPZ α vector. This plasmid was used to express the *M. bullatus* GH25-protein in *P. pastoris*.

pGAPZ α -His-UMAG02727-Myc-His

This plasmid contains the *U. maydis* gene 02727 without secretion signal amplified using the primers 5168 and 5169 and cloned via *EcoRI* and *XbaI* into the empty pGAPZ α vector. This plasmid was used to express the *U. maydis* GH25-protein in *P. pastoris*.

4.4 Microbiological methods

4.4.1 Transformation of *E. coli*

The transformation of *E. coli* cells was done by rubidium chloride-mediated transformation (Cohen et al., 1972). To produce chemo-competent bacterial cells 100 ml dYT medium supplemented with 10 mM MgCl₂ and 10 mM MgSO₄ was inoculated with 1 ml of a freshly grown overnight culture and incubated at 37 °C at 200 rpm until the OD₆₀₀ reached 0.5. The cells were centrifuged at 1500 x g for 15 min at 4 °C and the pellet was resuspended in 33 ml ice-cold RF1 solution. After 30 – 60 min of incubation at 4 °C on ice, the cells were again pelleted by centrifugation at 1500 x g for 15 min at 4 °C. The cell pellet was

resuspended in 5 ml ice-cold RF2 solution and incubated 15 min on ice. In the end, the cell suspension was stored at -80 °C after shock freezing it in 1.5 ml microcentrifuge tubes as 50 µl aliquots.

RF1-Solution	100 mM RbCl 50 mM MnCl ₂ x 4 H ₂ O 30 mM K-Acetate 10 mM CaCl ₂ x 2 H ₂ O 15 % (v/v) Glycerine in H ₂ O bid., pH 5.8 (Acetate), sterile filtered
RF2-Solution	10 mM MOPS 10 mM RbCl 75 mM CaCl ₂ x 2 H ₂ O 15 % (v/v) Glycerine in H ₂ O bid., pH 5.8 (NaOH), sterile filtered

To transform chemo-competent *E. coli* cells, one aliquot of cells was thawed on ice and 1 – 5 ng of plasmid DNA or 1 – 5 µl ligation mixture were added. After incubation for 30 min on ice the mixture was heat-shocked at 42 °C for 45 sec and then cooled on ice for 2 min. Afterwards 200 µl of dYT liquid media was added and the mix was incubated for 1 h at 37 °C and 200 rpm. 200 µl of this transformation mixture were plated on YT agar medium containing the antibiotic used for selection and incubated at 37 °C overnight.

4.4.2 Blue-white screen of *E. coli* transformants

To clone A-tailed PCR products into the pGEM®-T Easy vector, a blue-white selection approach was used. Insertion of the cloned PCR product into the plasmid backbone interrupts the *lacZ* gene, which leads to a lack of β-galactosidase expression. Colonies that contain the inserted PCR fragment therefore appear white on 5-bromo-4-chloro-3-indolyl-β-D-galactopyranoside (X-Gal) containing plates and are easily distinguishable from blue colonies in which β-galactosidase expression is active. For this screening, X-Gal solution (2 % X-Gal, dissolved in DMSO) was added to a f.c. of 0.08 % one hour before the transformation on selective YT-agar plates.

4.4.3 Transformation von *P. pastoris*

The transformation of *P. pastoris* was done by electroporation. For this an overnight culture was started in 5 ml YPD at 30 °C and 200 rpm. On the next day 0.25 ml of this overnight culture were used to inoculate 500 ml YPD and grown to a maximum OD₆₀₀ = 1.5. The cells were harvested by centrifugation at 1500 x g for 5 min at 4 °C and afterwards resuspended

in 500 ml of ice-cold H₂O_{bid}. Centrifugation was repeated under the same conditions and the pellet resuspended in 250 ml of ice-cold H₂O_{bid}. Afterwards the pellet was centrifuged a third time and the pellet resuspended in 20 ml of ice-cold 1 M sorbitol. The cells were pelleted a last time and resuspended in 1 ml ice-cold 1 M sorbitol for a final volume of 1.5 ml. 80 µl of those competent *P. pastoris* cells were mixed with 5-10 µg of linearized DNA (maximum volume of 10 µl) and transferred to an ice-cold 0.2 cm electroporation cuvette (Peqlab/VWR, Langenfeld, Germany). The cuvette was incubated for 5 min on ice and afterwards transferred to an Eporator® electroporation device (Eppendorf, Hamburg, Germany). For electroporation parameters for *P. pastoris* suggested by the manufacturer were used (1500 V, 5 ms). Immediately after electroporation 1 ml ice-cold 1 M sorbitol was added to the cuvette and the solution transferred to a sterile 15 ml tube. After incubation for 1-2 h at 30 °C without shaking 50 µl and 200 µl were spread on a YPD-agar plate containing 100 µg/ml Zeocin™ and incubated for 2-3 days until colonies formed. Transformants were transferred to a fresh YPD plate with appropriate antibiotic selection and tested for expression of the desired protein (chapter 4.6.4).

4.4.4 Transformation of *M. bullatus* and *U. maydis*

The preparation of protoplasts and subsequent transformation of *U. maydis* protoplasts was done as described in Schulz et al. (1990) and Gillissen et al. (1992) with changes mentioned as follows. An overnight culture of fungal cells was started from cells grown on PD medium in 4 mL YEPSL medium and incubated at 22 °C/ 28 °C at 200 rpm. Afterwards cultures were diluted in 50 mL YEPSL medium and grown until it reached an optical density of OD₆₀₀ = 0.8. Cells were pelleted by centrifugation for 15 min at 2000 x g and 4 °C. The pellet was washed in 20 ml of ice cold SCS, and further centrifuged for 10 min at 2000 x g, before being treated with 3 ml SCS solution with 20 mg/ml of Glucanex (Lysing Enzyme from *T. harzianum*, # L1412, Sigma-Aldrich, Deisenhofen, Germany). Protoplastation was monitored under the microscope. The reaction was stopped after 20 min of incubation, when 50 % of the cells had reached a spherical shape due to lysis of the cell wall, by adding 10 ml ice-cold SCS to the mix. The protoplasts were spun down for 10 min at 1300 x g at 4 °C and washed twice with 10 ml ice-cold SCS. Afterwards the pellet was resuspended in 10 ml ice-cold STC and centrifuged for 10 min at 1300 x g at 4 °C. Finally, the pellet was dissolved in 500 µl ice-cold STC, and stored in aliquots of 50 µl at -80°C after shock freezing in liquid N₂.

For transformation of protoplasts 5 µg of linearized plasmid DNA (in max. volume of 10 µl) along with 15 µg Heparin was added to an aliquot of protoplasts. After incubation on ice for

10 min, 500 µl STC/PEG solution was added to it and mixed gently by pipetting up and down; this step was followed by another 10 min on ice. The transformation mix was added to 10 ml of molten regeneration (reg) agar (hand warm) and rapidly poured over a layer of already solidified reg-agar containing appropriate antibiotic solution (Table 5). The plates were incubated for 4-7 days at 22 °C/ 28 °C until small colonies appeared which were afterwards singled and grown on PD agar plates containing the respective antibiotics. The resulting single colonies were used for DNA extraction (chapter 4.5.1.2) and verified via Southern blot analysis (chapter 4.5.3.2).

SCS solution	20 mM Na-Citrate, pH 5.8 1 M Sorbitol in H ₂ O _{bid.} , sterile filtered
STC solution	10 mM Tris-HCl, pH 7.5 100 mM CaCl ₂ 1 M Sorbitol in H ₂ O _{bid.} , sterile filtered
STC/PEG solution	15 mL STC 10 g PEG4000

4.4.5 Mating assays of *M. bullatus* and *U. maydis*

To check for filamentous growth of *M. bullatus* and *U. maydis*, the strains can be grown on PDA medium supplemented with activated charcoal (Table 3), as the dikaryotic hyphae form aerial hyphae on this artificial media and appear as white and fluffy colonies. For that, strains were grown in 4 ml YEPSL medium at 22 °C/28 °C at 200 rpm to an optical density of OD₆₀₀ = 0.6. The cells were harvested at 2000 x g for 5 min and resuspended in H₂O_{bid.} to an OD₆₀₀ = 1.0. 5 µl of each culture were spotted on the plates. To test whether two strains can mate, they were mixed before in a ratio of 1:1. Photographs were taken 24 h – 48 h after incubation at 22 °C/ 28 °C.

4.4.6 Induction of filament and appressoria formation on artificial surfaces

A culture of fungal cells was started from cells grown on PDA medium in 4 ml YEPSL medium and incubated at 22 °C/ 28 °C at 200 rpm overnight. Afterwards cultures were diluted in 50 ml YEPSL medium and grown until it reached an optical density of OD₆₀₀ = 0.8.

Cells were harvested by centrifugation at 2000 x g for 5 min and the resulting pellet was resuspended in 2 % YEPSL to an OD₆₀₀ = 1.0. The cells were spray inoculated using airbrush guns (Conrad Electronics GmbH, Hirschau, Germany) to Parafilm M (Pechiney Plastic Packaging, Chicago, USA) and incubated for 16-20 h at 22 °C/ 28 °C at on wet filter paper inside a sealed petri dish. To quantify filament formation, the samples were mounted for microscopy and the percentage of filaments relative to total cells was determined. All experiments were done in at least three biological replicates. To induce appressoria formation strains were prepared as described before and mixed with HDD (f.c. 35 µg/ml) prior to spray inoculation on Parafilm M. Cells were incubated as described above. To quantify appressoria, surfaces were gently rinsed with water and Calcofluor white staining solution (Sigma-Aldrich, Deisenhofen, Germany) was added. To quantify the proportion of appressoria, filaments stained with Calcofluor white showing an appressoria were counted relative to filaments showing no appressoria.

4.4.7 Microbial confrontation assays

An overnight culture of fungal or bacterial cells was started from cells grown on PDA or KingsB-Agar plates in 4 ml YEPSL or KingsB medium and incubated at 22 °C/ 28 °C at 200 rpm. Afterwards cultures were diluted in 4 ml YEPSL or KingsB medium and grown to an optical density of OD₆₀₀ = 0.8-1. 100µl of bacterial cultures were spread on a PDA plate and remaining liquid on the plate was dried. Afterwards 10 µl of *M. bullatus* or *U. maydis* were dropped onto the bacterial cultures. The plates were incubated for 2 - 4 days at 22 °C and bacterial inhibition could be visualized as a halo formation around fungal cultures.

4.5 Molecular biological methods

4.5.1 Isolation of nucleic acids

4.5.1.1 Plasmid DNA isolation from *E. coli*

To isolate plasmid DNA from *E. coli* cells the QIAprep Mini Plasmid Prep Kit (Qiagen, Hilden, Germany) was used. This kit works on the principle of alkaline lysis. For that, 2 ml of a thickly grown overnight culture was pelleted at 12000 x g for 2 min in a 2 ml microcentrifuge tube. The pellet was resuspended in 250 µl P1 buffer and to lyse the cells, 250 µl P2 buffer were added, and the suspension was mixed by repeatedly inverting the tube. After incubating the mixture for 1 min at room temperature, 300 µl P3 buffer were added to neutralize the lysed cell extract and to precipitate proteins. The cell debris and precipitated proteins were pelleted by centrifugation at 12000 x g for 10 min. Afterwards 600 µl of the

supernatant were transferred into a 1.5 ml microcentrifuge tube containing 600 µl isopropanol. To precipitate plasmid DNA, the tubes were incubated at -20 °C for 30 min and afterwards centrifuged at 12000 x g for 10 min. The supernatant was discarded, and the resulting pellet was washed by adding 800 µl of 80 % EtOH and centrifugation for 10 min at 12000 x g. In the end, the supernatant was completely removed and the resulting pellet containing plasmid DNA was resuspended in 50 µl sterile water.

4.5.1.2 Isolation of genomic DNA from *M. bullatus* and *U. maydis*

For the isolation of fungal genomic DNA (gDNA), a modified version of the protocol from (Hoffman & Winston, 1987) was used. 2 ml of a thickly grown fungal overnight culture were pelleted at 12000 x g for 2 min in a 2 ml microcentrifuge tube. After discarding the supernatant, ~ 0.3 g glassbeads (0.4-0.6 mm), 400 µl Ustilago lysis buffer and 500 µl of Phenol/Chloroform/Isoamylalcohol 25:24:1 (Roth, Karlsruhe, Germany) was added to the cell pellet. Then, the microcentrifuge tube was incubated for 20 min on a Vibrax-VXR shaker (IKA, Staufen, Germany) at 2500 rpm for 20 min. To separate the phases, the tube was spun down for 15 min at 12000 x g. The upper clear phase, which contains the extracted DNA, was transferred to a fresh 1.5 ml microcentrifuge tube, and precipitated by addition of 400 µl isopropanol and centrifugation at 12000 x g for 2 min. Afterwards, the pellet was washed twice with 75 % EtOH at 12000 x g for 2 min. In the end the supernatant was discarded, the resulted pellet was dried for 1 min at room temperature and dissolved in 50 µl TE-buffer containing 20 µg/ml RNaseA by incubation in a Thermomixer (Eppendorf, Hamburg, Germany) at 55 °C, 1200 rpm, 30 min. The extracted DNA was stored at -20 °C.

Ustilago lysis buffer

50 mM Tris-HCl, pH 7.5
50 mM Na₂-EDTA
1 % (w/v) SDS
in H₂O bid.

4.5.1.3 RNA-Extraction of Latex-peeled samples

To extract RNA of surface associated organisms the microbes were peeled off from the surface by using liquid Latex. For this experiment 4 weeks old sterile plants (*A. thaliana* Col-O grown in MS-media; Table 3) were fixed between two fingers (if the material is bigger it can also be fixed on double sided tape) and liquid latex was applied to the leaf surface by using a small brush. The latex was dried by using a hair dryer (cold air! – during this procedure, the color changes from white to transparent) and could afterwards be carefully peeled off by using a thin tweezer. The material was immediately shock frozen in liquid N₂.

Afterwards the frozen latex pieces were grinded with liquid N₂, and the RNA was isolated by using TRIzol® reagent (Invitrogen, Darmstadt, Germany) following the recommended instructions. The material was filled into a 1.5 ml reaction tube and 1 ml TRIzol® reagent was immediately added and mixed. The sponge-like Latex debris were removed and the supernatant was transferred to a fresh 1.5 ml centrifuge tube with 200 µl chloroform. The sample was mixed by inversion of the tubes and centrifuged at 12000 x g for 15 min to separate phases. The upper aqueous phase was transferred to a fresh 1.5 ml reaction tube containing 500 µl isopropanol. After incubation at room temperature for 10 min, the RNA was precipitated by centrifugation at 12000 x g for 10 min. The supernatant was discarded, and the pelleted RNA was washed with 1 ml 75 % EtOH and centrifuged at 7500 x g for 5 min. In the end, the supernatant was removed, and the pellet was dissolved in 35 µl RNase-free H₂O at 55 °C for 10 min.

4.5.1.4 DNase-digest after RNA extraction

For removal of residual DNA inside extracted RNA samples, the Ambion®TURBO DNasefree™ Kit (Thermo Fisher Scientific Inc., Bonn, Germany) was used according to the manufacturer's instructions. For that, 4 µl 10x DNase buffer and 1 µl DNase were added to the extracted RNA and the mixture was incubated at 37 °C for 30 min. Next, 4 µl inactivation reagent were added and the sample was incubated for 5 min at room temperature. In the end, the sample was centrifuged at 7500 x g for 2 min and 35 µl were transferred to a fresh 1.5 ml reaction tube. The amount of RNA was assessed by photometric measurement on a NanoDrop 2000c spectrophotometer (Thermo Fisher Scientific Inc., Bonn, Germany) and quality was afterwards assessed by loading 1 µg of RNA on a 1 % TBE gel (see chapter 4.5.3.1).

4.5.1.5 Purification of DNA

Plasmid DNA and PCR fragments of restriction digest mixtures were purified using the NucleoSpin gel and PCR Clean-up kit (Machery-Nagel, Düren, Germany) either directly or via gel extraction. The purification was done according to the manufacturer's instructions.

4.5.2 *In vitro* modification of nucleic acids

4.5.2.1 Restriction of DNA

The enzymatic digest of DNA was done with type II restriction endonucleases (NEB, Frankfurt/Main, Germany). The amount of digested DNA ranged from 1 – 5 µg. The reaction was set up according to the manufacturer's instructions. A common digestion reaction was composed as follows:

1 – 5 µg	DNA (plasmid or cleaned-up PCR product)
2 µl	10x NEB buffer (P1-4)
0.5 U	restriction enzyme
Ad 20 µl	H ₂ O bid.

4.5.2.2 Ligation of DNA fragments

To ligate DNA fragments the T4 DNA ligase (Thermo scientific, Bonn, Germany) was used according to the manufacturer's instructions. For the ligation of a desired insert with a corresponding vector backbone, a molar ratio of 3:1 – 10:1 was used to ensure a higher abundance of insert. A standard ligation mixture was set up as follows:

50 ng	vector DNA
3 – 10x	Insert DNA
2 µl	10x T4 DNA ligase buffer
1 µl	T4 DNA ligase
Ad 20 µl	H ₂ O bid.

The ligation reaction was incubated for 1 h at room temperature or overnight at 4 °C.

4.5.2.3 A-tailing of PCR products

For ligation of blunt-end DNA-fragments, produced by proof-reading polymerases, in the pGEM®-T vector system A-tails were added. For this 0.2 volume of the GoTaq® Green Master Mix (Promega, Walldorf, Germany) was added to 20 µl of DNA-fragment and samples were incubated for 20 min at 72 °C.

4.5.2.4 Fragment assembly using pGEM®-T Easy vector system

To ligate a DNA-fragment in the pGEM®-T Easy vector system manufacturer's instructions were followed. For the ligation of a desired insert DNA-fragment in a corresponding vector backbone, a molar ratio of 2:1 - 3:1 was used.

4. Material & Methods

50 ng	pGem®T-Easy vector
2 – 3x	Insert DNA
5 µl	2x Rapid Ligation & T4 DNA Ligase Buffer
1 µl	T4 DNA ligase (3 U/µl)
Ad 10 µl	H2Obid.

The ligation reaction was incubated for 1 h at room temperature or overnight at 4 °C.

4.5.2.5 Fragment assembly using Gibson Assembly system

The reaction is carried out under isothermal conditions using three enzymatic activities: a 5' exonuclease generates long overhangs, a polymerase fills in the gaps of the annealed single strand regions, and a DNA ligase seals the nicks of the annealed and filled-in gaps. To assemble fragments with the NEBuilder® HiFi DNA Assembly Master Mix (NEB, Frankfurt/Main, Germany) adjoining fragments need to overlap with 15-20 bp. The reaction mix was prepared as following:

50-100 ng	Vector DNA
0.2 pmol	Insert DNA (each fragment)
7.5 µl	NEBuilder® HiFi DNA Assembly Master Mix
Ad 10 µl	H2Obid.

Samples were incubated at 50 °C for 60 min and stored at -20 °C for subsequent transformation.

4.5.2.6 Polymerase chain reaction (PCR)

For the amplification of DNA fragments via polymerase chain reaction (PCR) different polymerases were used depending on the purpose of the experiment. For common cloning processes of genes from all organisms used in this study the Phusion® *Hot Start High Fidelity* DNA-Polymerase (Finnzymes/Thermo Scientific, Bonn, Germany) was used due to its proof-reading ability. For the cloning long DNA-fragments (>5kb), KOD Xtreme™ Hot Start DNA Polymerase (Merck Millipore, Darmstadt, Germany) was used. General analytical tests like colony PCR and all other PCRs that were not used for further cloning processes, were done with the GoTaq® Green Master Mix (Promega, Walldorf, Germany). Every PCR reaction was set up in a 20 µl or 50 µl reaction volume depending on its purpose of use. PCR reactions were set up according to the manufacturer's instructions.

4.5.2.7 cDNA synthesis

After isolation of RNA and DNase treatment (RNA-Extraction of Latex-peeled samples & DNase-digest after RNA extraction), cDNA was synthesized by using the RevertAid H Minus First Strand cDNA Synthesis Kit (Thermo Scientific, Bonn, Germany) according to the manufacturer's instructions. For one reaction, 10 µg total RNA was transcribed into cDNA using oligo(dT)₁₈ primer in a total reaction volume of 12 µl. Due to high GC-contents in the *M. bullatus* genome, samples were incubated at 65 °C for 5 min and afterwards chilled on ice. 4 µl 5x Reaction buffer, 1 µl RiboLock RNase Inhibitor (20 U/µl), 2 µl 10 mM dNTP Mix and 1 µl RevertAid H Minus M-MuIV Reverse Transcriptase (200 U/µl) was added to the sample which was then incubated at 25 °C for 5 min followed by synthesis of cDNA for 60 min at 45 °C. To stop the reaction samples were heated up to 70 °C for 5 min. The cDNA was placed at -20 °C for short term and at -80 °C for long term storage.

4.5.2.8 Sequencing of DNA

Sequencing reactions were performed by Eurofins (formerly GATC, Cologne, Germany). For sequencing of plasmids or PCR products DNA was cleaned up with the NucleoSpin gel and PCR Clean-up kit (Machery-Nagel, Düren, Germany) as described in chapter 4.5.1.5. DNA sequencing results were analyzed using Clone Manager 9 software (SciEd, Denver, US).

4.5.2.9 Sequencing of RNA

Sequencing library preparation was done using the Illumina TruSeq mRNA stranded Kit (Illumina, San Diego, USA). Illumina sequencing of mRNA was performed with 150 bp paired end reads at the Cologne Center for Genomics (CCG, Cologne, Germany) on an Illumina HiSeq 4000 (Illumina, San Diego, USA).

4.5.3 Separation and detection of nucleic acids

4.5.3.1 Agarose gel electrophoresis

Agarose gel electrophoresis was performed for the separation and estimation of size of nucleic acids. Agarose gels of 0.6 – 2 % Agarose concentration were prepared in 1x TAE buffer, by boiling in a microwave. After the buffer had cooled to ~60 °C, ethidium bromide (f.c. 0.25 µg/ml) was added. After solidification of the gel, the samples containing 1x DNA-loading dye were loaded for separation into the pockets of the gel and were run in a chamber containing 1x TAE buffer. Separation of DNA was done at constant voltage of 80-120 V depending on the size and percentage of the gel in parallel to a DNA marker of defined

4. Material & Methods

marker size. DNA bands were visualized by UV radiation at 365 nm using a gel documentation unit (Peqlab/VWR, Langenfeld, Germany).

50x TAE-buffer

2 M Tris-Base
2 M Acetic acid
50 mM EDTA pH 8.0

6x DNA loading dye

50 % (w/v) Sucrose
0.13 % (w/v) Bromophenol blue

4.5.3.2 Southern Blot analysis

After transformation of *M. bullatus* & *U. maydis* (chapter 4.4.4), transformants were singled and DNA was isolated (chapter 4.5.1.5) and subjected to Southern blot analysis (Southern, 2006) to check for the right integration into the genome. For that, 5 µg of DNA was fragmented via restriction enzyme digest. The restriction enzyme was selected to lead to fragment sizes of the locus that define a distinguishable size difference between transformed locus of interests and corresponding wild type locus. The DNA digest was incubated overnight in a volume of 200 µl. The fragmented DNA was afterwards precipitated by adding 15 µl 3 M potassium acetate and 1 mL 100 % ethanol and incubation of the samples at -20 °C for 30 min followed by centrifugation for 15 min at 17000 x g. The DNA pellets were then washed with 750 µl 80 % ethanol and afterwards again centrifuged for 5 min at 17000 x g. After centrifugation for 5 min at 17000 x g, the supernatant was removed, and the pellet was resuspended in 20 µl 1x DNA loading dye. The samples were separated via agarose gel electrophoresis (see chapter 4.5.3.1) in a 0.8 % agarose gel in 1x TAE buffer and separation of the fragment was documented using a gel documentation unit (Peqlab/VWR, Langenfeld, Germany). To facilitate the transfer of big DNA fragments, depurination of large fragments was achieved by incubating the gel in 0.125 N HCl for 15 min and afterwards neutralizing the gel in 0.4 N NaOH for 30 min. Transfer of nucleic acids was done in 0.4 N NaOH transfer solution via capillary forces to a Hybond-N+ nylon membrane (GE, Munich, Germany) following the protocol by Southern (1975). For that, the transfer buffer was sucked overnight into paper towels through the gel and DNA fragments onto the nylon membrane lying on top of the gel. On the next day the DNA fragments were fixed to the nylon membrane by UV cross-linking using an ultraviolet crosslinker (Roth, Karlsruhe, Germany). The membrane was then immediately pre-hybridized for 1 h at 65 °C in 20 mL hybridization buffer in a hybridization oven (UVP HB-1000 Hybridizer, VWR, Langenfeld, Germany). Nucleic acids were detected by using digoxigenin (DIG)-labeled

DNA probes, synthesized by using the PCR DIG Labeling Mix kit (Roche, Mannheim, Germany) following the manufacturer's instructions. To denature the DIG-labeled PCR products, they were added to 20 mL of hybridization buffer and heated for 10 min to 100 °C. The prehybridization buffer was exchanged with probe-containing buffer and hybridization was performed at 65 °C in the hybridization oven overnight. Afterwards the membrane was washed twice with southern wash buffer for 15 min at 65 °C in the hybridization oven followed by two 5 min washing steps with DIG wash buffer at room temperature and 30 min incubation in DIG buffer 2. Afterwards, the membrane was incubated in antibody solution for 30 min followed by two washing steps in DIG wash buffer for 15 min each. After incubation in DIG buffer 3 for 5 min, 2.4 ml CDP-Star solution was added. The blot was put into an autoclaving bag and analyzed by using a ChemiDoc MP System (BioRad, Munich, Germany) for 1 – 10 min depending on signal intensity.

1 M sodium phosphate buffer	Solution 1: 1 M Na ₂ HPO ₄ Solution 2: 1M NaH ₂ PO ₄ * H ₂ O Solution 2 is added to solution 1 until the pH reaches 7.0
Southern hybridization buffer	500 mM Sodium phosphate buffer, pH 7.0 7 % (w /v) SDS
Southern wash buffer	0.1 M Sodium phosphate buffer, pH 7.0 1 % (w /v) SDS
DIG buffer 1	0.1 M Maleic acid, pH 7.5 0.15 M NaCl
DIG buffer 2	0.1 M Maleic acid, pH 7.5 0.15 M NaCl 1 % (w /v) Milk powder
DIG buffer 3	0.1 M Maleic acid, pH 9.5 0.1 M NaCl 0.05 M MgCl ₂
DIG wash buffer	0.1 M Maleic acid, pH 7.5 0.15 M NaCl 0.3 % (v /v) Tween-20

DIG Antibody solution	0.1 M Maleic acid, pH 7.5 0.15 M NaCl 1 % (w /v) Milk powder 0.01 % (v/v) Anti-Dig Antibody
CDP-Star solution	0.1 M Maleic acid, pH 9.5 0.1 M NaCl 0.05 M MgCl ₂ 1 % (v/v) CDP-star solution

4.6 Biochemical methods

4.6.1 Separation of proteins via SDS-PAGE

Separation of proteins was done according to (Laemmli, 1970) by Sodium dodecyl sulfate polyacrylamide gel electrophoresis (SDS-PAGE), where denatured and negatively charged proteins are separated according to their molecular size in an electric field. To denature the proteins, samples were boiled for 5 min at 99 °C in 1x SDS gel loading buffer containing 100 mM DTT. The gels for SDS-PAGE composed of an upper stacking and a lower separating gel and were casted using the Mini Protean System (BioRad, Munich, Germany). Samples were loaded into the casted gel pockets and gels were run in 1x SDS running buffer in a gel chamber at a constant voltage of 120-160V for 1 h. To estimate the molecular mass, the PageRuler prestained protein ladder (Thermo Fisher Scientific Inc., Bonn, Germany) was used.

6x SDS-gel loading buffer	4M Tris-HCl, pH 6.8 6 % (w /v) SDS 0.15 % (w /v) Bromophenol blue 60 % (v /v) Glycerol
SDS running buffer	25 mM Tris-HCl, pH 8.3 192 mM Glycine 4 mM SDS
Stacking gel	5 % (v/v) Acrylamide 0.1 % (w/v) SDS in 125 mM Tris-HCl, pH 6.8 0.1 % (w/v) Ammonium persulfate 0.1 % (v/v) Tetramethylethylenediamine (TEMED)
Separating gel	12 % (v/v) Acrylamide 0.1 % (w/v) SDS in 375 mM Tris-HCl, pH 8.8 0.1 % (w/v) Ammonium persulphate 0.04 % (v/v) TEMED

4.6.2 Staining of SDS-PAGE gels

SDS-PAGE gels containing sample proteins were stained with coomassie brilliant blue staining solution for 3 to 4 h at RT. Destaining was performed with coomassie brilliant blue destain solution until the desired stain is reached. The destain solution should be changed several times during washing.

Coomassie brilliant blue staining solution	40 % (v/v) H ₂ O _{bid.} 45 % (v/v) Methanol 10 % (v/v) Acetic acid 0.1 % (w/v) Coomassie blue R350
Coomassie brilliant blue destaining solution	40 % (v/v) H ₂ O _{bid.} 45 % (v/v) Methanol 10 % (v/v) Acetic acid

4.6.3 Immunological detection of proteins via chemiluminescence (Western blot)

After separation of proteins by SDS-PAGE, the proteins were transferred to a Polyvinylidene fluoride (PVDF; Amersham Hybond P 0.45 PVDF blotting membrane, GE Healthcare, Munich, Germany) membrane and desired tagged proteins were detected by immunostaining using specific antibodies. Prior to blotting, the PVDF membrane was activated by adding pure MeOH and Whatman paper were soaked in transfer buffer. The SDS protein gel was first washed with H₂O_{bid.} and afterwards with transfer buffer to remove remaining SDS-running buffer. The blot was built from bottom to top as follows: Whatman paper, activated PVDF-membrane, SDS-gel, Whatman paper. The blot was transferred to a Trans-Blot Turbo Transfer system (BioRad, Munich, Germany) and proteins were transferred by adding a constant voltage of 25 V and 1 Ampere (A) for 25 - 30 min, depending on the size of the desired protein. After blotting the transferred proteins were fixed by adding methanol to the membrane. For immunological detection of proteins, the membrane was first incubated in blocking solution for 1 h at RT or overnight at 4 °C. Antibodies were diluted in antibody solution according to manufacturer instructions. The membrane was incubated with the primary antibody, which is specific for the tag of the desired protein, for 1 h at RT or at 4 °C overnight. Afterwards excessive and unspecific bound antibody was removed from the membrane by washing it three times with TBS-T buffer for 5 min and the secondary antibody, which is specific to the primary antibody, was added for 1 h at RT. Again, excessive, and unspecific bound secondary antibody was

4. Material & Methods

removed from the membrane by washing it three times with TBS-T buffer. The desired tagged protein was visualized by addition of the enhanced chemiluminescence reagent SuperSignal™ West Pico (Thermo Fisher Scientific Inc., Bonn, Germany) to the membrane, which was placed in a plastic bag. The enhanced chemiluminescence reagent is processed by the Horseradish peroxidase, which is bound to the secondary antibody and releases a chemiluminescent signal (475 nm) which is documented using a ChemiDoc™ MP system (BioRad, Munich, Germany).

Western transfer buffer	39 mM glycine 48 mM Tris-base 0.0375 % SDS 20 % Methanol
TBS-T buffer	50 mM Tris-HCl, pH 7.5 150 mM NaCl 0.1 % (v/v) Tween-20 0.2

Table 11: Antibodies used in this study.

Antibody	Organism	Working dilution	Supplier
His	Mouse	1/10000	Sigma-Aldrich (Deisenhofen, Germany)
Mouse IgG	Goat	1/3000	Thermo Fisher Scientific Inc., (Bonn, Germany)

4.6.4 Expression of heterologous proteins in *P. pastoris*

A small-scale expression was performed to identify recombinant *P. pastoris* clones that are expressing the correct protein. For this a single colony was used to inoculate an overnight culture in 10 ml YPD medium (Table 3). 0.1 ml of this overnight culture were used to inoculate 50 ml YPD and were grown at 30 °C and 200 rpm. After 24 h and 48 h 1 ml of this culture was transferred to a microcentrifuge tube and centrifuged at 17000 x g for 3 min. The supernatant was transferred to a new tube and both, pellet and supernatant, were shock frozen in liquid N₂ and stored at -80 °C until ready to assay by western blot.

4.7 Plant methods

4.7.1 Plant material and growth conditions

All *A. thaliana* plants were grown in Phyto chambers at 22 °C on a short-day period (8 h light) with 33-40 % humidity. During the night temperature was decreased to 18 °C (16 h dark). For gnotobiotic experiments plants were grown in 12-well petri dishes on 1/2MS-agar. Millet plants were grown in a greenhouse at 22 °C on long day period (16h light and 8h night period). Maize was grown in a greenhouse at 28 °C on a long day period (16 h light) with 80% humidity and a 8 h night period at 22 °C.

Table 12: *A. thaliana* ecotypes used in this study

Ecotype	Origin	Experiment
Columbia-0 (Col-0)	United states of America	Gnotobiotic experiments
Wassilewskija-0 (Ws-0)	Russia	Albugo spore propagation

4.7.2 Seed sterilization

A. thaliana seeds were collected in a 1.5 ml reaction tube and treated with 600 µl 1.5 % NaClO/ 0.02 % Triton for 5 min under vigorous shaking. All further steps were carried out under sterile conditions. The supernatant was removed, and the seeds were washed 5 times with H₂O_{bid}. Seeds were stored for vernalization in 500 µl 0.1 % agar light-tight at 4 °C for 1 week.

4.7.3 Infections of *A. thaliana* with *A. laibachii*

Three to four sterilized *A. thaliana* seeds were sown on 0.5x MS medium (**Table 3**) covered with autoclaving bag discs in 12-well petri dishes. After 2 weeks additional seedlings were removed, so that only one plant remained per well. Infections with *A. laibachii* were performed three weeks after sawing. Overnight liquid cultures of *M. bullatus* and SynCom bacterial strains were diluted and grown to an OD₆₀₀ = 0.6. The cultures were spun down at 2000 x g for 10 min, the pellets dissolved in 10mM MgCl₂ and 500 µl of each culture was evenly sprayed on each *A. thaliana* seedling using airbrush guns (Conrad Electronics GmbH, Hirschau, Germany). Two days later, a spore solution of *A. laibachii* was prepared as described in Propagation of *A. laibachii* and the zoospores were pelleted at 2000 x g for 10 min. The supernatant was removed, and the spores were treated with 2 ml of an antibiotic mix (Kanamycin 500 µg/ml, Rifampicin 500 µg/ml, Streptomycin 625 µg/ml and Gentamycin 250 µg/ml) for 25 min at room temperature in darkness. Afterwards spores

4. Material & Methods

were washed 3 times with sterile water and spore number was adjusted to 15×10^4 spores/ml in 10mM MgCl₂. 500 µl of *A. laibachii* spore solution was sprayed on each *A. thaliana* seedling and disease symptoms on the leaves could be quantified 2 weeks later as a percentage between infected and non-infected leaves.

4.7.4 Virulence assay of *U. maydis* on maize

Virulence assays of *U. maydis* on maize were performed and symptoms were classified as described in Redkar and Doehlemann (2016a). *U. maydis* strains that were used for infection of *Z. mays* were grown overnight in YEPsLight liquid medium at 28 °C under constant shaking at 200 rpm until reaching OD₆₀₀ of 0.6–1.0. Subsequently, the cells were harvested by centrifugation (10 min at 2.400 g) and resuspended in sterile water at an OD₆₀₀ of 1.0. Syringe infections were made with 300–500 µl of the cell suspension into the interior of leaf whorl of 7-day-old corn plants for seedling infections. The injection site was chosen to be approximately 1 cm above the earth, which is about 2.5 to 3 cm above the basal plant meristem. Here, the leaf sheaths of the first and second leaf and the leaf blades of the third and fourth sheet were pierced by the syringe which later shows an infection mark after the symptom development. Disease symptoms on maize seedlings infected by *U. maydis* were scored after 6 dpi and the following scoring theme was applied.

Table 13: Classification of disease symptoms in infected maize seedlings

Disease symptom	Description of symptom
No symptoms	The leaf does not show any disease symptoms or sign of infection
Chlorosis	The leaf has chlorotic areas around the infection site on the infected leaf and younger leaves
Small tumors	Tumors around the infection area are ≤ 1 mm on the infected leaf and younger leaves
Normal tumors	Tumors around the infection area are ≥ 1 mm on the infected leaf and younger leaves
Big tumors	Very big tumors are formed on the infected leaf or younger leaves including the plant stem that leads to an overall bending of the plant
Dead plant	Plant has died due to <i>U. maydis</i> infection

4.8 Microscopy

4.8.1 WGA-AF488/Propidium iodide co-staining of colonised maize tissue

To visualize growth of *M. bullatus* after coleoptile infections a WGA-AF488 and propidium iodide co-staining was performed as described in Redkar et al. (2018).

4.8.2 Fluorescence microscopy

Imaging was performed by using a Nikon Eclipse Ti inverted microscope (Nikon Instruments Microscopes and Digital Imaging Systems, Alzenau, Germany) using the filter set indicated in Table 14. High resolution digital images were recorded using a Hamamatsu C11440 ORCA-flash4.0LT camera (Hamamatsu Photonics, Herrsching am Ammersee, Germany).

Table 14: Filters used for fluorescence microscopy with their respective spectra

Filter	Excitation spectra	Detection spectra	Purpose of use
eGFP HC Filter set	455 nm – 490 nm	500 nm – 540 nm	eGFP detection
DAPI Filter set	350 nm – 400 nm	415 nm – 475 nm	DAPI detection
DsRed filter	540 nm – 580 nm	600 nm – 690 nm	PI detection, chlorophyll autofluorescence

4.8.3 Image processing and measurement

M. bullatus and *U. maydis* cells were analyzed and counted using the Nikon Instruments NIS-Elements (Nikon Instruments Microscopes and Digital Imaging Systems, Alzenau, Germany) software and the CorelDraw Graphics Suite (Corel Corporation, Ottawa, Canada).

4.9 Bioinformatics and computational data analysis

4.9.1 RNAseq analysis

RNAseq data was provided by the Cologne Center for Genomics, Cologne, Germany. Reads from RNAseq data were mapped with Bowtie v2.2.9 (Langmead & Salzberg, 2012) and TopHat v2.1.1 (Kim et al., 2013) against the reference genomes of *M. bullatus* (this study) and *A. thaliana* TAIR10 genome (obtained from the Arabidopsis Information Resource (TAIR) download server (<ftp://ftp.arabidopsis.org/home/tair>) on December 12th, 2017). Differentially expressed genes were determined with the R package "limma" on 'voom'-transformed count data.

4.9.2 Further bioinformatic analysis tools

De novo genome sequencing of *M. bullatus* was performed at the Max Planck Sequencing service by using SMRT sequencing (Pacific Biosciences, Munich, Germany) and the received raw reads were assembled by using the HGAP pipeline. Gene prediction of the assembled genome sequence was done with the Augustus software tool (Stanke und Waack 2003), which was trained with the *U. maydis* genome sequence. RNA-Seq reads of

4. Material & Methods

M. bullatus axenic cultures were used to generate exon and intron hints and to start a second gene prediction. Functional gene annotation was performed by using Blast2Go (BioBam Bioinformatics, Valencia, Spain). The Secretome was investigated by using SignalP 4.0 (Petersen et al., 2011) and functional domains in secreted proteins were predicted by doing an Inter-Pro Scan (Jones et al., 2014). Potential Transmembrane domains were predicted by using TMHMM 2.0 (Krogh et al., 2001). AntiSmash 4.0 (Blin et al., 2017) was used to predict potential secondary metabolite clusters. Heat-maps were performed using the heatmap.2 function of the package gplots v3.0.1 in R-studio v3.5.1 (RStudio Inc., Boston, Massachusetts, USA). An analysis of variance (ANOVA) model was used for pairwise comparison of the conditions, with Tukey & HSD test to determine significant differences among them (P values <0.05).

Data availability

Genome information and RNA sequencing have been submitted to NCBI Genbank and are available under the following links:

<https://www.ncbi.nlm.nih.gov/geo/query/acc.cgi?acc=GSE148670>

5 Bibliography

- Abril, A. B., Torres, P. A., & Bucher, E. H. (2005). The importance of phyllosphere microbial populations in nitrogen cycling in the Chaco semi-arid woodland. *Journal of Tropical Ecology*, 21(1), 103-107. doi:10.1017/S0266467404001981
- Agler, M. T., Ruhe, J., Kroll, S., Morhenn, C., Kim, S.-T., Weigel, D., & Kemen, E. M. (2016). Microbial Hub Taxa Link Host and Abiotic Factors to Plant Microbiome Variation. *PLOS Biology*, 14(1), e1002352. doi:10.1371/journal.pbio.1002352
- Agrios, G. N. (2005). *Plant pathology*: Academic Press. San Diego. US.
- Ahmed, A., Rushworth, J. V., Hirst, N. A., & Millner, P. A. (2014). Biosensors for Whole-Cell Bacterial Detection. *Clinical Microbiology Reviews*, 27(3), 631-646. doi:10.1128/cmr.00120-13
- Ali, S., Laurie, J. D., Linning, R., Cervantes-Chávez, J. A., Gaudet, D., & Bakkeren, G. (2014). An Immunity-Triggering Effector from the Barley Smut Fungus *Ustilago hordei* Resides in an Ustilaginaceae-Specific Cluster Bearing Signs of Transposable Element-Assisted Evolution. *PLoS Pathog*, 10(7), e1004223. doi:10.1371/journal.ppat.1004223
- Alquères, S., Meneses, C., Rouws, L., Rothballer, M., Baldani, I., Schmid, M., & Hartmann, A. (2013). The bacterial superoxide dismutase and glutathione reductase are crucial for endophytic colonization of rice roots by *Gluconacetobacter diazotrophicus* PAL5. *Mol Plant Microbe Interact*, 26(8), 937-945. doi:10.1094/mpmi-12-12-0286-r
- Aronson, J. M., Cooper, B. A., & Fuller, M. S. (1967). Glucans of oomycete cell walls. *Science*, 155(3760), 332-335. doi:10.1126/science.155.3760.332
- Arutchevi, J. I., Bhaduri, S., Uppara, P. V., & Doble, M. (2008). Mannosylerythritol lipids: a review. *Journal of Industrial Microbiology and Biotechnology*, 35(12), 1559-1570. doi:10.1007/s10295-008-0460-4
- Asai, S., & Shirasu, K. (2015). Plant cells under siege: plant immune system versus pathogen effectors. *Curr Opin Plant Biol*, 28, 1-8. doi:10.1016/j.pbi.2015.08.008
- Ausubel, F. M. (2002). *Short protocols in molecular biology : a compendium of methods from Current protocols in molecular biology* (5th ed.). New York: Wiley.
- Avis, T. J., & Bélanger, R. R. (2002). Mechanisms and means of detection of biocontrol activity of *Pseudozyma* yeasts against plant-pathogenic fungi. *FEMS Yeast Res*, 2(1), 5-8. doi:10.1111/j.1567-1364.2002.tb00062.x
- Backer, R., Rokem, J. S., Ilangumaran, G., Lamont, J., Praslickova, D., Ricci, E., Subramanian, S., & Smith, D. L. (2018). Plant Growth-Promoting Rhizobacteria: Context, Mechanisms of Action, and Roadmap to Commercialization of Biostimulants for Sustainable Agriculture. *Front Plant Sci*, 9(1473). doi:10.3389/fpls.2018.01473

5. Bibliography

- Bakkeren, G., Kämper, J., & Schirawski, J. (2008). Sex in smut fungi: Structure, function and evolution of mating-type complexes. *Fungal Genetics and Biology*, *45*, S15-S21. doi:10.1016/j.fgb.2008.04.005
- Barda, O., Shalev, O., Alster, S., Buxdorf, K., Gafni, A., & Levy, M. (2015). Pseudozyma aphidis Induces Salicylic-Acid-Independent Resistance to Clavibacter michiganensis in Tomato Plants. *Plant Dis*, *99*(5), 621-626. doi:10.1094/pdis-04-14-0377-re
- Bardin, M., Ajouz, S., Comby, M., Lopez-Ferber, M., Graillot, B., Siegwart, M., & Nicot, P. C. (2015). Is the efficacy of biological control against plant diseases likely to be more durable than that of chemical pesticides? *Front Plant Sci*, *6*, 566. doi:10.3389/fpls.2015.00566
- Begerow, D., Bauer, R., & Boekhout, T. (2000). Phylogenetic placements of ustilaginomycetous anamorphs as deduced from nuclear LSU rDNA sequences* *Part 174 of the series 'Studies in Heterobasidiomycetes'. *Mycological Research*, *104*(1), 53-60. doi:10.1017/S0953756299001161
- Begerow, D., Stoll, M., & Bauer, R. (2006). A phylogenetic hypothesis of Ustilaginomycotina based on multiple gene analyses and morphological data. *Mycologia*, *98*(6), 906-916. doi:10.1080/15572536.2006.11832620
- Bélanger, R. R., Labbé, C., Lefebvre, F., & Teichmann, B. (2012). Mode of action of biocontrol agents: all that glitters is not gold. *Canadian Journal of Plant Pathology*, *34*(4), 469-478. doi:10.1080/07060661.2012.726649
- Benevenuto, J., Teixeira-Silva, N. S., Kuramae, E. E., Croll, D., & Monteiro-Vitorello, C. B. (2018). Comparative Genomics of Smut Pathogens: Insights From Orphans and Positively Selected Genes Into Host Specialization. *Front Microbiol*, *9*(660). doi:10.3389/fmicb.2018.00660
- Berg, G., Grube, M., Schloter, M., & Smalla, K. (2014). Unraveling the plant microbiome: looking back and future perspectives. *Front Microbiol*, *5*, 148. doi:10.3389/fmicb.2014.00148
- Blin, K., Wolf, T., Chevrette, M. G., Lu, X., Schwalen, C. J., Kautsar, S. A., Suarez Duran, H. G., de Los Santos, E. L. C., Kim, H. U., Nave, M., Dickschat, J. S., Mitchell, D. A., Shelest, E., Breitling, R., Takano, E., Lee, S. Y., Weber, T., & Medema, M. H. (2017). antiSMASH 4.0-improvements in chemistry prediction and gene cluster boundary identification. *Nucleic Acids Res*, *45*(W1), W36-w41. doi:10.1093/nar/gkx319
- Boekhout, T. (1995). <i>PSEUDOZYMA</i> BANDONI EMEND. BOEKHOUT, A GENUS FOR YEAST-LIKE ANAMORPHS OF USTILAGINALES. *The Journal of General and Applied Microbiology*, *41*(4), 359-366. doi:10.2323/jgam.41.359
- Bölker, M., Urban, M., & Kahmann, R. (1992). The a mating type locus of U. maydis specifies cell signaling components. *Cell*, *68*(3), 441-450. doi:10.1016/0092-8674(92)90182-C
- Bordenstein, S. R., & Theis, K. R. (2015). Host Biology in Light of the Microbiome: Ten Principles of Holobionts and Hologenomes. *PLoS Biol*, *13*(8), e1002226. doi:10.1371/journal.pbio.1002226

- Bösch, K., Frantzeskakis, L., Vraneš, M., Kämper, J., Schipper, K., & Göhre, V. (2016). Genetic Manipulation of the Plant Pathogen *Ustilago maydis* to Study Fungal Biology and Plant Microbe Interactions. *Journal of visualized experiments : JoVE*(115), 54522. doi:10.3791/54522
- Bottin, A., Kämper, J., & Kahmann, R. (1996). Isolation of a carbon source-regulated gene from *Ustilago maydis*. *Mol Gen Genet*, 253(3), 342-352. doi:10.1007/pl00008601
- Boyer, J. S. (1982). Plant productivity and environment. *Science*, 218(4571), 443-448. doi:10.1126/science.218.4571.443
- Brefort, T., Doehlemann, G., Mendoza-Mendoza, A., Reissmann, S., Djamei, A., & Kahmann, R. (2009). *Ustilago maydis* as a Pathogen. *Annu Rev Phytopathol*, 47, 423-445. doi:10.1146/annurev-phyto-080508-081923
- Brefort, T., Tanaka, S., Neidig, N., Doehlemann, G., Vincon, V., & Kahmann, R. (2014). Characterization of the largest effector gene cluster of *Ustilago maydis*. *PLoS Pathog*, 10(7), e1003866. doi:10.1371/journal.ppat.1003866
- Brito, L. F., López, M. G., Straube, L., Passaglia, L. M. P., & Wendisch, V. F. (2020). Inorganic Phosphate Solubilization by Rhizosphere Bacterium *Paenibacillus sonchi*: Gene Expression and Physiological Functions. *Front Microbiol*, 11(3122). doi:10.3389/fmicb.2020.588605
- Brown, J. K. M., & Rant, J. C. (2013). Fitness costs and trade-offs of disease resistance and their consequences for breeding arable crops. *Plant Pathology*, 62(S1), 83-95. doi:10.1111/ppa.12163
- Burch, A. Y., Zeisler, V., Yokota, K., Schreiber, L., & Lindow, S. E. (2014). The hygroscopic biosurfactant syringafactin produced by *Pseudomonas syringae* enhances fitness on leaf surfaces during fluctuating humidity. *Environ Microbiol*, 16(7), 2086-2098. doi:10.1111/1462-2920.12437
- Burrill, T. J. (1883). New Species of *Micrococcus* (Bacteria). *The American Naturalist*, 17, 319-320.
- Buxdorf, K., Rahat, I., Gafni, A., & Levy, M. (2013). The epiphytic fungus *Pseudozyma aphidis* induces jasmonic acid- and salicylic acid/nonexpressor of PR1-independent local and systemic resistance. *Plant Physiol*, 161(4), 2014-2022. doi:10.1104/pp.112.212969
- Buzzini, P., & Martini, A. (2000). Biodiversity of killer activity in yeasts isolated from the Brazilian rain forest. *Can J Microbiol*, 46(7), 607-611. doi:10.1139/w00-032
- Calderón, C. E., Rotem, N., Harris, R., Vela-Corcía, D., & Levy, M. (2019). *Pseudozyma aphidis* activates reactive oxygen species production, programmed cell death and morphological alterations in the necrotrophic fungus *Botrytis cinerea*. *Mol Plant Pathol*, 20(4), 562-574. doi:10.1111/mpp.12775
- Carrión, V. J., Perez-Jaramillo, J., Cordovez, V., Tracanna, V., de Hollander, M., Ruiz-Buck, D., Mendes, L. W., van Ijcken, W. F. J., Gomez-Exposito, R., Elsayed, S. S., Mohanraju, P., Arifah, A., van der Oost, J., Paulson, J. N., Mendes, R., van Wezel, G. P., Medema, M. H., & Raaijmakers, J. M. (2019). Pathogen-induced activation of

5. Bibliography

- disease-suppressive functions in the endophytic root microbiome. *Science*, 366(6465), 606-612. doi:10.1126/science.aaw9285
- Carvalho, F. P. (2006). Agriculture, pesticides, food security and food safety. *Environmental Science & Policy*, 9(7), 685-692. doi:10.1016/j.envsci.2006.08.002
- Cavalier-Smith, T., & Chao, E. E. (2006). Phylogeny and megasystematics of phagotrophic heterokonts (kingdom Chromista). *J Mol Evol*, 62(4), 388-420. doi:10.1007/s00239-004-0353-8
- Cawoy, H., Debois, D., Franzil, L., De Pauw, E., Thonart, P., & Ongena, M. (2014). Lipopeptides as main ingredients for inhibition of fungal phytopathogens by *Bacillus subtilis*/amyloliquefaciens. *Microb Biotechnol*, 8(2), 281-295. doi:10.1111/1751-7915.12238
- Chialva, M., Salvioli di Fossalunga, A., Daghino, S., Ghignone, S., Bagnaresi, P., Chiapello, M., Novero, M., Spadaro, D., Perotto, S., & Bonfante, P. (2018). Native soils with their microbiotas elicit a state of alert in tomato plants. *New Phytologist*, 220(4), 1296-1308. doi:10.1111/nph.15014
- Christensen, J. J. (1963). *Corn smut caused by Ustilago maydis*. [Worcester, Mass.] :: American Phytopathological Society.
- Ciancio, A., Pieterse, C. M. J., & Mercado-Blanco, J. (2019). Editorial: Harnessing Useful Rhizosphere Microorganisms for Pathogen and Pest Biocontrol - Second Edition. *Front Microbiol*, 10(1935). doi:10.3389/fmicb.2019.01935
- Cohen, S. N., Chang, A. C. Y., & Hsu, L. (1972). Nonchromosomal Antibiotic Resistance in Bacteria: Genetic Transformation of *Escherichia coli* by R-Factor DNA. *Proceedings of the National Academy of Sciences*, 69(8), 2110-2114. doi:10.1073/pnas.69.8.2110
- Compant, S., Duffy, B., Nowak, J., Clément, C., & Barka, E. A. (2005). Use of plant growth-promoting bacteria for biocontrol of plant diseases: principles, mechanisms of action, and future prospects. *Appl Environ Microbiol*, 71(9), 4951-4959. doi:10.1128/aem.71.9.4951-4959.2005
- Compant, S., Samad, A., Faist, H., & Sessitsch, A. (2019). A review on the plant microbiome: Ecology, functions, and emerging trends in microbial application. *J Adv Res*, 19, 29-37. doi:10.1016/j.jare.2019.03.004
- Coyte, K. Z., Schluter, J., & Foster, K. R. (2015). The ecology of the microbiome: Networks, competition, and stability. *Science*, 350(6261), 663-666. doi:10.1126/science.aad2602
- Csuros, M., Rogozin, I. B., & Koonin, E. V. (2011). A Detailed History of Intron-rich Eukaryotic Ancestors Inferred from a Global Survey of 100 Complete Genomes. *PLOS Computational Biology*, 7(9), e1002150. doi:10.1371/journal.pcbi.1002150
- Cui, H., Tsuda, K., & Parker, J. E. (2015). Effector-triggered immunity: from pathogen perception to robust defense. *Annu Rev Plant Biol*, 66, 487-511. doi:10.1146/annurev-arplant-050213-040012

- de Jonge, R., Bolton, M. D., Kombrink, A., van den Berg, G. C., Yadeta, K. A., & Thomma, B. P. (2013). Extensive chromosomal reshuffling drives evolution of virulence in an asexual pathogen. *Genome Res*, 23(8), 1271-1282. doi:10.1101/gr.152660.112
- Djamei, A., Schipper, K., Rabe, F., Ghosh, A., Vincon, V., Kahnt, J., Osorio, S., Tohge, T., Fernie, A. R., Feussner, I., Feussner, K., Meinicke, P., Stierhof, Y.-D., Schwarz, H., Macek, B., Mann, M., & Kahmann, R. (2011). Metabolic priming by a secreted fungal effector. *Nature*, 478(7369), 395-398. doi:10.1038/nature10454
- Doehlemann, G., Reissmann, S., Aßmann, D., Fleckenstein, M., & Kahmann, R. (2011). Two linked genes encoding a secreted effector and a membrane protein are essential for *Ustilago maydis*-induced tumour formation. *Molecular Microbiology*, 81(3), 751-766. doi:10.1111/j.1365-2958.2011.07728.x
- Doehlemann, G., van der Linde, K., Aßmann, D., Schwammbach, D., Hof, A., Mohanty, A., Jackson, D., & Kahmann, R. (2009). Pep1, a Secreted Effector Protein of *Ustilago maydis*, Is Required for Successful Invasion of Plant Cells. *PLoS Pathog*, 5(2), e1000290. doi:10.1371/journal.ppat.1000290
- Droby, S., Cohen, L., Daus, A., Weiss, B., Horev, B., Chalutz, E., Katz, H., Keren-Tzur, M., & Shachnai, A. (1998). Commercial Testing of Aspire: A Yeast Preparation for the Biological Control of Postharvest Decay of Citrus. *Biological Control*, 12(2), 97-101. doi:10.1006/bcon.1998.0615
- Dufour, R., & Areas, A. T. T. f. R. (2001). *Biointensive Integrated Pest Management (IPM): ATTRA*.
- Dutheil, J. Y., Mannhaupt, G., Schweizer, G., M.K. Sieber, C., Münsterkötter, M., Güldener, U., Schirawski, J., & Kahmann, R. (2016). A Tale of Genome Compartmentalization: The Evolution of Virulence Clusters in Smut Fungi. *Genome Biology and Evolution*, 8(3), 681-704. doi:10.1093/gbe/evw026
- Eastgate, J. A. (2000). *Erwinia amylovora*: the molecular basis of fireblight disease. *Mol Plant Pathol*, 1(6), 325-329. doi:10.1046/j.1364-3703.2000.00044.x
- Eden-Green, S., & Billing, E. (1974). Fireblight. *Review of Plant Pathology*, 53(5), 353-365.
- Edgerton, M. D. (2009). Increasing crop productivity to meet global needs for feed, food, and fuel. *Plant Physiol*, 149(1), 7-13. doi:10.1104/pp.108.130195
- Eitzen, K., Sengupta, P., Kroll, S., Kemen, E., & Doehlemann, G. (2021). A fungal member of the *Arabidopsis thaliana* phyllosphere antagonizes *Albugo laibachii* via a GH25 lysozyme. *eLife*, 10, e65306. doi:10.7554/eLife.65306
- Fastrez, J. (1996). Phage lysozymes. *Exs*, 75, 35-64.
- Ferraz, P., Cássio, F., & Lucas, C. (2019). Potential of Yeasts as Biocontrol Agents of the Phytopathogen Causing Cacao Witches' Broom Disease: Is Microbial Warfare a Solution? *Front Microbiol*, 10, 1766. doi:10.3389/fmicb.2019.01766
- Freimoser, F. M., Rueda-Mejia, M. P., Tilocca, B., & Migheli, Q. (2019). Biocontrol yeasts: mechanisms and applications. *World J Microbiol Biotechnol*, 35(10), 154. doi:10.1007/s11274-019-2728-4

5. Bibliography

- Gafni, A., Calderon, C. E., Harris, R., Buxdorf, K., Dafa-Berger, A., Zeilinger-Reichert, E., & Levy, M. (2015). Biological control of the cucurbit powdery mildew pathogen *Podosphaera xanthii* by means of the epiphytic fungus *Pseudozyma aphidis* and parasitism as a mode of action. *Front Plant Sci*, 6, 132. doi:10.3389/fpls.2015.00132
- Gao, F.-k., Dai, C.-c., & Liu, X.-z. (2010). Mechanisms of fungal endophytes in plant protection against pathogens. *African Journal of Microbiology Research*, 4(13), 1346-1351.
- Gao, Z., Karlsson, I., Geisen, S., Kowalchuk, G., & Jousset, A. (2019). Protists: Puppet Masters of the Rhizosphere Microbiome. *Trends Plant Sci*, 24(2), 165-176. doi:10.1016/j.tplants.2018.10.011
- García-Pedrajas, M. D., Nadal, M., Bölker, M., Gold, S. E., & Perlin, M. H. (2008). Sending mixed signals: redundancy vs. uniqueness of signaling components in the plant pathogen, *Ustilago maydis*. *Fungal Genet Biol*, 45 Suppl 1, S22-30. doi:10.1016/j.fgb.2008.04.007
- Garrido-Oter, R., Nakano, R. T., Dombrowski, N., Ma, K.-W., McHardy, A. C., & Schulze-Lefert, P. (2018). Modular Traits of the Rhizobiales Root Microbiota and Their Evolutionary Relationship with Symbiotic Rhizobia. *Cell Host & Microbe*, 24(1), 155-167.e155. doi:10.1016/j.chom.2018.06.006
- Gillissen, B., Bergemann, J., Sandmann, C., Schroeer, B., Bölker, M., & Kahmann, R. (1992). A two-component regulatory system for self/non-self recognition in *Ustilago maydis*. *Cell*, 68(4), 647-657. doi:10.1016/0092-8674(92)90141-x
- Gladyshev, E. A., & Arkhipova, I. R. (2011). A widespread class of reverse transcriptase-related cellular genes. *Proceedings of the National Academy of Sciences*, 108(51), 20311-20316. doi:10.1073/pnas.1100266108
- Goswami, R. S. (2012). Targeted gene replacement in fungi using a split-marker approach. *Methods Mol Biol*, 835, 255-269. doi:10.1007/978-1-61779-501-5_16
- Guinebretiere, M. H., Nguyen-The, C., Morrison, N., Reich, M., & Nicot, P. (2000). Isolation and characterization of antagonists for the biocontrol of the postharvest wound pathogen *Botrytis cinerea* on strawberry fruits. *J Food Prot*, 63(3), 386-394. doi:10.4315/0362-028x-63.3.386
- Haefele, D. M., & Lindow, S. E. (1987). Flagellar Motility Confers Epiphytic Fitness Advantages upon *Pseudomonas syringae*. *Appl Environ Microbiol*, 53(10), 2528-2533. doi:10.1128/aem.53.10.2528-2533.1987
- Halisky, P. M., & Barbe, G. D. (1962). A Study of *Melanopsichium pennsylvanicum* Causing Gall Smut on *Polygonum*. *Bulletin of the Torrey Botanical Club*, 89(3), 181-186. doi:10.2307/2482566
- Hardoim, P. R., Overbeek, L. S. v., Berg, G., Pirttilä, A. M., Compant, S., Campisano, A., Döring, M., & Sessitsch, A. (2015). The Hidden World within Plants: Ecological and Evolutionary Considerations for Defining Functioning of Microbial Endophytes. *Microbiology and Molecular Biology Reviews*, 79(3), 293-320. doi:doi:10.1128/MMBR.00050-14

- Hash, J. H., & Rothlauf, M. V. (1967). The N,O-diacetylmuramidase of *Chalaropsis* species. I. Purification and crystallization. *J Biol Chem*, 242(23), 5586-5590.
- Hassani, M. A., Durán, P., & Hacquard, S. (2018). Microbial interactions within the plant holobiont. *Microbiome*, 6(1), 58. doi:10.1186/s40168-018-0445-0
- Heimel, K., Scherer, M., Vranes, M., Wahl, R., Pothiratana, C., Schuler, D., Vincon, V., Finkernagel, F., Flor-Parra, I., & Kämper, J. (2010). The Transcription Factor Rbf1 Is the Master Regulator for b-Mating Type Controlled Pathogenic Development in *Ustilago maydis*. *PLoS Pathog*, 6(8), e1001035. doi:10.1371/journal.ppat.1001035
- Hernandez, M. N., & Lindow, S. E. (2019). *Pseudomonas syringae* Increases Water Availability in Leaf Microenvironments via Production of Hygroscopic Syringafactin. *Appl Environ Microbiol*, 85(18). doi:10.1128/aem.01014-19
- Hill, S. (1990). *Pest control in sustainable agriculture*. Paper presented at the Proceedings of the entomological society of Ontario.
- Hirsch, A. M., & Fujishige, N. A. (2008). Commensalisms. In S. E. Jørgensen & B. D. Fath (Eds.), *Encyclopedia of Ecology* (pp. 679-683). Oxford: Academic Press.
- Hoffman, C. S., & Winston, F. (1987). A ten-minute DNA preparation from yeast efficiently releases autonomous plasmids for transformation of *Escherichia coli*. *Gene*, 57(2-3), 267-272. doi:10.1016/0378-1119(87)90131-4
- Hokkanen, H. M. T. (1991). Trap Cropping in Pest Management. *Annual Review of Entomology*, 36(1), 119-138. doi:10.1146/annurev.en.36.010191.001003
- Holden, M. H., Ellner, S. P., Lee, D.-H., Nyrop, J. P., & Sanderson, J. P. (2012). Designing an effective trap cropping strategy: the effects of attraction, retention and plant spatial distribution. *Journal of Applied Ecology*, 49(3), 715-722. doi:10.1111/j.1365-2664.2012.02137.x
- Hood, M. E., & Antonovics, J. (2000). Intratetrad mating, heterozygosity, and the maintenance of deleterious alleles in *Microbotryum violaceum* (= *Ustilago violacea*). *Heredity*, 85(3), 231-241. doi:10.1046/j.1365-2540.2000.00748.x
- Horner, N. R., Grenville-Briggs, L. J., & van West, P. (2012). The oomycete *Pythium oligandrum* expresses putative effectors during mycoparasitism of *Phytophthora infestans* and is amenable to transformation. *Fungal Biology*, 116(1), 24-41. doi:10.1016/j.funbio.2011.09.004
- Hyde, K. D., Xu, J., Rapior, S., Jeewon, R., Lumyong, S., Niego, A. G. T., Abeywickrama, P. D., Aluthmuhandiram, J. V. S., Brahamanage, R. S., Brooks, S., Chaiyasen, A., Chethana, K. W. T., Chomnunti, P., Chepkirui, C., Chuankid, B., de Silva, N. I., Doilom, M., Faulds, C., Gentekaki, E., Gopalan, V., Kakumyan, P., Harishchandra, D., Hemachandran, H., Hongsanant, S., Karunarathna, A., Karunarathna, S. C., Khan, S., Kumla, J., Jayawardena, R. S., Liu, J.-K., Liu, N., Luangharn, T., Macabeo, A. P. G., Marasinghe, D. S., Meeks, D., Mortimer, P. E., Mueller, P., Nadir, S., Nataraja, K. N., Nontachaiyapoom, S., O'Brien, M., Penkhrue, W., Phukhamsakda, C., Ramanan, U. S., Rathnayaka, A. R., Sadaba, R. B., Sandargo, B., Samarakoon, B. C., Tennakoon, D. S., Siva, R., Sriprom, W., Suryanarayanan, T. S., Sujarit, K., Suwannarach, N., Suwunwong, T., Thongbai, B., Thongklang, N., Wei, D., Wijesinghe, S. N., Winiski, J., Yan, J., Yasanthika, E., & Stadler, M. (2019). The

5. Bibliography

- amazing potential of fungi: 50 ways we can exploit fungi industrially. *Fungal Diversity*, 97(1), 1-136. doi:10.1007/s13225-019-00430-9
- Jin, C. W., Li, G. X., Yu, X. H., & Zheng, S. J. (2010). Plant Fe status affects the composition of siderophore-secreting microbes in the rhizosphere. *Annals of Botany*, 105(5), 835-841. doi:10.1093/aob/mcq071
- Jones, J. D., & Dangl, J. L. (2006). The plant immune system. *Nature*, 444(7117), 323-329. doi:10.1038/nature05286
- Jones, P., Binns, D., Chang, H. Y., Fraser, M., Li, W., McAnulla, C., McWilliam, H., Maslen, J., Mitchell, A., Nuka, G., Pesseat, S., Quinn, A. F., Sangrador-Vegas, A., Scheremetjew, M., Yong, S. Y., Lopez, R., & Hunter, S. (2014). InterProScan 5: genome-scale protein function classification. *Bioinformatics*, 30(9), 1236-1240. doi:10.1093/bioinformatics/btu031
- Kaffarnik, F., Müller, P., Leibundgut, M., Kahmann, R., & Feldbrügge, M. (2003). PKA and MAPK phosphorylation of Prf1 allows promoter discrimination in *Ustilago maydis*. *The EMBO Journal*, 22(21), 5817-5826. doi:10.1093/emboj/cdg554
- Kämper, J., Kahmann, R., Bölker, M., Ma, L.-J., Brefort, T., Saville, B. J., Banuett, F., Kronstad, J. W., Gold, S. E., Müller, O., Perlin, M. H., Wösten, H. A. B., de Vries, R., Ruiz-Herrera, J., Reynaga-Peña, C. G., Snetselaar, K., McCann, M., Pérez-Martín, J., Feldbrügge, M., Basse, C. W., Steinberg, G., Ibeas, J. I., Holloman, W., Guzman, P., Farman, M., Stajich, J. E., Sentandreu, R., González-Prieto, J. M., Kennell, J. C., Molina, L., Schirawski, J., Mendoza-Mendoza, A., Greilinger, D., Münch, K., Rössel, N., Scherer, M., Vraneš, M., Ladendorf, O., Vincon, V., Fuchs, U., Sandrock, B., Meng, S., Ho, E. C. H., Cahill, M. J., Boyce, K. J., Klose, J., Klosterman, S. J., Deelstra, H. J., Ortiz-Castellanos, L., Li, W., Sanchez-Alonso, P., Schreier, P. H., Häuser-Hahn, I., Vaupel, M., Koopmann, E., Friedrich, G., Voss, H., Schlüter, T., Margolis, J., Platt, D., Swimmer, C., Gnirke, A., Chen, F., Vysotskaia, V., Mannhaupt, G., Güldener, U., Münsterkötter, M., Haase, D., Oesterheld, M., Mewes, H.-W., Mauceli, E. W., DeCaprio, D., Wade, C. M., Butler, J., Young, S., Jaffe, D. B., Calvo, S., Nusbaum, C., Galagan, J., & Birren, B. W. (2006). Insights from the genome of the biotrophic fungal plant pathogen *Ustilago maydis*. *Nature*, 444(7115), 97-101. doi:10.1038/nature05248
- Kämper, J., Reichmann, M., Romeis, T., Bölker, M., & Kahmann, R. (1995). Multiallelic recognition: Nonself-dependent dimerization of the bE and bW homeodomain proteins in *Ustilago maydis*. *Cell*, 81(1), 73-83. doi:10.1016/0092-8674(95)90372-0
- Kaupert Neto, A. A., Borin, G. P., Goldman, G. H., Damásio, A. R., & Oliveira, J. V. (2016). Insights into the plant polysaccharide degradation potential of the xylanolytic yeast *Pseudozyma brasiliensis*. *FEMS Yeast Res*, 16(2), fov117. doi:10.1093/femsyr/fov117
- Kemen, E., & Jones, J. D. (2012). Obligate biotroph parasitism: can we link genomes to lifestyles? *Trends Plant Sci*, 17(8), 448-457. doi:10.1016/j.tplants.2012.04.005
- Khrunyk, Y., Münch, K., Schipper, K., Lupas, A. N., & Kahmann, R. (2010). The use of FLP-mediated recombination for the functional analysis of an effector gene family in the biotrophic smut fungus *Ustilago maydis*. *New Phytologist*, 187(4), 957-968. doi:10.1111/j.1469-8137.2010.03413.x

- Kim, D., Pertea, G., Trapnell, C., Pimentel, H., Kelley, R., & Salzberg, S. L. (2013). TopHat2: accurate alignment of transcriptomes in the presence of insertions, deletions and gene fusions. *Genome Biology*, *14*(4), R36. doi:10.1186/gb-2013-14-4-r36
- Kitamoto, D., Yanagishita, H., Shinbo, T., Nakane, T., Kamisawa, C., & Nakahara, T. (1993). Surface active properties and antimicrobial activities of mannosylerythritol lipids as biosurfactants produced by *Candida antarctica*. *Journal of Biotechnology*, *29*(1), 91-96. doi:10.1016/0168-1656(93)90042-L
- Kjær, B., Jensen, H. P., Jensen, J., & Jørgensen, J. H. (1990). Associations between three ml-o powdery mildew resistance genes and agronomic traits in barley. *Euphytica*, *46*(3), 185-193. doi:10.1007/BF00027217
- Köhl, J., Kolnaar, R., & Ravensberg, W. J. (2019). Mode of Action of Microbial Biological Control Agents Against Plant Diseases: Relevance Beyond Efficacy. *Front Plant Sci*, *10*, 845. doi:10.3389/fpls.2019.00845
- Kojic, M., & Holloman, W. K. (2000). Shuttle vectors for genetic manipulations in *Ustilago maydis*. *Can J Microbiol*, *46*(4), 333-338. doi:10.1139/w00-002 %M 10779869
- Konishi, M., Morita, T., Fukuoka, T., Imura, T., Kakugawa, K., & Kitamoto, D. (2007). Production of different types of mannosylerythritol lipids as biosurfactants by the newly isolated yeast strains belonging to the genus *Pseudozyma*. *Appl Microbiol Biotechnol*, *75*(3), 521-531. doi:10.1007/s00253-007-0853-8
- Krogh, A., Larsson, B., von Heijne, G., & Sonnhammer, E. L. (2001). Predicting transmembrane protein topology with a hidden Markov model: application to complete genomes. *J Mol Biol*, *305*(3), 567-580. doi:10.1006/jmbi.2000.4315
- Kroll, S., Agler, M. T., & Kemen, E. (2017). Genomic dissection of host-microbe and microbe-microbe interactions for advanced plant breeding. *Curr Opin Plant Biol*, *36*, 71-78. doi:10.1016/j.pbi.2017.01.004
- Krombach, S., Reissmann, S., Kreibich, S., Bochen, F., & Kahmann, R. (2018). Virulence function of the *Ustilago maydis* sterol carrier protein 2. *New Phytologist*, *220*(2), 553-566. doi:10.1111/nph.15268
- Kruse, J., Doehlemann, G., Kemen, E., & Thines, M. (2017). Asexual and sexual morphs of *Moesziomyces* revisited. *IMA Fungus*, *8*(1), 117-129. doi:10.5598/imafungus.2017.08.01.09
- Laemmli, U. K. (1970). Cleavage of Structural Proteins during the Assembly of the Head of Bacteriophage T4. *Nature*, *227*(5259), 680-685. doi:10.1038/227680a0
- Langmead, B., & Salzberg, S. L. (2012). Fast gapped-read alignment with Bowtie 2. *Nat Methods*, *9*(4), 357-359. doi:10.1038/nmeth.1923
- Laur, J., Ramakrishnan, G. B., Labbé, C., Lefebvre, F., Spanu, P. D., & Bélanger, R. R. (2018). Effectors involved in fungal-fungal interaction lead to a rare phenomenon of hyperbiotrophy in the tritrophic system biocontrol agent-powdery mildew-plant. *New Phytol*, *217*(2), 713-725. doi:10.1111/nph.14851
- Laurie, J. D., Ali, S., Linning, R., Mannhaupt, G., Wong, P., Güldener, U., Münsterkötter, M., Moore, R., Kahmann, R., Bakkeren, G., & Schirawski, J. (2012). Genome

5. Bibliography

- comparison of barley and maize smut fungi reveals targeted loss of RNA silencing components and species-specific presence of transposable elements. *Plant Cell*, 24(5), 1733-1745. doi:10.1105/tpc.112.097261
- Lefebvre, F., Joly, D. L., Labbé, C., Teichmann, B., Linning, R., Belzile, F., Bakkeren, G., & Bélanger, R. R. (2013). The transition from a phytopathogenic smut ancestor to an anamorphic biocontrol agent deciphered by comparative whole-genome analysis. *Plant Cell*, 25(6), 1946-1959. doi:10.1105/tpc.113.113969
- Levy, A., Salas Gonzalez, I., Mittelviehhaus, M., Clingenpeel, S., Herrera Paredes, S., Miao, J., Wang, K., Devescovi, G., Stillman, K., Monteiro, F., Rangel Alvarez, B., Lundberg, D. S., Lu, T.-Y., Lebeis, S., Jin, Z., McDonald, M., Klein, A. P., Feltcher, M. E., Rio, T. G., Grant, S. R., Doty, S. L., Ley, R. E., Zhao, B., Venturi, V., Pelletier, D. A., Vorholt, J. A., Tringe, S. G., Woyke, T., & Dangl, J. L. (2018). Genomic features of bacterial adaptation to plants. *Nature Genetics*, 50(1), 138-150. doi:10.1038/s41588-017-0012-9
- Lim, C. S., Weinstein, B. N., Roy, S. W., & Brown, C. M. (2021). Analysis of Fungal Genomes Reveals Commonalities of Intron Gain or Loss and Functions in Intron-Poor Species. *Molecular Biology and Evolution*. doi:10.1093/molbev/msab094
- Lindow, S. E., & Brandl, M. T. (2003). Microbiology of the Phyllosphere. *Appl Environ Microbiol*, 69(4), 1875-1883. doi:doi:10.1128/AEM.69.4.1875-1883.2003
- Lugtenberg, B., & Kamilova, F. (2009). Plant-growth-promoting rhizobacteria. *Annu Rev Microbiol*, 63, 541-556. doi:10.1146/annurev.micro.62.081307.162918
- Ma, L.-S., Wang, L., Trippel, C., Mendoza-Mendoza, A., Ullmann, S., Moretti, M., Carsten, A., Kahnt, J., Reissmann, S., Zechmann, B., Bange, G., & Kahmann, R. (2018). The *Ustilago maydis* repetitive effector Rsp3 blocks the antifungal activity of mannose-binding maize proteins. *Nature Communications*, 9(1), 1711. doi:10.1038/s41467-018-04149-0
- Macho, Alberto P., & Zipfel, C. (2014). Plant PRRs and the Activation of Innate Immune Signaling. *Molecular Cell*, 54(2), 263-272. doi:10.1016/j.molcel.2014.03.028
- Martínez-Espinoza, A. D., García-Pedrajas, M. a. D., & Gold, S. E. (2002). The Ustilaginales as Plant Pests and Model Systems. *Fungal Genetics and Biology*, 35(1), 1-20. doi:10.1006/fgbi.2001.1301
- Martinez-Fleites, C., Korczynska, J. E., Davies, G. J., Cope, M. J., Turkenburg, J. P., & Taylor, E. J. (2009). The crystal structure of a family GH25 lysozyme from *Bacillus anthracis* implies a neighboring-group catalytic mechanism with retention of anomeric configuration. *Carbohydrate Research*, 344(13), 1753-1757. doi:10.1016/j.carres.2009.06.001
- Matei, A., Ernst, C., Günl, M., Thiele, B., Altmüller, J., Walbot, V., Usadel, B., & Doehlemann, G. (2018). How to make a tumour: cell type specific dissection of *Ustilago maydis*-induced tumour development in maize leaves. *New Phytologist*, 217(4), 1681-1695. doi:10.1111/nph.14960
- Mélida, H., Sandoval-Sierra, J. V., Diéguez-Uribeondo, J., & Bulone, V. (2013). Analyses of extracellular carbohydrates in oomycetes unveil the existence of three different cell wall types. *Eukaryotic cell*, 12(2), 194-203. doi:10.1128/EC.00288-12

- Mendes, R., Kruijt, M., de Bruijn, I., Dekkers, E., van der Voort, M., Schneider, J. H., Piceno, Y. M., DeSantis, T. Z., Andersen, G. L., Bakker, P. A., & Raaijmakers, J. M. (2011). Deciphering the rhizosphere microbiome for disease-suppressive bacteria. *Science*, 332(6033), 1097-1100. doi:10.1126/science.1203980
- Mendoza-Mendoza, A., Berndt, P., Djamei, A., Weise, C., Linne, U., Marahiel, M., Vranes, M., Kämper, J., & Kahmann, R. (2009). Physical-chemical plant-derived signals induce differentiation in *Ustilago maydis*. *Mol Microbiol*, 71(4), 895-911. doi:10.1111/j.1365-2958.2008.06567.x
- Mercier, J., & Lindow, S. E. (2000). Role of leaf surface sugars in colonization of plants by bacterial epiphytes. *Appl Environ Microbiol*, 66(1), 369-374. doi:10.1128/aem.66.1.369-374.2000
- Metcalf, J. A., Funkhouser-Jones, L. J., Brileya, K., Reysenbach, A.-L., & Bordenstein, S. R. (2014). Antibacterial gene transfer across the tree of life. *eLife*, 3, e04266. doi:10.7554/eLife.04266
- Middelhoven, W. J. (1997). Identity and biodegradative abilities of yeasts isolated from plants growing in an arid climate. *Antonie Van Leeuwenhoek*, 72(2), 81-89. doi:10.1023/a:1000295822074
- Muccilli, S., & Restuccia, C. (2015). Bioprotective Role of Yeasts. *Microorganisms*, 3(4), 588-611. doi:10.3390/microorganisms3040588
- Myers, J. H., & Cory, J. S. (2017). Biological control agents: invasive species or valuable solutions? *Impact of biological invasions on ecosystem services* (pp. 191-202): Springer.
- Nicot, P., P., Blum, B., Köhl, J., & Ruocco, M. (2011). Perspectives for future research-and-development projects on biological control of plant pests and diseases *Classical and augmentative biological control against diseases and pests: critical status analysis and review of factors influencing their success*. Zürich (switzerland): IOBC - International Organisation for Biological and Integrated Control of Noxious Animals and Plants.
- Nikoh, N., McCutcheon, J. P., Kudo, T., Miyagishima, S.-y., Moran, N. A., & Nakabachi, A. (2010). Bacterial Genes in the Aphid Genome: Absence of Functional Gene Transfer from *Buchnera* to Its Host. *PLOS Genetics*, 6(2), e1000827. doi:10.1371/journal.pgen.1000827
- Nishimoto, R. (2019). Global trends in the crop protection industry. *J Pestic Sci*, 44(3), 141-147. doi:10.1584/jpestics.D19-101
- Oguchi, R., Onoda, Y., Terashima, I., & Tholen, D. (2018). Leaf anatomy and function *The leaf: a platform for performing photosynthesis* (pp. 97-139): Springer.
- Ökmen, B., Kemmerich, B., Hilbig, D., Wemhöner, R., Aschenbroich, J., Perrar, A., Huesgen, P. F., Schipper, K., & Doehlemann, G. (2018). Dual function of a secreted fungalsin metalloprotease in *Ustilago maydis*. *New Phytologist*, 220(1), 249-261. doi:10.1111/nph.15265

5. Bibliography

- Ökmen, B., Schwammbach, D., Bakkeren, G., Neumann, U., & Doehlemann, G. (2021). The *Ustilago hordei*–Barley Interaction is a Versatile System for Characterization of Fungal Effectors. *Journal of Fungi*, 7(2). doi:10.3390/jof7020086
- Parniske, M. (2008). Arbuscular mycorrhiza: the mother of plant root endosymbioses. *Nat Rev Microbiol*, 6(10), 763-775. doi:10.1038/nrmicro1987
- Parratt, S. R., & Laine, A.-L. (2016). The role of hyperparasitism in microbial pathogen ecology and evolution. *The ISME Journal*, 10(8), 1815-1822. doi:10.1038/ismej.2015.247
- Pawlowska, T. E., Gaspar, M. L., Lastovetsky, O. A., Mondo, S. J., Real-Ramirez, I., Shakya, E., & Bonfante, P. (2018). Biology of Fungi and Their Bacterial Endosymbionts. *Annu Rev Phytopathol*, 56, 289-309. doi:10.1146/annurev-phyto-080417-045914
- Petersen, T. N., Brunak, S., von Heijne, G., & Nielsen, H. (2011). SignalP 4.0: discriminating signal peptides from transmembrane regions. *Nat Methods*, 8(10), 785-786. doi:10.1038/nmeth.1701
- Piątek, M., Lutz, M., & Yorou, N. S. (2015). A molecular phylogenetic framework for *Anthracozygia* (Ustilaginales), including five new combinations (inter alia for the asexual *Pseudozyma flocculosa*), and description of *Anthracozygia grodzinskae* sp. nov. *Mycological Progress*, 14(10), 88. doi:10.1007/s11557-015-1114-3
- Pieterse, C. M. J., Zamioudis, C., Berendsen, R. L., Weller, D. M., Wees, S. C. M. V., & Bakker, P. A. H. M. (2014). Induced Systemic Resistance by Beneficial Microbes. *Annu Rev Phytopathol*, 52(1), 347-375. doi:10.1146/annurev-phyto-082712-102340
- Pineda, A., Zheng, S. J., van Loon, J. J., Pieterse, C. M., & Dicke, M. (2010). Helping plants to deal with insects: the role of beneficial soil-borne microbes. *Trends Plant Sci*, 15(9), 507-514. doi:10.1016/j.tplants.2010.05.007
- Punja, Z. K., & Utkhede, R. S. (2003). Using fungi and yeasts to manage vegetable crop diseases. *Trends in Biotechnology*, 21(9), 400-407. doi:10.1016/S0167-7799(03)00193-8
- Rabe, F., Bosch, J., Stirnberg, A., Guse, T., Bauer, L., Seitner, D., Rabanal, F. A., Czedik-Eysenberg, A., Uhse, S., Bindics, J., Genencher, B., Navarrete, F., Kellner, R., Ekker, H., Kumlehn, J., Vogel, J. P., Gordon, S. P., Marcel, T. C., Münsterkötter, M., Walter, M. C., Sieber, C. M. K., Mannhaupt, G., Güldener, U., Kahmann, R., & Djamei, A. (2016). A complete toolset for the study of *Ustilago bromivora* and *Brachypodium* sp. as a fungal-temperate grass pathosystem. *eLife*, 5, e20522. doi:10.7554/eLife.20522
- Rau, A., Hogg, T., Marquardt, R., & Hilgenfeld, R. (2001). A new lysozyme fold. Crystal structure of the muramidase from *Streptomyces coelicolor* at 1.65 Å resolution. *J Biol Chem*, 276(34), 31994-31999. doi:10.1074/jbc.M102591200
- Ray, D. K., Mueller, N. D., West, P. C., & Foley, J. A. (2013). Yield Trends Are Insufficient to Double Global Crop Production by 2050. *PLoS One*, 8(6), e66428. doi:10.1371/journal.pone.0066428

- Redkar, A. (2015). *Functional Characterization of an Organ Specific Effector See1 of Ustilago Maydis*. Philipps-Universität Marburg.
- Redkar, A., & Doehlemann, G. (2016). Ustilago maydis Virulence Assays in Maize. *Bio-protocol*, 6(6), e1760. doi:10.21769/BioProtoc.1760
- Redkar, A., Hoser, R., Schilling, L., Zechmann, B., Krzymowska, M., Walbot, V., & Doehlemann, G. (2015). A Secreted Effector Protein of Ustilago maydis Guides Maize Leaf Cells to Form Tumors. *Plant Cell*, 27(4), 1332-1351. doi:10.1105/tpc.114.131086
- Rosenberg, E., & Zilber-Rosenberg, I. (2016). Microbes Drive Evolution of Animals and Plants: the Hologenome Concept. *mBio*, 7(2), e01395. doi:10.1128/mBio.01395-15
- Röttjers, L., & Faust, K. (2018). From hairballs to hypotheses—biological insights from microbial networks. *FEMS Microbiology Reviews*, 42(6), 761-780. doi:10.1093/femsre/fuy030
- Ruocco, M., Woo, S., Vinale, F., Lanzuise, S., & Lorito, M. (2011). Identified difficulties and conditions for field success of biocontrol. 2. Technical aspects: factors of efficacy *Classical and augmentative biological control against diseases and pests: critical status analysis and review of factors influencing their success* (pp. 45). Zürich (Switzerland): IOBC - International Organisation for Biological and Integrated Control of Noxious Animals and Plants.
- Sambrook, J., Fritsch, E. F., & Maniatis, T. (1989). *Molecular cloning: a laboratory manual*: Cold spring harbor laboratory press.
- Saravi, S. S. S., & Shokrzadeh, M. (2011). Role of pesticides in human life in the modern age: a review. *Pesticides in the modern world-risks and benefits*, 3-12.
- Savary, S., Willocquet, L., Pethybridge, S. J., Esker, P., McRoberts, N., & Nelson, A. (2019). The global burden of pathogens and pests on major food crops. *Nat Ecol Evol*, 3(3), 430-439. doi:10.1038/s41559-018-0793-y
- Scherer, M., Heimel, K., Starke, V., & Kämper, J. r. (2006). The Clp1 Protein Is Required for Clamp Formation and Pathogenic Development of Ustilago maydis. *Plant Cell*, 18(9), 2388-2401. doi:10.1105/tpc.106.043521
- Schilling, L., Matei, A., Redkar, A., Walbot, V., & Doehlemann, G. (2014). Virulence of the maize smut Ustilago maydis is shaped by organ-specific effectors. *Mol Plant Pathol*, 15(8), 780-789. doi:10.1111/mpp.12133
- Schipper, K. (2009). *Charakterisierung eines Ustilago maydis Genclusters, das für drei neuartige sekretierte Effektoren kodiert* Philipps-Universität Marburg.
- Schirawski, J., Mannhaupt, G., Münch, K., Brefort, T., Schipper, K., Doehlemann, G., Di Stasio, M., Rössel, N., Mendoza-Mendoza, A., Pester, D., Müller, O., Winterberg, B., Meyer, E., Ghareeb, H., Wollenberg, T., Münsterkötter, M., Wong, P., Walter, M., Stukenbrock, E., Güldener, U., & Kahmann, R. (2010). Pathogenicity Determinants in Smut Fungi Revealed by Genome Comparison. *Science*, 330(6010), 1546-1548. doi:10.1126/science.1195330

5. Bibliography

- Schulz, B., Banuett, F., Dahl, M., Schlesinger, R., Schäfer, W., Martin, T., Herskowitz, I., & Kahmann, R. (1990). The b alleles of *U. maydis*, whose combinations program pathogenic development, code for polypeptides containing a homeodomain-related motif. *Cell*, *60*(2), 295-306.
- Schuster, M., Schweizer, G., & Kahmann, R. (2018). Comparative analyses of secreted proteins in plant pathogenic smut fungi and related basidiomycetes. *Fungal Genet Biol*, *112*, 21-30. doi:10.1016/j.fgb.2016.12.003
- Seitner, D., Uhse, S., Gallei, M., & Djamei, A. (2018). The core effector Cce1 is required for early infection of maize by *Ustilago maydis*. *Mol Plant Pathol*, *19*(10), 2277-2287. doi:10.1111/mpp.12698
- Shade, A., Jacques, M. A., & Barret, M. (2017). Ecological patterns of seed microbiome diversity, transmission, and assembly. *Curr Opin Microbiol*, *37*, 15-22. doi:10.1016/j.mib.2017.03.010
- Sharma, R., Mishra, B., Runge, F., & Thines, M. (2014). Gene Loss Rather Than Gene Gain Is Associated with a Host Jump from Monocots to Dicots in the Smut Fungus *Melanopsichium pennsylvanicum*. *Genome Biology and Evolution*, *6*(8), 2034-2049. doi:10.1093/gbe/evu148
- Sharma, R., Ökmen, B., Doehlemann, G., & Thines, M. (2019). Saprotrophic yeasts formerly classified as *Pseudozyma* have retained a large effector arsenal, including functional Pep1 orthologs. *Mycological Progress*, *18*(5), 763-768. doi:10.1007/s11557-019-01486-2
- Shelton, A. M., & Badenes-Perez, F. R. (2006). Concepts and applications of trap cropping in pest management. *Annu Rev Entomol*, *51*, 285-308. doi:10.1146/annurev.ento.51.110104.150959
- Shivas, R. G., & Brown, J. F. (1984). Identification and enumeration of yeasts on *Banksia collina* and *Callistemon viminalis* leaves. *Transactions of the British Mycological Society*, *83*(4), 687-689. doi:10.1016/S0007-1536(84)80188-6
- Shoresh, M., Harman, G. E., & Mastouri, F. (2010). Induced systemic resistance and plant responses to fungal biocontrol agents. *Annu Rev Phytopathol*, *48*, 21-43. doi:10.1146/annurev-phyto-073009-114450
- Southern, E. (2006). Southern blotting. *Nature Protocols*, *1*(2), 518-525. doi:10.1038/nprot.2006.73
- Spaink, H. P. (2000). Root nodulation and infection factors produced by rhizobial bacteria. *Annu Rev Microbiol*, *54*, 257-288. doi:10.1146/annurev.micro.54.1.257
- Srivastava, D. A., Harris, R., Breuer, G., & Levy, M. (2021). Secretion-Based Modes of Action of Biocontrol Agents with a Focus on *Pseudozyma aphidis*. *Plants (Basel)*, *10*(2). doi:10.3390/plants10020210
- Stone, B. W. G., Weingarten, E. A., & Jackson, C. R. The Role of the Phyllosphere Microbiome in Plant Health and Function *Annual Plant Reviews online* (pp. 533-556).

- Stringlis, I. A., Yu, K., Feussner, K., de Jonge, R., Van Bentum, S., Van Verk, M. C., Berendsen, R. L., Bakker, P. A. H. M., Feussner, I., & Pieterse, C. M. J. (2018). MYB72-dependent coumarin exudation shapes root microbiome assembly to promote plant health. *Proceedings of the National Academy of Sciences*, *115*(22), E5213-E5222. doi:10.1073/pnas.1722335115
- Syed Ab Rahman, S. F., Singh, E., Pieterse, C. M. J., & Schenk, P. M. (2018). Emerging microbial biocontrol strategies for plant pathogens. *Plant Sci*, *267*, 102-111. doi:10.1016/j.plantsci.2017.11.012
- Teichmann, B., Linne, U., Hewald, S., Marahiel, M. A., & Bölker, M. (2007). A biosynthetic gene cluster for a secreted cellobiose lipid with antifungal activity from *Ustilago maydis*. *Mol Microbiol*, *66*(2), 525-533. doi:10.1111/j.1365-2958.2007.05941.x
- Trivedi, P., Leach, J. E., Tringe, S. G., Sa, T., & Singh, B. K. (2020). Plant–microbiome interactions: from community assembly to plant health. *Nature Reviews Microbiology*, *18*(11), 607-621. doi:10.1038/s41579-020-0412-1
- Tsuda, K., & Katagiri, F. (2010). Comparing signaling mechanisms engaged in pattern-triggered and effector-triggered immunity. *Curr Opin Plant Biol*, *13*(4), 459-465. doi:10.1016/j.pbi.2010.04.006
- Van Wees, S. C., Van der Ent, S., & Pieterse, C. M. (2008). Plant immune responses triggered by beneficial microbes. *Curr Opin Plant Biol*, *11*(4), 443-448. doi:10.1016/j.pbi.2008.05.005
- Vánky, K. (1977). *Moesziomyces*, a new genus of Ustilaginales. *Botaniska Notiser*, *130*, 131-135.
- Vannier, N., Agler, M., & Hacquard, S. (2019). Microbiota-mediated disease resistance in plants. *PLoS Pathog*, *15*(6), e1007740. doi:10.1371/journal.ppat.1007740
- Vollmer, W., Joris, B., Charlier, P., & Foster, S. (2008). Bacterial peptidoglycan (murein) hydrolases. *FEMS Microbiology Reviews*, *32*(2), 259-286. doi:10.1111/j.1574-6976.2007.00099.x
- Vorholt, J. A. (2012). Microbial life in the phyllosphere. *Nat Rev Microbiol*, *10*(12), 828-840. doi:10.1038/nrmicro2910
- Wang, Q. M., Begerow, D., Groenewald, M., Liu, X. Z., Theelen, B., Bai, F. Y., & Boekhout, T. (2015). Multigene phylogeny and taxonomic revision of yeasts and related fungi in the Ustilaginomycotina. *Stud Mycol*, *81*, 55-83. doi:10.1016/j.simyco.2015.10.004
- William Roy, S., & Gilbert, W. (2006). The evolution of spliceosomal introns: patterns, puzzles and progress. *Nature Reviews Genetics*, *7*(3), 211-221. doi:10.1038/nrg1807
- Wilson, M., & Lindow, S. (1993). Interactions between the biological control agent *Pseudomonas fluorescens* A506 and *Erwinia amylovora* in pear blossoms. *Phytopathology*, *83*(1), 117-123.
- Xin, X. F., Nomura, K., Aung, K., Velásquez, A. C., Yao, J., Boutrot, F., Chang, J. H., Zipfel, C., & He, S. Y. (2016). Bacteria establish an aqueous living space in plants crucial for virulence. *Nature*, *539*(7630), 524-529. doi:10.1038/nature20166

5. Bibliography

- Xing-Feng, H., M., C. J., F., R. K., Ruifu, Z., Qirong, S., & M., V. J. (2014). Rhizosphere interactions: root exudates, microbes, and microbial communities. *Botany*, *92*(4), 267-275. doi:10.1139/cjb-2013-0225
- Yang, H.-H., Yang, S. L., Peng, K.-C., Lo, C.-T., & Liu, S.-Y. (2009). Induced proteome of *Trichoderma harzianum* by *Botrytis cinerea*. *Mycological Research*, *113*(9), 924-932.
- Zalila-Kolsi, I., Ben Mahmoud, A., Ali, H., Sellami, S., Nasfi, Z., Tounsi, S., & Jamoussi, K. (2016). Antagonist effects of *Bacillus* spp. strains against *Fusarium graminearum* for protection of durum wheat (*Triticum turgidum* L. subsp. durum). *Microbiological Research*, *192*, 148-158. doi:10.1016/j.micres.2016.06.012
- Zhao, Z., Liu, H., Wang, C., & Xu, J.-R. (2013). Comparative analysis of fungal genomes reveals different plant cell wall degrading capacity in fungi. *BMC genomics*, *14*, 274-274. doi:10.1186/1471-2164-14-274
- Zuo, W., Ökmen, B., Depotter, J. R. L., Ebert, M. K., Redkar, A., Misas Villamil, J., & Doehlemann, G. (2019). Molecular Interactions Between Smut Fungi and Their Host Plants. *Annu Rev Phytopathol*, *57*, 411-430. doi:10.1146/annurev-phyto-082718-100139

6 Appendix

Table 15: Cazymes of Ustilaginomycetes.

BEPS: Bacterial exopolysaccharides; BPG: Bacterial peptidoglycan; CW: Cell wall; ESR, energy storage and recovery; PCW: Plant cell wall; PG, protein glycosylation; FCW: Fungal cell wall.

	cellulose						hemicellulose															hemicellulose or pectin							
	GH						GH										CE						GH						
	6	7	45	61	74	94	10	11	26	27	29	31	35	36	39	51	53	54	62	67	93		115	1	2	3	5	15	16
<i>A. flocculosa</i>	0	0	1	0	0	0	1	0	0	1	0	5	2	0	1	3	1	0	0	0	1	1	0	0	0	4	0	0	5
<i>S. reilianum</i>	0	0	3	0	0	0	2	1	0	1	0	3	1	0	0	2	0	0	1	0	0	1	1	0	0	3	0	0	3
<i>U. maydis</i>	0	0	3	0	0	0	2	1	0	0	0	3	1	0	0	3	0	0	1	0	1	1	1	0	0	1	0	0	4
<i>U. hordei</i>	0	0	3	0	0	0	2	1	0	2	0	3	1	0	0	3	0	1	1	0	0	1	1	0	0	4	0	0	3
<i>M. bullatus</i>	0	0	2	0	0	0	2	1	0	3	0	4	1	1	1	3	0	1	1	0	1	1	1	0	0	2	0	0	8

	pectin										Total PCWDE
	GH				PL				CE		
	28	78	88	105	1	3	4	9	11	8	
<i>A. flocculosa</i>	3	1	0	1	1	1	4	0	0	0	37
<i>S. reilianum</i>	1	0	0	2	1	0	0	0	0	1	27
<i>U. maydis</i>	2	0	0	2	1	0	0	0	0	1	26
<i>U. hordei</i>	2	0	0	2	1	0	0	0	0	1	32
<i>M. bullatus</i>	3	0	1	2	1	0	0	0	0	0	40

	Fungal cell wall degrading enzymes													Total FCWDE	Cell wall degrading enzymes					Total CWDE				
	GH														CE	GH								
	16	17	18	20	46	55	64	71	72	75	76	81	85		89	92	4	1	2		3	5	8	9
<i>A. flocculosa</i>	13	1	6	2	0	1	0	0	1	0	0	1	0	3	6	34	1	2	4	11	1	0	19	
<i>S. reilianum</i>	20	2	3	2	0	1	0	0	1	0	1	0	1	0	3	7	41	0	1	3	13	1	1	19
<i>U. maydis</i>	13	1	3	2	0	1	0	0	1	0	0	1	0	3	5	30	0	2	3	11	1	1	18	
<i>U. hordei</i>	15	2	4	2	0	1	0	0	1	0	1	0	1	0	3	6	36	1	1	4	12	1	1	20
<i>M. bullatus</i>	15	2	3	2	0	1	0	0	1	0	1	0	1	0	3	6	35	1	2	4	11	2	0	20

	Energy							Total ERS	Bacterial cell wall					Total BPG & BEPS
	GH								GH			PL		
	4	13	15	32	37	49	65		23	24	25	7	14	
<i>A. flocculosa</i>	0	5	1	2	2	0	0	10	0	0	0	0	0	0
<i>S. reilianum</i>	0	6	1	2	2	0	0	11	0	0	1	0	0	1
<i>U. maydis</i>	0	3	1	3	2	0	0	9	0	0	1	0	1	2
<i>U. hordei</i>	0	6	1	2	2	0	0	11	0	0	1	0	1	2
<i>M. bullatus</i>	0	6	1	2	2	0	0	11	0	0	1	0	1	2

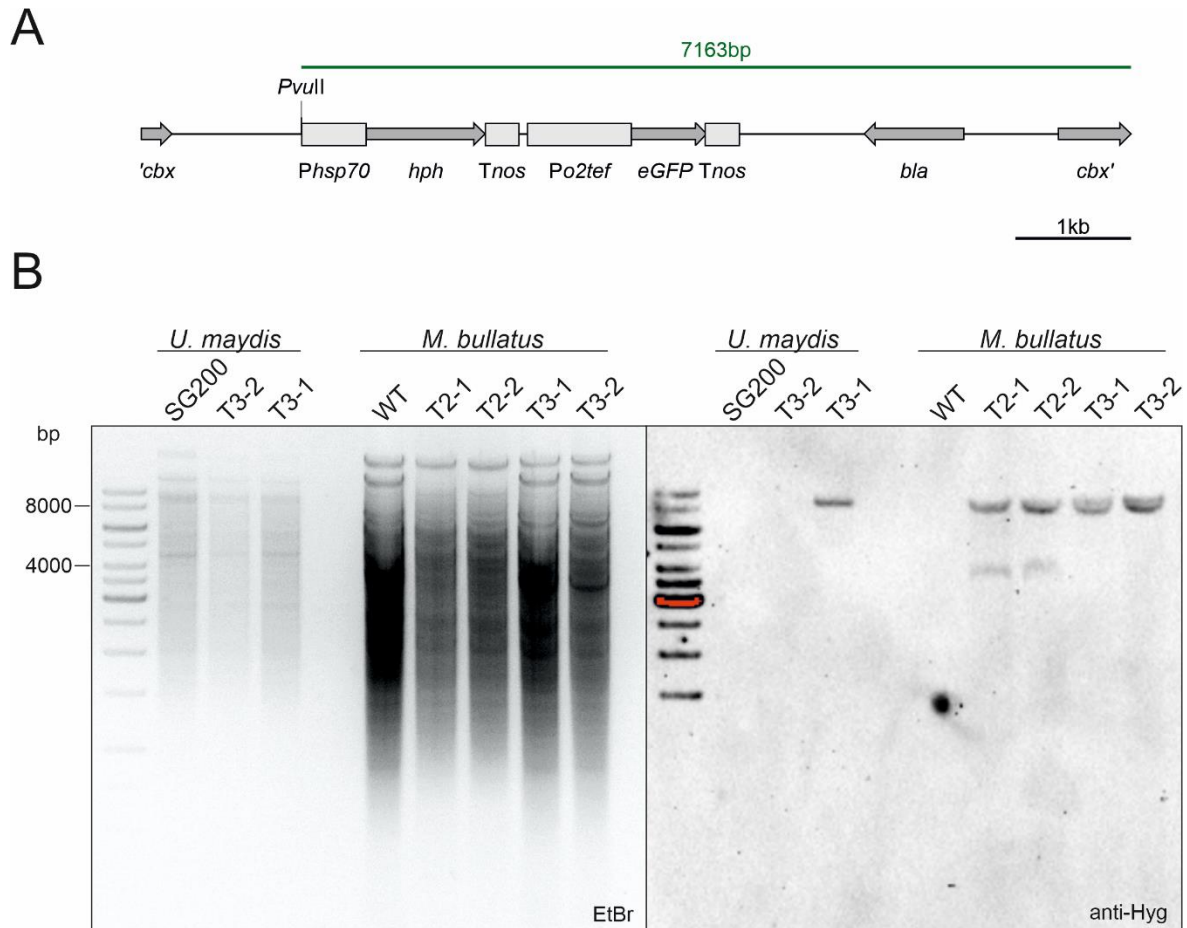


Figure 21: Verification of genomic eGFP-integration via Southern Blot. To show integration of the linearized plasmid DNA the genomic DNA was digested by using *PvuII*. The resulting band after hybridization with an hygromycin specific probe was expected to be bigger than 7163bp (**A**). Two *U. maydis* and four *Mba* transformants were subjected to southern blot analysis together with both wildtype strains. While no hybridization can be detected in the wildtype strains, one *U. maydis* and all *Mba* transformants show a band with the expected size (**B**).

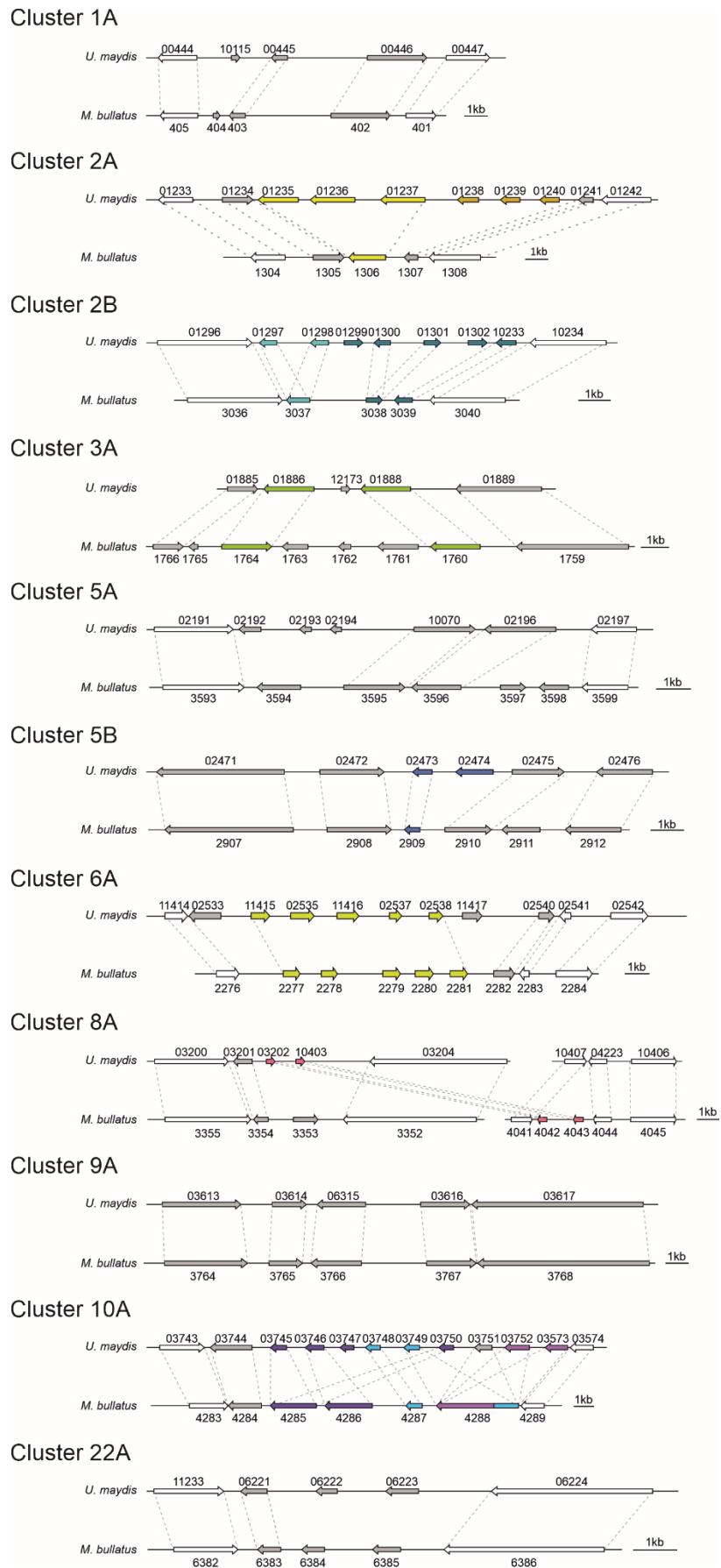


Figure 22: Virulence cluster comparison

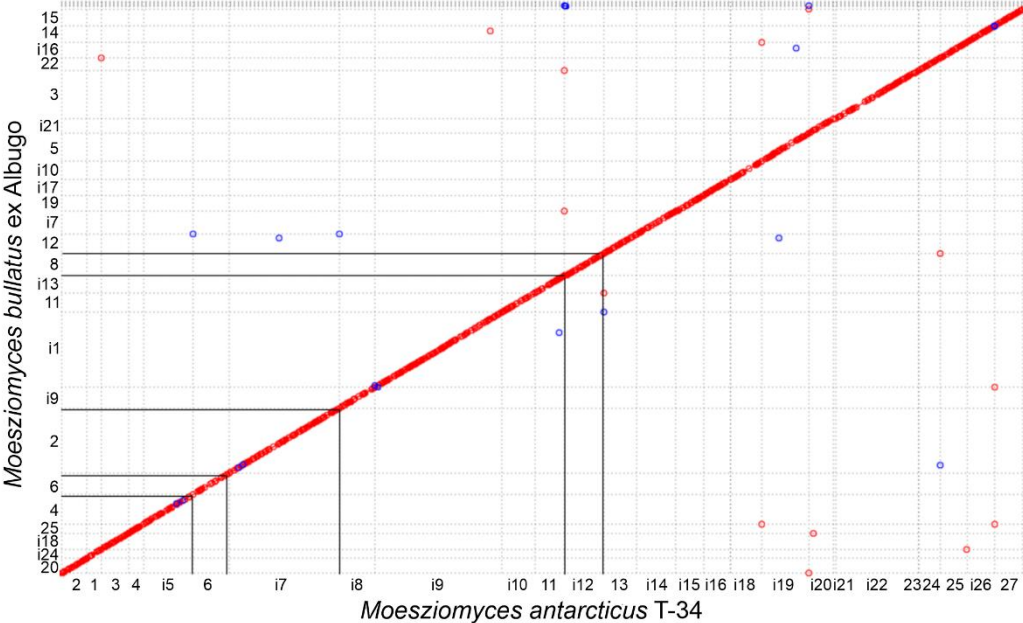


Figure 23: Genome comparison to *M. antarctica*. The genome of *M. bullatus* ex Albugo was mapped to the reference genome of the anamorphic relative *M. antarctica* T-34. This led to a high synteny in genome structure. Highlighted are the recombinated *Mba* contigs 2, 6 and 8.

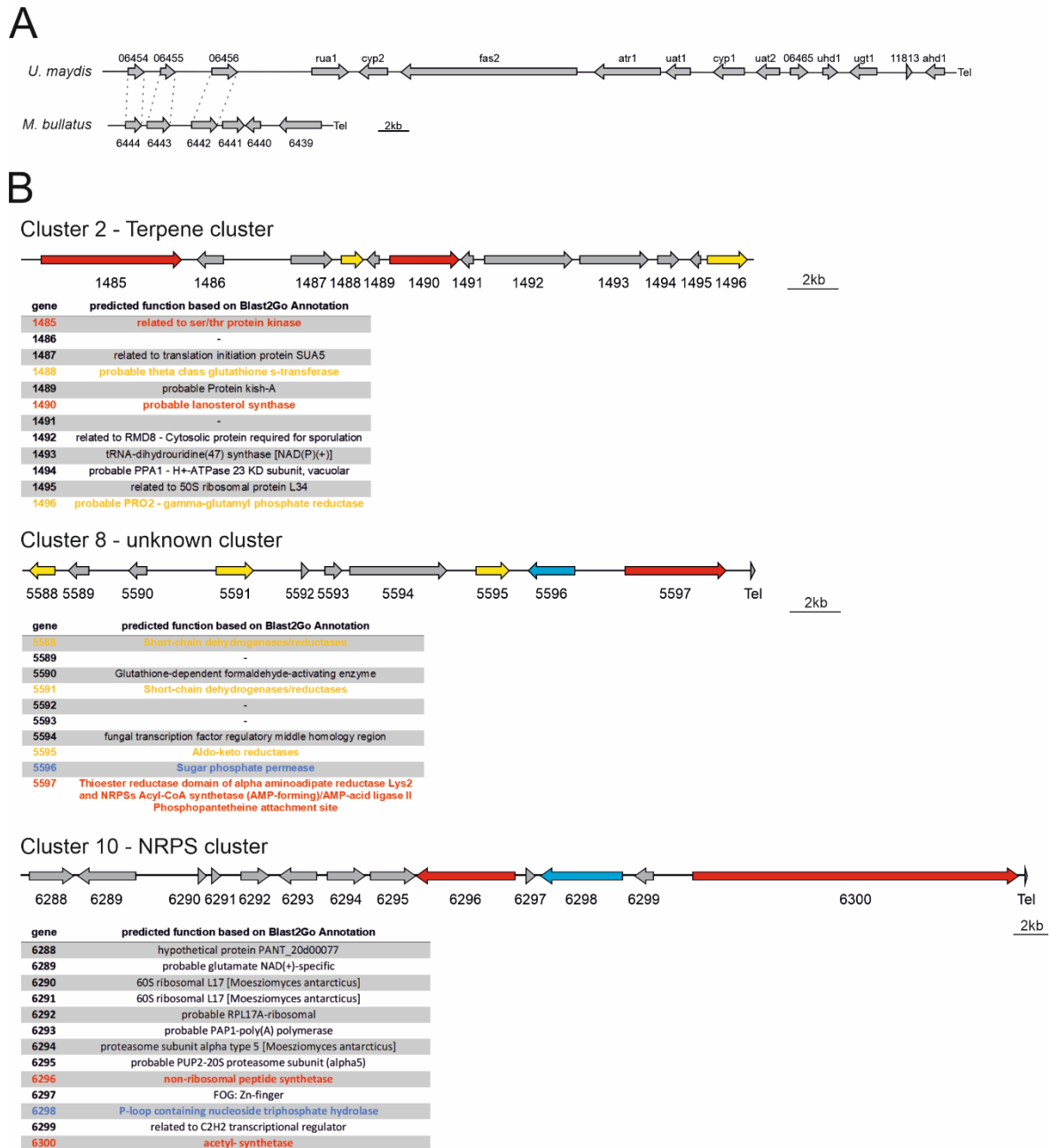


Figure 24: Secondary metabolites in *Mba*. Compared to the phytopathogen *U. maydis*, *Mba* has lost the secondary metabolite cluster for Ustilagic acid production (A). Furthermore, three unique clusters could be found. While cluster 2 is probably producing a terpene product, Cluster 8 belongs to the group of unknown clusters and cluster 10 has non-ribosomal peptide synthetase backbone gene (B).

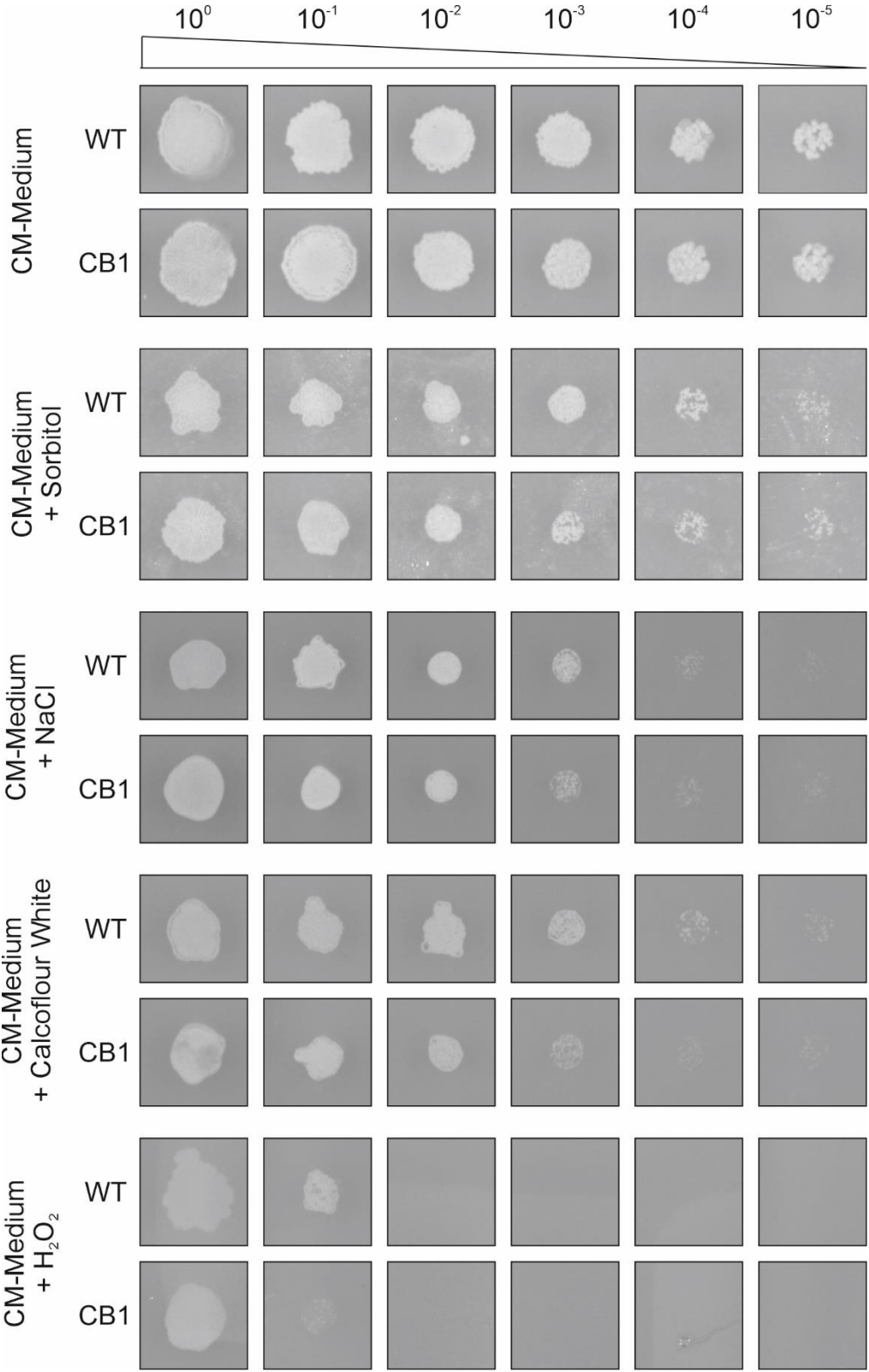


Figure 25: Stress test CB1. To exclude growth defects wildtype and CB1 strain were plated in a dilution series on CM-agar plates containing different stressors.

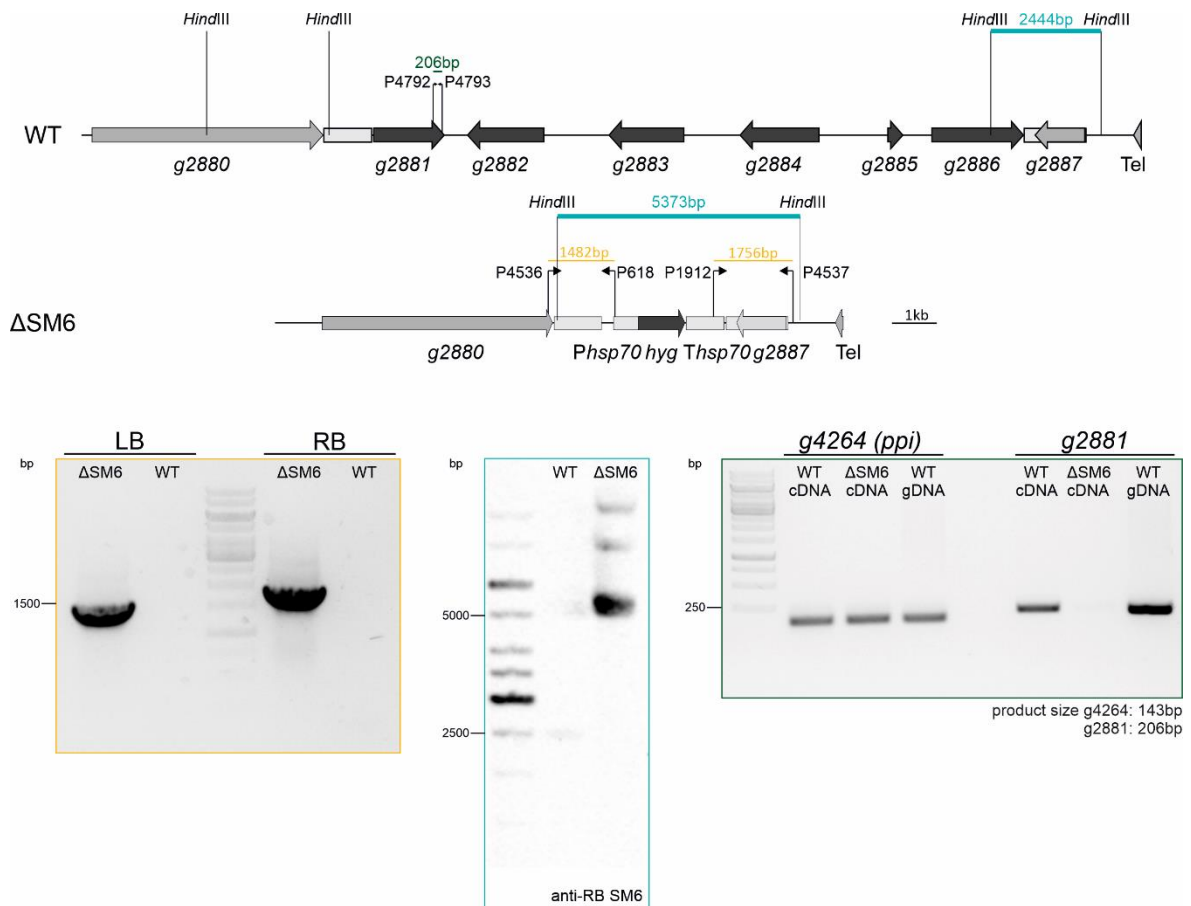


Figure 26: Verification of *Mba* Secondary metabolite cluster 6 knockout. To knockout the MEL cluster different attempts have been performed. First, integration of the knockout cassette was verified via PCR by amplifying each flanking side with primers located in the genomic region and inside of the knockout cassette. Furthermore, genomic DNA of wildtype and Δ SM6 strains had been subjected to southern blot analysis. A probe, hybridizing with the right boarder, was used to detect fragmented wildtype (2444 bp) and mutant (5373 bp) DNA, after cutting it with *HindIII*. Third, absence of *g2881* (coding for an Acetyltransferase) was verified by amplifying it from cDNA. *g4264* (coding for the housekeeping gene *ppi*) was used as a control for cDNA quality).

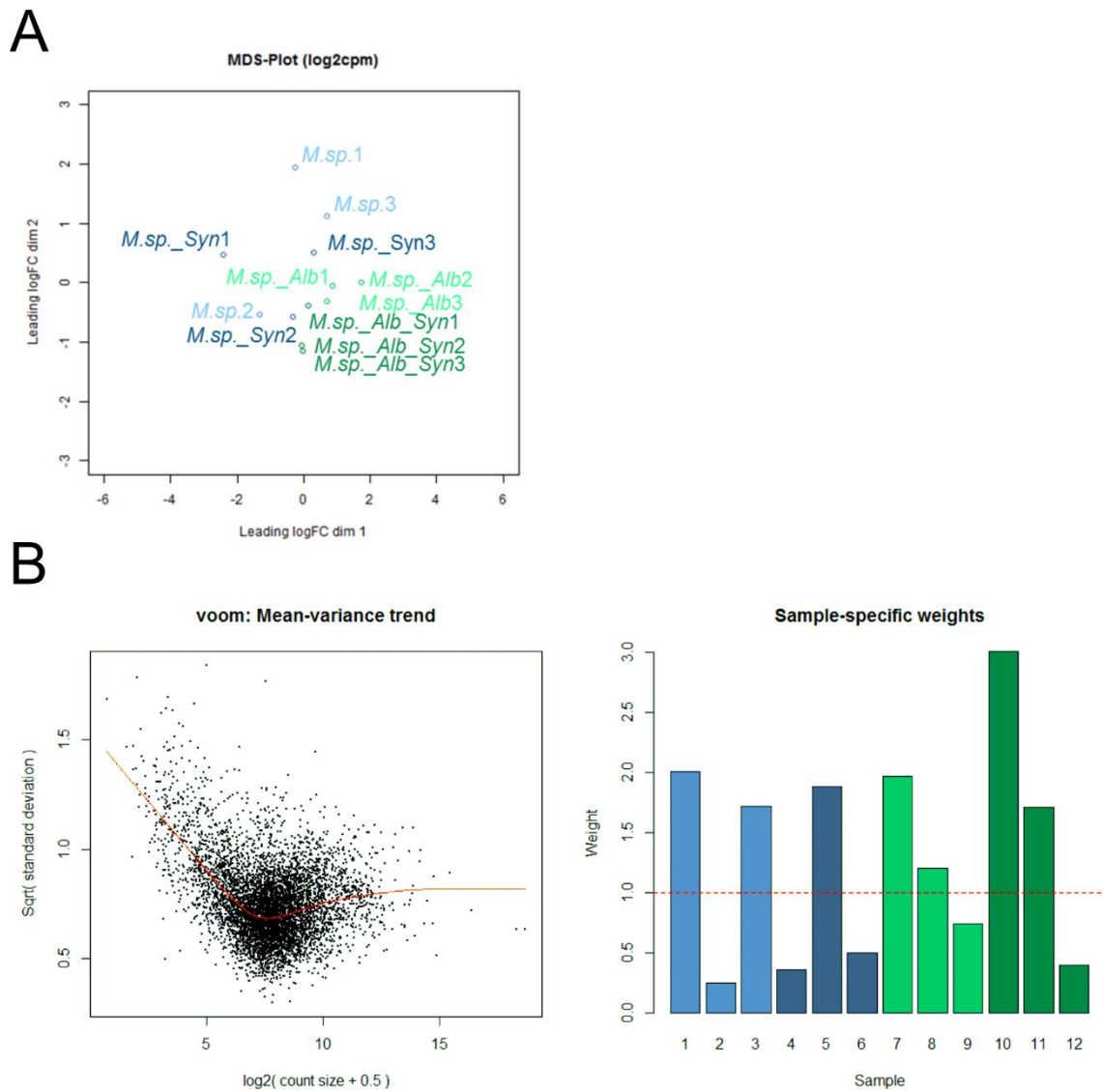
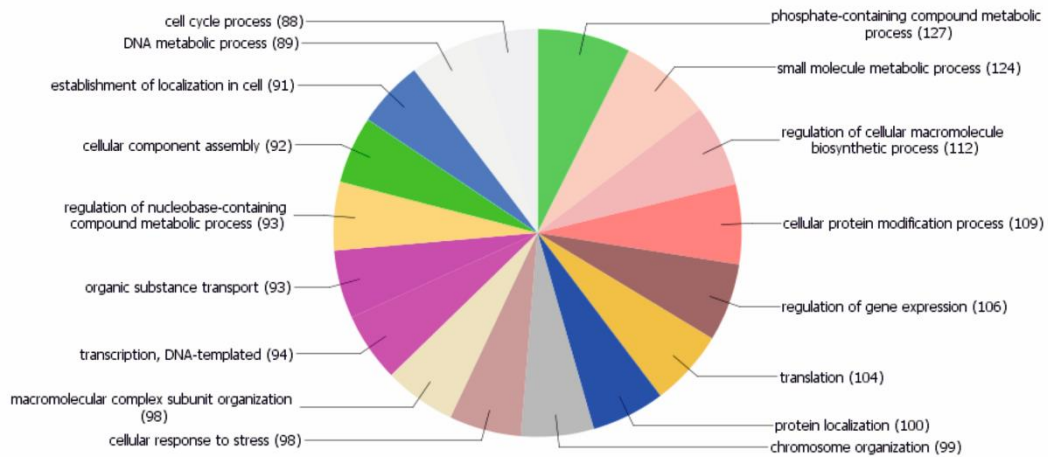


Figure 27: RNA-Seq Voom transformation. A multidimensional scaling plot shows high variance of the samples not containing *A. laibachii* as a community stabilizer (**A**). By voom-transformation of the raw data with sample-specific weighting variance should be lowered (**B**).

A

M. bullatus axenic culture vs. *M. bullatus* Peel
downregulated genes

Sequence Distribution [Biological Process]



B

M. bullatus Peel vs.
M. bullatus + *A. laibachii* Peel & *M. bullatus* + *A. laibachii*+ SynCom Peel
upregulated genes

Sequence Distribution [Biological Process]

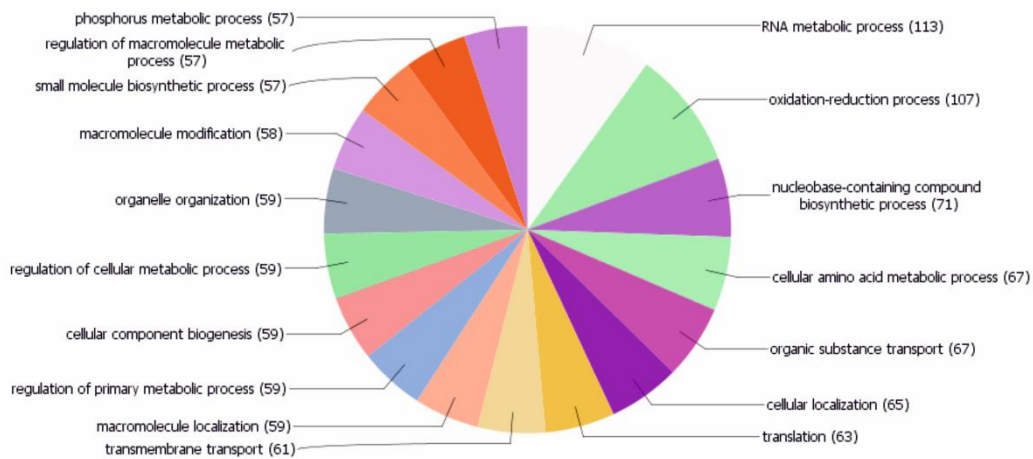


Figure 28: GO-term analysis RNA-Seq

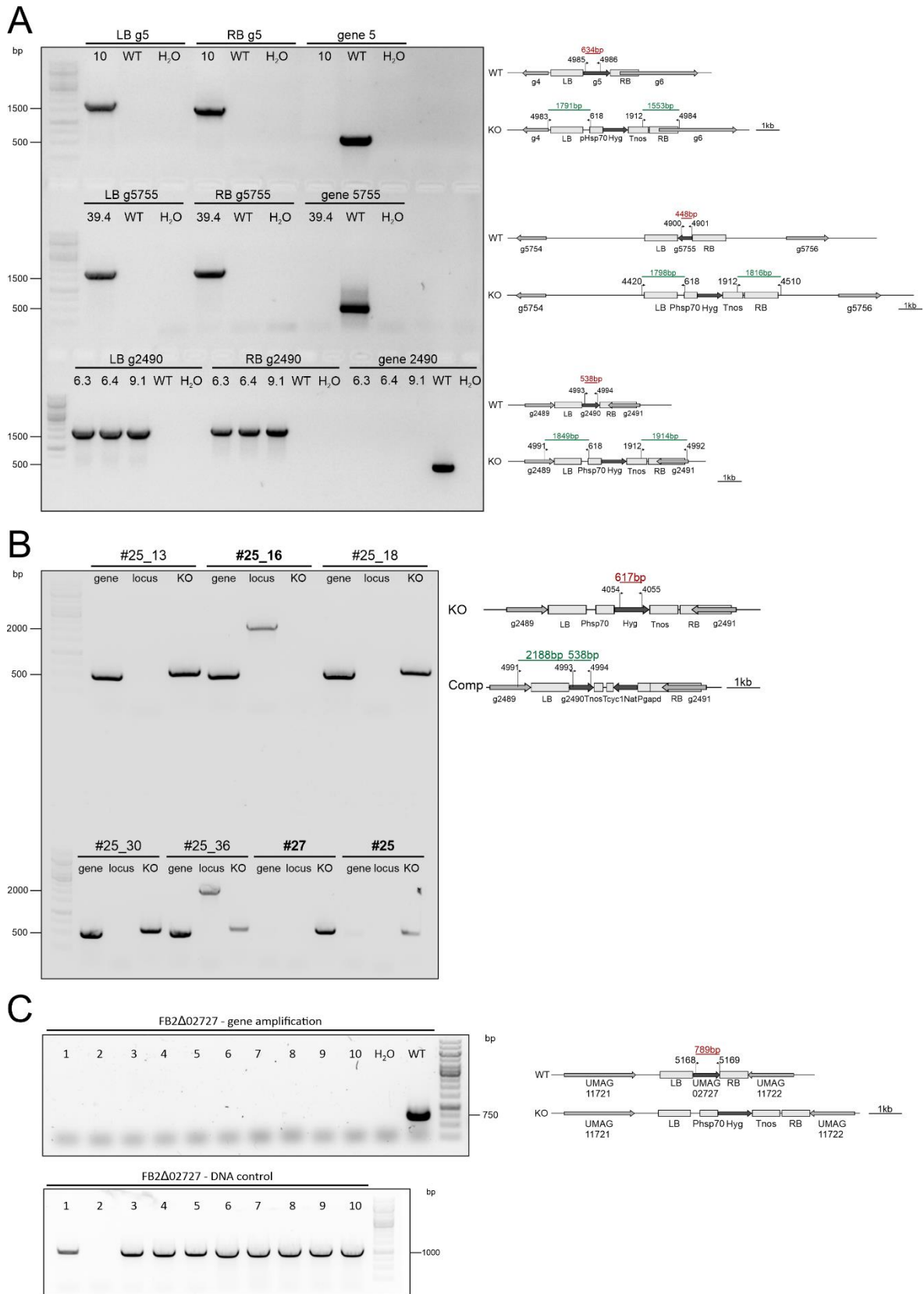


Figure 29: Knockout & Complementation PCR verification. *Mba* *g5*, *g5755* and *g2490* knockouts were verified by three PCR-reactions. Left and right border integration was proofed with one primer outside of the knockout cassette and one inside of it. Furthermore, absence of the gene was verified (**A**). For complementation, one primer set verified presence of the gene, and one the integration at the locus. Absence of the hygromycin gene was the last proof (**B**). In *U. maydis* complementation was proofed by absence of the gene and a second PCR with primers to amplify *tin2* to control DNA-preparation (**C**).

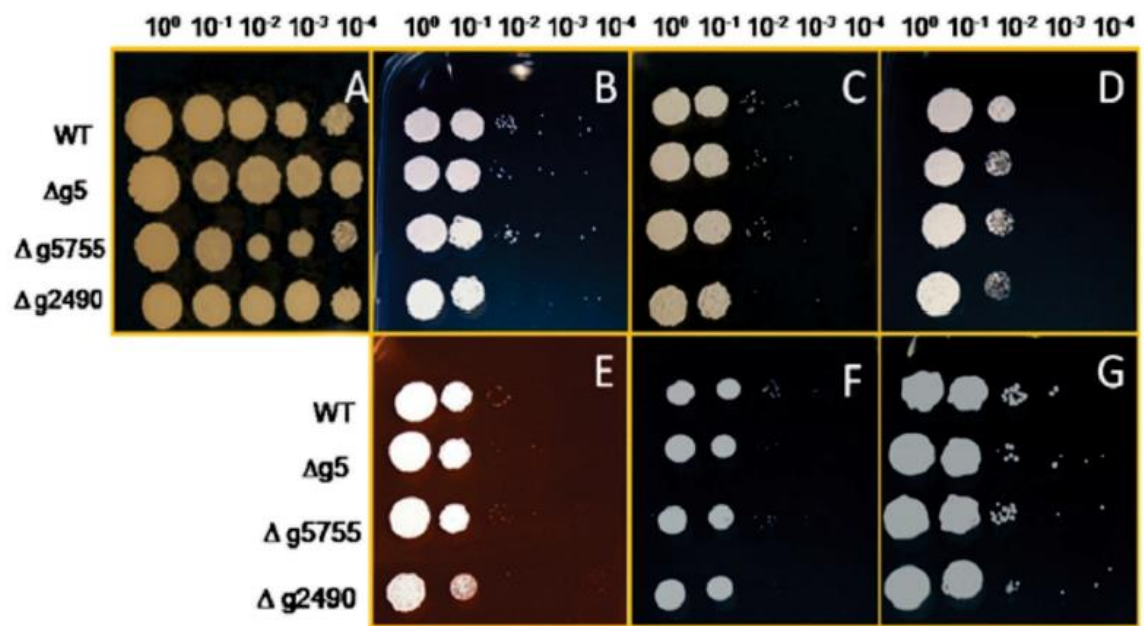


Figure 30: Stress test of *Mba* knockout strains. To exclude growth defects wildtype and knockout strains were plated in a dilution series on CM-agar plates containing different stressors.

Eidesstattliche Erklärung

Ich versichere, dass ich die von mir vorgelegte Dissertation selbständig angefertigt, die benutzten Quellen und Hilfsmittel vollständig angegeben und die Stellen der Arbeit – einschließlich Tabellen, Karten und Abbildungen –, die anderen Werken im Wortlaut oder dem Sinn nach entnommen sind, in jedem Einzelfall als Entlehnung kenntlich gemacht habe; dass diese Dissertation noch keiner anderen Fakultät oder Universität zur Prüfung vorgelegen hat; dass sie – abgesehen von unten angegebenen Teilpublikationen – noch nicht veröffentlicht worden ist, sowie, dass ich eine solche Veröffentlichung vor Abschluss des Promotionsverfahrens nicht vornehmen werde.

Die Bestimmungen der Promotionsordnung sind mir bekannt. Die von mir vorgelegte Dissertation ist von Prof. Dr. Gunther Döhlemann betreut worden.

Teile dieser Arbeit wurden in folgenden Artikeln veröffentlicht oder zur Veröffentlichung eingereicht:

Eitzen, K., Sengupta, P., Kroll, S., Kemen, E., & Doehlemann, G. (2021). A fungal member of the *Arabidopsis thaliana* phyllosphere antagonizes *Albugo laibachii* via a GH25 lysozyme. *eLife*, 10, e65306. doi:10.7554/eLife.65306

Datum:

Unterschrift:

Delimitation of own contribution

The results presented in this study were acquired by me independently and without other assistance than that stated here. The experiments were conceived and the publication “A fungal member of the *Arabidopsis thaliana* phyllosphere antagonizes *Albugo laibachii* via a GH25 lysozyme” was written in collaboration with Prof. Dr. Gunther Döhlemann, Prof. Dr. Eric Kemen and Priyamedha Sengupta. The experimental contributions of other persons that participated in this study are listed in the following:

Melanie Kastl generated the Δ 01987/Mb1682 strain and did the maize infections with this strain together with Dr. Bilal Ökmen as a part of her student internship.

Franca Arndt helped to verify the generation of *M. bullatus* CB1 strain and performed stress assays and plant infections with this strain as a part of her bachelor thesis. Furthermore, she generated *P. pastoris* strains expressing the GH25 enzymes and did first test expressions as a student helper.

Sarah Kroheck generated the *M. bullatus* Δ SM6 strain and performed microbial inhibition assays as a part of her bachelor thesis.

Priyamedha Sengupta performed the stress test of *M. bullatus* knockout strains.

Acknowledgment

First, I want to especially thank Prof. Dr. Gunther Döhlemann and Prof. Dr. Eric Kemen for giving me the opportunity to work in their fantastic groups. Both gave me the freedom to develop my own project while creating a supportive and constructive environment. This project was challenging but I learned a lot about experimental design and how to cope with unexpected problems.

I thank Prof. Dr. Alga Zuccaro for your helpful advice and critical discussions in every TAC meeting. Also, I want to thank Prof. Dr. Bart Thomma for being so kind to be the second reviewer of this thesis.

As I have really appreciated being a member of CEPLAS I would like to thank every member for all your dedication and hard work. You developed a great consortium in the past years and gave me possibility to further develop my own career and personality. In particular I want to say thank you to Justine Groenewold and Isabell Witt for organizing various excursions, scientific trainings and courses for personal development. All of this helped me to achieve my goals and to further develop my personality.

My special thank goes to every member of the AG Döhlemann. I enjoyed being a member of this group and every coffee break in the social kitchen was so much fun. And there was much coffee needed when working on a PhD thesis!

A big thanks to Ute and Rapha, who always kept the lab running and organized! Without you there would have been many empty cupboards and only chaos!

A special thank you to Elaine, Jan, and Selma, who always had great and helpful advice and made my years at the group unforgettable!

Also, I want to thank Priya, who is now continuing the *Moesziomyces* research. I had so much fun while sharing the lab with you!

Zu guter Letzt werde ich nun ins Deutsche wechseln, denn in diesem Teil möchte ich vor allem meiner Familie und meinen besten Freunden danken. Besonderer Dank geht dabei an meine Eltern und Schwiegereltern. Ihr habt mir besonders in den letzten Jahren so oft den Rücken freigehalten und ohne eure Hilfe wäre es mir nicht möglich gewesen diese Arbeit zu Ende zu schreiben!

Außerdem möchte ich meinen beiden besten Freundinnen Ramona und Maren für die schönen, aber wie immer zu seltenen, Tage und Abende danken, an denen ihr mich vom

ganzen Stress abgelenkt habt! Ihr hattet immer ein offenes Ohr für meine Probleme und habt mir oft geholfen wieder das Positive zu sehen!

Als letztes möchte ich mich bei meinem Mann Marcel bedanken. Du musstest in den letzten Jahren so oft meinen Frust und meine Enttäuschung aushalten und hast trotz allem immer zu mir gestanden und mich versucht wieder aufzufangen. Ich bin froh, dass du immer an meiner Seite bist, und könnte mir niemand anderes wünschen!